

MARTIN MARIETTA ENERGY SYSTEMS LIBRARIES



3 4456 0353189 0

ORNL-1478  
Progress  
10a

**AEC RESEARCH AND DEVELOPMENT REPORT**

**HOMOGENEOUS REACTOR PROJECT**

**QUARTERLY PROGRESS REPORT**

**FOR PERIOD ENDING JANUARY 1, 1953**

**DECLASSIFIED**

CLASSIFICATION CHANGED TO  
BY AUTHORITY OF: AEC 4-1-55  
OAC 6-8-59



**CENTRAL RESEARCH LIBRARY  
DOCUMENT COLLECTION**

**LIBRARY LOAN COPY**

**DO NOT TRANSFER TO ANOTHER PERSON**

If you wish someone else to see this document,  
send in name with document and the library will  
arrange a loan.

**OAK RIDGE NATIONAL LABORATORY**  
OPERATED BY  
**CARBIDE AND CARBON CHEMICALS COMPANY**  
A DIVISION OF UNION CARBIDE AND CARBON CORPORATION



POST OFFICE BOX P  
OAK RIDGE, TENNESSEE

This document contains Restricted Data as defined in the Atomic Energy Act of 1946. Its transmission or the disclosure of its contents in any manner to an unauthorized person is prohibited.

[REDACTED]

10A

ORNL-1478

[REDACTED]

Contract No. W-7405-eng-26

**HOMOGENEOUS REACTOR PROJECT**  
**QUARTERLY PROGRESS REPORT**  
**for Period Ending January 1, 1953**

Project Director - J. A. Swartout  
Engineering - C. E. Winters  
Chemistry - S. C. Lind, C. H. Secoy  
Corrosion - E. G. Bohlmann  
Chemical Technology - F. L. Steahly, F. R. Bruce

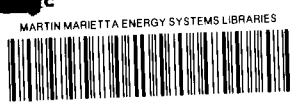
Compiled by W. E. Thompson

DATE ISSUED

\_\_\_\_\_

**OAK RIDGE NATIONAL LABORATORY**  
Operated by  
**CARBIDE AND CARBON CHEMICALS COMPANY**  
A Division of Union Carbide and Carbon Corporation  
Post Office Box P  
Oak Ridge, Tennessee

[REDACTED]



3 4456 0353189 0

INTERNAL DISTRIBUTION

1. G. T. Felbeck (C&CCC)
- 2-3. Chemistry Library
4. Physics Library
5. Health Physics Library
6. Metallurgy Library
- 7-8. Reactor Experimental  
Engineering Library
- 9-10. Central Research Library
- 11-20. Central Files
21. R. E. Aven
22. S. E. Beall
23. E. P. Blizard
24. E. G. Bohlmann
25. G. E. Boyd
26. W. M. Breazeale
27. R. C. Briant
28. R. B. Briggs
29. F. R. Bruce
30. J. H. Buck
31. A. D. Callihan
32. D. W. Cardwell
33. G. H. Cartledge
34. C. E. Center
35. G. H. Clewett
36. T. E. Cole
37. D. D. Cowen
38. J. S. Culver
39. J. L. English
40. D. E. Ferguson
41. W. R. Gall
42. J. P. Gill
43. R. J. Goldstein
44. C. B. Graham
45. J. C. Griess
46. C. S. Harrill
47. P. N. Haubenreich
48. C. G. Heisig
49. A. Hollaender
50. A. S. Householder
51. W. B. Humes (K-25)
52. G. R. Jenkins (C&CCC, South  
Charleston)
53. G. H. Jenks
54. C. P. Keim
55. M. T. Kelley
56. E. M. King
57. A. S. Kitzes
58. C. E. Larson
59. L. B. Emlet (Y-12)
60. S. C. Lind
61. R. S. Livingston
62. R. N. Lyon
63. W. L. Marshall
64. H. F. McDuffie
65. J. R. McWherter
66. E. C. Miller
67. K. Z. Morgan
68. E. J. Murphy
69. L. R. Quarles
70. P. M. Reyling
71. W. L. Ross
72. H. C. Savage
73. C. H. Secoy
74. C. L. Segaser
75. E. D. Shipley
76. A. H. Snell
77. I. Spiewak
78. F. L. Steahly
79. C. D. Susano
80. J. A. Swartout
81. E. H. Taylor
82. W. E. Thompson
83. M. Tobias
84. S. Visner
85. W. P. Walker
86. A. M. Weinberg

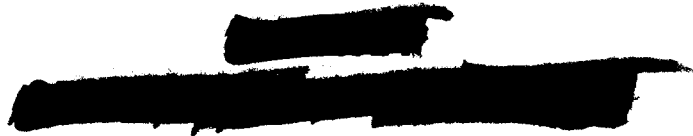


- |                               |                    |
|-------------------------------|--------------------|
| 87. T. A. Welton              | 91. F. C. Zapp     |
| 88. E. P. Wigner (Consultant) | 92. P. C. Zmola    |
| 89. C. E. Winters             | 93. G. C. Williams |
| 90. F. C. VonderLage          |                    |

*EXTERNAL DISTRIBUTION*

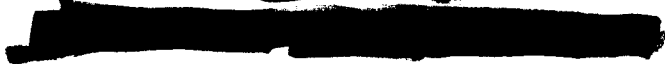
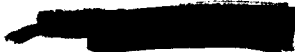
- 94-104. Argonne National Laboratory
- 105. Armed Forces Special Weapons Project (Sandia)
- 106-110. Atomic Energy Commission, Washington
- 111. Battelle Memorial Institute
- 112-114. Brookhaven National Laboratory
- 115. Bureau of Ships
- 116-117. California Research and Development Company
- 118-123. Carbide and Carbon Chemicals Company (Y-12 Plant)
- 124. Chicago Patent Group
- 125. Chief of Naval Research
- 126. Department of the Navy - Op 36
- 127-131. duPont Company
- 132-134. General Electric Company (ANPP)
- 135-138. General Electric Company, Richland
- 139. Hanford Operations Office
- 140-147. Idaho Operations Office (1 copy to Phillips Petroleum Co.)
- 148. Iowa State College
- 149-152. Knolls Atomic Power Laboratory
- 153-154. Los Alamos Scientific Laboratory
- 155. Massachusetts Institute of Technology (Kaufman)
- 156-158. Mound Laboratory
- 159. National Advisory Committee for Aeronautics, Cleveland
- 160. National Advisory Committee for Aeronautics, Washington
- 161-162. New York Operations Office
- 163-164. North American Aviation, Inc.
- 165. Nuclear Development Associates, Inc.
- 166. Patent Branch, Washington
- 167. Rand Corporation
- 168. San Francisco Operations Office
- 169. Savannah River Operations Office, Augusta
- 170. Savannah River Operations Office, Wilmington
- 171-172. University of California Radiation Laboratory
- 173. Vitro Corporation of America
- 174. Walter Kidde Nuclear Laboratories, Inc.
- 175-178. Westinghouse Electric Corporation
- 179-186. Wright Air Development Center
- 187-201. Technical Information Service, Oak Ridge





Reports previously issued in this series are as follows:

ORNL-527	Date Issued, December 28, 1949
ORNL-630	Period Ending February 28, 1950
ORNL-730	Feasibility Report - Date Issued, July 6, 1950
ORNL-826	Period Ending August 31, 1950
ORNL-925	Period Ending November 30, 1950
ORNL-990	Period Ending February 28, 1951
ORNL-1057	Period Ending May 15, 1951
ORNL-1121	Period Ending August 15, 1951
ORNL-1221	Period Ending November 15, 1951
ORNL-1280	Period Ending March 15, 1952
ORNL-1318	Period Ending July 1, 1952
ORNL-1424	Period Ending October 1, 1952





## SUMMARY

### PART I HOMOGENEOUS REACTOR EXPERIMENT

After the repair of the fuel leak that occurred in July, the entire HRE system was checked for leaks by a helium leak test, hydrostatic tests, and by water balance, all of which indicated the system to be free from leaks. Operation of the reactor was resumed on October 8, and experiments to evaluate the effectiveness of the D<sub>2</sub>O reflector between 200 and 250°C and to obtain the temperature coefficient of reactivity in this temperature range were carried out. A value of  $7.9 \pm 1.0\%$   $k_{eff}$  was obtained at 225°C for the entire reflector by doubling the value observed from full to the core equator and correcting for the control rod. The temperature coefficient of reactivity was measured from 217 to 228°C and gave, by extrapolation, a value of  $1.54 \times 10^{-3}$   $k_{eff}/^{\circ}\text{C}$  for the coefficient at 250°C.

These two experiments completed the low-power experimental program. The power level was then increased to about 35 kw, and after about 30 min of operation at this power level, the building-air monitors indicated that active gas was leaking into the building. The activity was traced to a small leak in the fuel gas condenser that operates at atmospheric pressure. It was not considered feasible to install a replacement condenser, and therefore a closed cooling system was provided for the existing condenser and arrangements were made to operate under a pressure of 5 psi so that any

leakage would be into the reactor system rather than out of it.

Operation was resumed on November 6 at the 1-kw power level with the fuel at 200°C and 1000 psi. After two days of operation, a leak occurred in a lead-gasketed flange in the differential pressure cell used for measuring oxygen flow into the fuel system. With the loss of pressure in the oxygen feed line, fuel backed through this line to the leak and spilled out into the cell. Approximately 500 g of U<sup>235</sup> leaked out before the off-gas monitor alarmed and the fuel dumped.

It was possible to remove the troublesome parts of the oxygen system with remote tools and disassemble them for examination without difficulty or overexposure to radiation.

The entire oxygen addition system is being revised, since both fuel leaks have occurred there, and installation of the new system is expected to be completed by January 1, 1953.

Based on chemical analyses for dissolved nickel in the fuel solution, the generalized corrosion rate in the HRE to date appears to be about 1 mpy.

Further studies with the electric analog-computer HRE simulator have been made and are reported.

### PART II BOILING REACTOR RESEARCH

Construction of the HRE Building No. 2 has been postponed for at least a year. The Teapot boiling reactor will be mocked up and tested at Y-12





before it is installed in its final location for actual operation.

The chemical stability of uranyl sulfate solutions in a boiling reactor is being studied, particularly with regard to whether sufficient dissolved oxygen will be present to prevent  $UO_3$  precipitation.

Preliminary plans have been made for a boiling-reactor reactivity-response experiment at Los Alamos.

The effect of dissolved gas on the superheat required for bubble formation in superheated uranium sulfate solutions is being investigated.

Equipment for two experiments on vapor removal from boiling liquids is being constructed. Preliminary tests have been made to determine the liquid entrainment in vapor rising from a high-pressure boiling liquid at high power release rates.

An investigation of the equilibrium response of a simple, closed-vessel boiling reactor to changes in demand for steam reveals that only at very low vapor fraction and low pressure will good response be obtained. In some other cases at low pressure, the power output will increase with pressure until a higher pressure is reached, at which point the power output will decrease toward zero with further increase in pressure.

### PART III

## GENERAL HOMOGENEOUS REACTOR STUDIES

### Intermediate-Scale Homogeneous Reactor Design

The design now proposed for the ISHR is that of a two-region thorium converter that will use for fuel a

solution of  $UO_2SO_4$  in  $D_2O$  containing 5 g of uranium per liter and will be constructed of stainless steel. The blanket may contain  $ThO_2-D_2O$  slurry or thorium oxide pellets in  $D_2O$ . Thorium concentrations up to 60% of the blanket volume have been studied. A power density of 50 kw per liter in the core gives a core diameter of 4 ft for a 48-megawatt reactor and, allowing for a 2-ft blanket, the vessel is 8 ft in diameter. The flow rates are 5000 gpm through the core and 1000 gpm through the blanket. Both the core and the blanket will operate at 1000 psia and 250°C maximum temperature. The core-tank wall thickness is 1/4 inch.

Under these conditions and with 1000 g of thorium per liter in the blanket, a conversion ratio of 0.79 atom of  $U^{233}$  produced per atom of  $U^{235}$  destroyed is expected. Reducing the core-tank wall thickness to 1/8 in. will increase this ratio to 0.9. The ratio could be increased further by using zirconium for construction of the core tank or by increasing the concentration of thorium in the blanket. A density of 4218 g of thorium per liter as pellets in the blanket with a 1/8-in. stainless steel core vessel wall yields a conversion ratio of 1.0008 atoms of  $U^{233}$  produced per atom of  $U^{235}$  destroyed.

The system of auxiliaries serving the reactor is similar to that previously proposed for the plutonium and power producing reactor, except, of course, that now two nearly duplicate systems are required.

The heat exchanger originally designed for the plutonium and power producing reactor is satisfactory for



[REDACTED]

the fuel system of this reactor. A new design may be required for the blanket system, however.

#### Controls and Instrumentation

A valve test loop is being constructed to test valve-trim materials, high-pressure seals, valve operators, and other components in service with uranyl sulfate solutions at 250°C and 1000 psi.

A general design has been developed for a spectrophotometer to be used in monitoring uranium concentration in uranyl sulfate fuel solutions. The use of ultrasonic liquid-level indicators is also being investigated.

#### Engineering Development

On the basis of experiments with small-scale core models, it appears that rotating flow through the core of an intermediate-scale reactor of the type now being designed is not satisfactory because of high pressure drop across the core. Therefore present investigations of rotating flow are being de-emphasized so that greater effort can be devoted to the more promising straight-through flow arrangements.

The use of straight-through flow requires a gas separator in the external circuit, and, at present, pipe-line separators appear most attractive. Models have been tested, and further tests of refined models are planned.

Because of difficulties experienced with the operation of the pulsafeeder fuel feed pump in the HRE, an extensive

program of development and testing on this type of pump has been undertaken. With modifications, mainly to the diaphragm, pumping head, check valves, and motor speed, a smoothly running pump of improved performance and reliability has been produced. Development and testing are being continued. Testing of an alternate, piston-type pump is now in progress.

Slurry circulating experiments with a pulsafeeder pump, let-down valve, and heat exchanger are in progress. These and additional experiments will aid in the eventual conversion of the HRE mockup to a slurry circulating system.

A small test facility is being installed for use in studying the effects of temperature, pressure, and fission-product poisons on the operation of high-pressure, catalytic recombiners. Both packed-bed and shell-and-tube types of recombiner units will be tested.

#### Corrosion

Ten pump loops are now in operation in the dynamic corrosion program. This scale of testing would have been impossible to attain or maintain without the successful organization of methods of pump repair in the Y-12 shops. To date, nine Westinghouse model 100-A pumps and one model 30-A pump have been repaired. Performance of the model 100-A pump under a variety of conditions is discussed.

Progress on the construction of an all-titanium loop has been slowed somewhat by diversion of craft labor to

[REDACTED]

other higher priority work, but completion of this loop in the next quarter is anticipated.

A study of the effect of the formation of a corrosion film on the inside tube surface on the over-all heat transfer coefficient has been started. An experimental setup was designed to simulate HRE operating conditions, and initial results indicate that a coefficient at least as large as that used in HRE design calculations (about 1000 Btu/hr·°F·ft<sup>2</sup>) may be expected.

Precipitation of UO<sub>3</sub>·H<sub>2</sub>O from low-concentration solutions of uranyl sulfate or uranyl fluoride circulating in pump loops operating at 250°C continues to be observed. No satisfactory causative mechanism has been ascertained thus far. Preliminary results indicate that the addition of excess sulfuric acid to the solutions may prevent this precipitation.

During the past quarter, the emphasis in data taking has shifted from obtaining generalized corrosion rates by following changes in nickel concentration in the test solutions to obtaining data from examination of pin and coupon specimens. A summary of such results obtained to date is included in this report. The general indication corresponds to that obtained in the nickel rate studies; however, it is hoped that more definitive conclusions and recommendations will be indicated by the pin and coupon data. Unfortunately, more experience with the test techniques is obviously necessary before specific statements can be justified.

The small-scale dynamic test program continues in the equipment development stage.

Static tests in uranyl sulfate solutions are concerned with tests of synthetic gems, crevice corrosion, and stress corrosion.

An in-reactor loop for circulating homogeneous reactor fuels into the high-flux region of the LITR is being designed. The major components of the loop, which is designed to fit into a thimble in a standard beam hole, are a centrifugal pump, temperature control system, and sample holders. The total volume is 300 ml and the operating conditions are 250°C and 1000 psi.

#### Metallurgy

The experimental efforts of the Metallurgy group have been directed toward the development of welding techniques for heavy sections of stainless steels, assistance to the Corrosion group, radiation damage studies, and evaluation of the possibility of embrittling titanium in HRP corrosion environments.

Metallographic work is in progress to further study the severe intergranular corrosion attack that occurred in a type 304 stainless steel specimen holder under what was thought to be a relatively mild corrosion environment. The results are not complete but indicate the susceptibility of a sensitized material to concentration cell attack by oxygen-depleted uranyl sulfate, and the consequent requirement that material specifications, welding procedures, and heat treatment

[REDACTED]

[REDACTED]

[REDACTED]

[REDACTED]

be designed to ensure complete stabilization of austenitic stainless steels. Assistance has been given to the Corrosion, Instrument, and Design groups in the selection, procurement, and preparation of various test specimens and of engineering component parts.

Tentative specifications, based on continuing experimental welding work and covering procedures and qualification tests for the welding of heavy sections of type 347 stainless steel, have been written and distributed for criticism prior to recommendation for adoption.

Impact test specimens of several materials of interest to the HRP are undergoing irradiation in the ORNL graphite reactor and in the LITR. Tests on a carbon steel apparently further confirm the previously reported tendency of neutron irradiation to increase the transition temperature and decrease the fracture energy of such material.

Exposures of commercially pure titanium impact test specimens to uranyl sulfate solutions in static and dynamic tests thus far have not indicated any appreciable change in hydrogen content or in impact-vs.-temperature behavior. It should be noted, however, that the initial material, before corrosion exposure, contained substantially more hydrogen and was somewhat more brittle than would be desired in a completely acceptable structural material for HRP purposes. Work is continuing on higher purity material and on partly cold-worked specimens, as well as on other phases of the problem.

#### Aqueous Solution and Radiation Chemistry

Radiation studies in which the rate of corrosion of type 347 stainless steel is determined by measuring the rate of consumption of oxygen gas have been continued. For a uranyl fluoride solution containing 40 g of uranium per liter, the average corrosion rate was 3.5 mpy over a nine-week period, compared with an out-of-reactor rate of 0.9 mpy over a six-day period. An amount of uranium equivalent to the amount of nickel oxidized is precipitated from the solution.

The rate of production of hydrogen has been found to be unaffected by acidity in the pH range from 1.4 to 3.5 but is lowered by about 3% at a pH of 0.6 for a uranyl sulfate solution containing 40 g of uranium (93.2% enriched) per liter.

Introductory studies of the mechanism of the hydrogen-oxygen recombination reaction in solutions indicate that the reaction proceeds without the formation of a bonded, activated complex. There are also indications that both sulfate and hydrogen ions may be involved in the reaction.

Further studies of the catalytic decomposition of hydrogen peroxide show that Fe(III) is a better catalyst than Fe(II). A concentration of 6 to 10 ppm of Cu(II) is sufficient for complete promoter action. Manganese(II) has been found to have negligible catalytic effect.

Work on the solubility of uranium trioxide in uranyl sulfate and uranyl fluoride solutions has been hampered by corrosion difficulties and problems

[REDACTED]

[REDACTED]

[REDACTED]

in analysis. It appears that the corrosion problems have been solved, and useful data should be forthcoming. Work at present is largely concerned with efforts to improve the analytical techniques.

Phase study of the two-liquid phase region in the three-component system,  $UO_3-SO_3-H_2O$ , is in progress. Most of the past quarter has been devoted to the construction of apparatus by which a thermostatic method involving volume measurements can be employed. This technique, if successful, will yield information about the vapor phase, as well as about each of the liquid phases.

A study of the oxidation states of specific fission products in homogeneous reactor environment has been started. The initial work will be with iodine.

Corrosion of type 347 stainless steel by  $UO_2F_2-NaF$  solutions is being investigated. Results will be reported later.

Several members of the group have devoted a major portion of their time to the accumulation and preparation of material for the Reactor Handbook. A paper entitled "The Radiation Chemistry of Aqueous Reactor Solutions. I. Radiation-Induced Decomposition," by J. W. Boyle, W. F. Kieffer, C. J. Hochanadel, T. J. Sworski, and J. A. Ghormley has been accepted for publication by the *Journal of Reactor Science and Technology*. This paper is intended to be the first of a series in this general field. Another paper entitled "The Electrical Conductivity of Uranyl Sulfate and Uranyl Fluoride

Solutions," by R. D. Brown, W. B. Bunker, W. L. Marshall, and C. H. Secoy has been submitted to the American Chemical Society for presentation at the 123rd National Meeting at Los Angeles, March 15-19, 1953.

### Slurry Chemistry

During the past quarter, attention was directed to methods of preparing pure  $UO_3-H_2O$  platelets with the use of the commercially available trioxides as starting materials. Previous studies have indicated that a series of calcinations at 350 to 400°C and subsequent rehydrations at 250°C resulted in considerable purification from  $NO_3^-$  and a reduction in average particle size. Neither Mallinckrodt  $UO_3$  nor Harshaw  $UO_3$  appears to be suitable for use as a starting material without some pretreatment other than simple washing.

High purity  $UO_3 \cdot H_2O$  platelets suitable for use in a slurry were prepared by five calcination-hydration cycles with  $UO_3 \cdot H_2O$  rods used as starting material. The rods were prepared by the decomposition in water at 250°C of  $UO_4 \cdot 2H_2O$  precipitated from uranyl nitrate solution.

An alternate method of preparing pure platelets, which promises some reduction in the number of steps required to produce a satisfactory slurry, used ammonium uranyl carbonate as a starting material. The carbonate was prepared in two ways: by a metathesis of freshly precipitated ammonium diuranate with ammonium carbonate and by adsorption of the uranyl ion from a

[REDACTED]

[REDACTED]

[REDACTED]

[REDACTED]

nitrate solution and subsequent elution of it with ammonium carbonate.

It was demonstrated that sedimentation data for oxide slurries containing 200 to 500 g of uranium per liter could be used in obtaining particle size data in substantial agreement with those obtained from nitrogen adsorption surface area measurements.

Interest was aroused in the possible use of uranyl carbonate as a slurry fuel when it was found that a relatively pure material ( $UO_3/U = 0.96$ ) could be prepared by the reaction of the oxide platelets with carbon dioxide. The material showed excellent slurry properties. The addition of a low concentration of sodium carbonate served to deflocculate the fine particle agglomerates and produce virtually stable slurries at both high and low uranium concentrations.

An experiment on the effect of reactor irradiation on high purity platelets of natural uranium showed that at a fission density of about 0.2 watts per gram of oxide, slurry properties were essentially unimpaired by a three-week irradiation at  $250^\circ C$ .

Static corrosion tests on the effect of fission products on the corrosion of type 347 stainless steel by an oxide slurry indicated that the presence of the fission products should not increase corrosion.

#### Physical Studies of Slurries

Thorium oxide slurry properties are being investigated in concentrations up to 2000 g per liter. The investigation includes the design and construction of a thorium oxide slurry circulating loop.

[REDACTED]

[REDACTED]

[REDACTED]

The uranium oxide circulating loop has now operated for over 2000 hr without indication of abrasion or corrosion on the stainless steel parts. Modification of the pressurizer appears to have eliminated plating in the main stream, but a cake continues to build up in the pressurizer itself.

Critical experiments with slurries are now being performed. Sedimentation rates for  $UO_3 \cdot H_2O$  slurries have been measured and tentatively correlated by means of sedimentation theory.

Crystal habits of  $UO_3 \cdot H_2O$  are being investigated. Preliminary data on the thermal conductivity of  $UO_3 \cdot H_2O$  slurries and of  $ThO_2$  slurries have been obtained.

#### Chemical Processing

This quarter, the development of chemical processing for a homogeneous plutonium producing reactor has been limited to removal of plutonium from the reactor fuel solution and to study of radiation damage in the tributyl phosphate solvent-extraction process. It was established that in the presence of the mixture of hydrogen and oxygen expected in the reactor, hexavalent plutonium is reduced and precipitates in 24 hr at  $250^\circ C$ . If the plutonium is removed as it precipitates, the concentration of  $Pu^{240}$  in the product will not exceed 0.2%. At  $100^\circ C$ , some reduction of Pu(VI) was observed with the fuel solution in contact with mixtures of hydrogen and oxygen; however, no precipitation of plutonium occurred in 72 hours. These results indicate that special provisions must be made for removing plutonium from a reactor operating at  $100^\circ C$ , even to

[REDACTED]

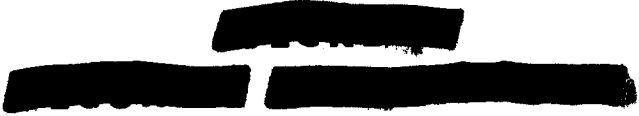
limit the concentration of Pu<sup>240</sup> in the product to 2%.

Tests with solvent exposed to Co<sup>60</sup> gamma emission indicated that no difficulties from solvent decomposition would be encountered in the tributyl

phosphate solvent extraction of homogeneous reactor fuel cooled only 15 days. However, the formation of surface-active agents and unsaturated compounds may cause some difficulties in solvent recovery.

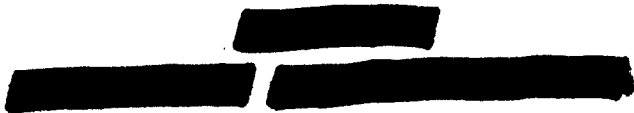
[REDACTED]

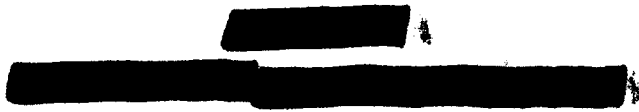
[REDACTED]



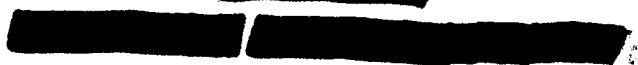
CONTENTS

	Page
SUMMARY . . . . .	v
PART I. HOMOGENEOUS REACTOR EXPERIMENT	
STATUS OF THE HRE . . . . .	3
Experimental Program . . . . .	3
Temperature coefficient . . . . .	3
Reflector effectiveness . . . . .	3
Reactor Operation . . . . .	4
Leak search . . . . .	4
Gas leak in condenser . . . . .	5
Fuel leak . . . . .	5
Corrosion . . . . .	6
HRE Simulator . . . . .	6
PART II. BOILING REACTOR RESEARCH	
BOILING REACTOR RESEARCH . . . . .	11
Over-all Program Change . . . . .	11
Building Design . . . . .	13
Teapot Design . . . . .	15
Stability of Boiling UO <sub>2</sub> SO <sub>4</sub> Solutions . . . . .	15
Nuclear Stability Studies . . . . .	16
Bubble Nucleation by Fission Fragments . . . . .	16
Power Removal from Volume Boiling Systems . . . . .	17
Unsteady-State Vapor Removal Tests . . . . .	17
Response of a Boiling Homogeneous Reactor to Changes in Steam Demand . . . . .	18
PART III. GENERAL HOMOGENEOUS REACTOR STUDIES	
INTERMEDIATE-SCALE HOMOGENEOUS REACTOR DESIGN . . . . .	23
Fuel System Flow Sheet . . . . .	23
Design Data . . . . .	27
Core Vessel . . . . .	27
Heat Exchanger . . . . .	31
Gas Separator . . . . .	32
Gas Production in the Reactor Core . . . . .	33
Recombiner System . . . . .	33



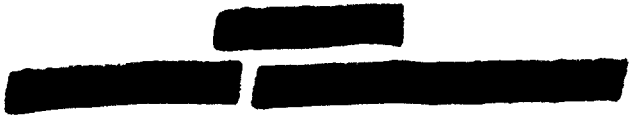


Evaporator System . . . . .	34
Fuel Dump System . . . . .	34
Fuel Feed System . . . . .	35
Control Rod Calculations . . . . .	35
Control Rod Operator . . . . .	36
Steam System . . . . .	36
Equipment Layout . . . . .	38
Critical Concentration and Neutron Balance . . . . .	38
Conversion Ratio as a Function of Radius . . . . .	39
Heating of Pellets in the Blanket . . . . .	40
Production of Tritium in a Three-Region Reactor . . . . .	40
CONTROLS AND INSTRUMENTATION . . . . .	43
Valves . . . . .	43
Concentration Indicator . . . . .	44
Liquid Level Indicator . . . . .	44
Densitrol . . . . .	44
ENGINEERING DEVELOPMENT . . . . .	45
Core and Gas-Separator Development . . . . .	45
Core development for straight-through flow . . . . .	45
Gas separators . . . . .	48
Single-core reactor studies . . . . .	50
Test Loop for 4000-gpm Pump . . . . .	52
Large Heat Exchangers . . . . .	52
Pulsafeeder Pump Development . . . . .	53
Seal Welded Head for the 1-gph Pulsafeeder Pump . . . . .	55
Positive-Displacement Triplex Pump Development . . . . .	55
Development of 1-gpm Pump with a Stellite Piston . . . . .	55
Small Canned-Rotor Pump Development . . . . .	57
Conversion of the HRE Mockup to Operate with Uranium Oxide Slurry . . . . .	59
Recombiner Development . . . . .	59
CORROSION . . . . .	61
Dynamic Corrosion Tests . . . . .	61
Pump Loop Corrosion Results . . . . .	63
Small-Scale Dynamic Corrosion Test Program . . . . .	74
Static Corrosion Studies . . . . .	74
Uranyl sulfate corrosion studies . . . . .	74
Uranyl fluoride corrosion studies . . . . .	75
In-Reactor Loop . . . . .	76
METALLURGY . . . . .	81
Service and Miscellaneous Work . . . . .	81
Welding of Type 347 Stainless Steel . . . . .	81





Radiation Damage Studies . . . . .	83
Properties of Titanium . . . . .	83
AQUEOUS SOLUTION AND RADIATION CHEMISTRY . . . . .	91
Radiation Studies of Uranyl Fluoride and Uranyl Sulfate Solutions . . . . .	91
Effect of Low Oxygen Pressure on Corrosion of Type 347 Stainless Steel in Radiation . . . . .	92
Radiation Chemistry of Aqueous Reactor Solutions . . . . .	92
Mechanism of the Hydrogen-Oxygen Recombination Reaction in Solutions . . . . .	93
Catalytic Decomposition of Hydrogen Peroxide in Uranyl Sulfate Solutions . . . . .	95
Solubility of Uranium Trioxide in Aqueous Uranyl Sulfate and Uranyl Fluoride . . . . .	95
Oxidation States of Fission Products in Reactors . . . . .	96
SLURRY CHEMISTRY . . . . .	97
UO <sub>3</sub> Chemistry . . . . .	97
Preparation of pure UO <sub>3</sub> ·H <sub>2</sub> O platelets . . . . .	97
Particle size determinations and sedimentation rates . . . . .	99
UO <sub>2</sub> CO <sub>3</sub> Chemistry . . . . .	101
Preparation of UO <sub>2</sub> CO <sub>3</sub> slurries . . . . .	101
Properties of UO <sub>2</sub> CO <sub>3</sub> and UO <sub>2</sub> CO <sub>3</sub> slurries . . . . .	102
Uranium Oxide Slurry Irradiation Studies . . . . .	103
Effect of Fission Products on Corrosion . . . . .	103
PHYSICAL STUDIES OF SLURRIES . . . . .	105
Thorium Oxide Studies . . . . .	105
Thorium Oxide Circulating Loops . . . . .	105
Uranium Slurry Pump Loops . . . . .	107
Critical Experiments . . . . .	107
Sedimentation Studies . . . . .	107
Thermal Conductivity of Slurries . . . . .	109
Crystal Structure of UO <sub>3</sub> ·H <sub>2</sub> O . . . . .	109
CHEMICAL PROCESSING . . . . .	113
Plutonium Chemistry in Uranyl Sulfate Solutions . . . . .	113
Radiation Damage . . . . .	114
RELATED BASIC CHEMISTRY RESEARCH . . . . .	117
Capture Cross Section of Protactinium-233 . . . . .	117
Chemistry of Corrosion . . . . .	117
Nucleation of Bubbles in Superheated Solutions by Fission Recoils . . . . .	117
Uranyl-Sensitized Reaction of Hydrogen and Oxygen . . . . .	117
Oxidation of Uranium(IV) by Gamma Rays . . . . .	118



**Part I**

**HOMOGENEOUS REACTOR EXPERIMENT**



# HRP QUARTERLY PROGRESS REPORT

## STATUS OF THE HRE

S. E. Beall, Section Chief

J. W. Hill

T. H. Thomas

P. M. Wood

S. I. Kaplan

D. E. Eissenberg

V. K. Pare'

J. J. Hairston

J. L. Redford

M. A. Bell

C. W. Keller

S. Visner

### EXPERIMENTAL PROGRAM

On October 8, after a recheck for leaks (see section of this chapter on "Reactor Operation"), the reactor was recharged with fuel solution, and operation was resumed for the purpose of evaluating the effectiveness of the D<sub>2</sub>O reflector between 200 and 250°C and also for obtaining the temperature coefficient of reactivity in this temperature range. The concentration data obtained in these runs were not so accurate as the previous data at lower temperatures, primarily because of sampling difficulties encountered with the activated fuel solution. The sampling frequency was restricted to one sample in 8 hr, the size of sample was limited to 20 ml, and the possibilities of contamination of the sample were increased. As a result, the accuracy of the concentration was probably no better than ±1.5%.

**Temperature Coefficient.** The upper limit of the range of temperatures for which the critical concentration was measured was extended from 217 to 228°C. The results are consistent with those obtained previously and are in good agreement with theoretical calculations.<sup>(1)</sup> A cubic equation was fitted to the data to obtain the extrapolated value of  $1.54 \times 10^{-3} k_{eff}/^{\circ}\text{C}$  for the temperature coefficient of reactivity at 250°C. This value agrees with the calculations to within 5%.

**Reflector Effectiveness.** The effect of reflector level on reactivity

at temperatures near 225°C was measured by two methods. For reflector levels from 100% full to a point 6 in. below the top of the core, the fuel concentration was maintained constant and the reactor was kept critical by varying both the reflector level and core temperature. In this manner, the value of the reflector level was deduced from the temperature coefficient of reactivity. Data were also taken over the range of reflector levels from full to the equator of the core by maintaining the temperature at approximately 225°C and varying the fuel concentration with the reflector level. Because of mechanical difficulties, the control rod remained fully inserted.

The data indicate a linear dependence for reflector levels below the top of the core. The value of  $7.9 \pm 1.0\% k_{eff}$  is obtained for the value of the entire reflector by doubling the value observed from full to the core equator and correcting for the control rod. The value of the reflector effectiveness calculated from theory is 8.5% if an empirical correction is made for the presence of the control rod.

### REACTOR OPERATION

A fuel spill from a check valve in the oxygen addition line was described in the previous report.<sup>(2)</sup> After the fuel solution was recovered and the area was decontaminated, a new check valve was installed without difficulty. At the same time, a

<sup>(1)</sup>S. E. Beall *et al.*, HRP Quar. Prog. Rep. Oct. 1, 1952, ORNL-1424, p. 4.

<sup>(2)</sup>*Ibid.*, p. 3.

## HRP QUARTERLY PROGRESS REPORT

revision was made in the fuel concentration system to eliminate instability that resulted in unexpected concentration changes.

**Leak Search.** With considerably greater appreciation for the consequences of a leak in the fuel system, it was decided to examine the entire piping once more for leaks that might have developed since the previous leak test. The leak search was performed by helium, hydrostatic, and water balance methods. The first method employed a Consolidated Engineering Co. leak detector of the mass spectrometer type. Reactor piping and equipment were pressurized with helium to a pressure several atmospheres greater than the operating level. While the system remained at pressure, a portable probe was used to sniff welds, flanges, and pipe surfaces. Although no leaks were detected in the fuel system, two were located in the off-gas system at screwed connections and were stopped by welding over the threads.

This type of helium leak test, in a system that is not thoroughly dry, may fail to show leaks at points of water holdup. Therefore a second test was conducted with the system under hydrostatic pressure. One disadvantage of this test in a system of large volume is that its sensitivity is determined by the accuracy with which temperature and pressure changes can be measured. For the HRE, it was calculated that a leak greater than  $20 \text{ cm}^3$  per day might be detected. After much effort in degassing the system and maintaining constant temperature conditions, the reactor system was considered satisfactory by this standard.

In neither of the tests described above was it possible to have the reactor at its normal operating temperature of  $250^\circ\text{C}$ . Because of the possibility that some leaks not evident at room temperature would appear at the higher temperature, it was decided

to operate the system with an accurately weighed quantity of water at 1000 psi and above  $200^\circ\text{C}$  continuously for one week. The sensitivity of this test was limited to a leak rate of  $70 \text{ cm}^3$  per day because of weighing inaccuracies. The result of the water balance test was a 0.5% gain in water weight, and the reactor was considered sufficiently leak tight for operation until the activity level of the fuel could be increased to a level easily detectable by monitors on the shield ventilating system.

Following the leak tests, the flame and catalytic recombiners in the fuel off-gas line were operated for 16 hr at flow rates as high as 15 cfm STP (corresponding to 1000-kw operation and gas produced at the rate of 2 molecules of hydrogen per 100 ev). During this time it was found that the instability in the fuel concentration system had been corrected by the system revision mentioned earlier.

**Gas Leak in Condenser.** With the completion of the low-power experimental program, the reactor power level was increased, by factors of 10 to 50, until a power level of about 35 kw was attained. Although it has not yet been possible to make an accurate determination of operating power at any level, approximations have been made by measurements of  $\text{Ce}^{141}$  activity in the fuel, by neutron flux measurements with foils in the reflector space, and by calculations based on temperature rise and heat capacity. After the reactor was operated for 30 min at the 35-kw level, it became evident from air monitors that active gas was leaking into the building. The activity was first traced to the floor drain and then to the cooling water from the fuel-gas condenser, which operates at atmospheric pressure. A series of tests proved the existence of a leak between the expanded tube and shell side of the condenser. It is possible that this leak was caused by flashbacks from the flame recombiner, because it is known

## PERIOD ENDING JANUARY 1, 1953

that the jacket-to-shell seal was leak-tight during the leak tests described above. It was not considered feasible to install a replacement condenser; so a decision was made to attach a separate, closed cooling system to the existing condenser. The new cooling system is equipped with a condenser, a circulating pump, and a storage tank containing demineralized water that make possible operation of the leaking condenser under a pressure of approximately 5 psi and ensure that water will leak into the system at a rate of a few cubic centimeters per day instead of gas leaking out.

**Fuel Leak.** After the condenser revisions were completed, operation was resumed on November 6 at the 1-kw power level, with the fuel at 200°C and 1000 psi. After two days of operation, a leak occurred in a lead-gasketed differential pressure cell that measures oxygen flow into the fuel system. As the oxygen leakage rate approached the oxygen feed rate, fuel solution backed into the oxygen line through a check valve, through the oxygen control valve, and began to spill through the gasket seal into the reflector cell of the shield. Approximately 500 g of  $U^{235}$  was lost before the off-gas monitron alarmed and dumped the fuel.

It was possible to open the reflector cell within 1 hr for remote inspection. The activity level was measured at 150 to 200 r/hr. By flushing with water, removing the contaminated concrete block, and allowing the fission-product activity to decay for 48 hr, the activity level was reduced to about 10 r/hr. At this level it was possible to remove the troublesome parts of the oxygen system with remote tools. The parts were disassembled remotely without difficulty or over-exposures, and the cause of the leak was determined to be the lead gasket on one flange of the differential pressure cell. Normally, the oxygen control valve between the flow device

and the fuel would have prevented back leakage. However, after the valve was disassembled, the seat was found to be loose, which permitted fuel solution to pass through to the leaking gasket.

It may be recalled that the previous fuel loss was from the oxygen addition line also, but that leak was at a point about 20 ft downstream from the control valve. In an effort to eliminate the possibility of another leak, it was decided to revise the entire oxygen system. The new system includes two spring-loaded check valves in series, a monitron to dump the fuel should activity appear in the line, an improved control valve, and a differential pressure cell with welded flanges. Installation of the new parts should be completed by January 1, 1953, at which time the experimental program can be resumed.

During this quarter the reactor was operated for a total of 194 hr, during which 228 kwhr was accumulated, for an average power level of approximately 1 kw.

### CORROSION

The corrosion of the type 347 stainless steel of which the HRE fuel system is constructed, has been followed by determining the nickel content of the fuel solution. The concentration of uranium in the  $UO_2SO_4$  solution has been varied between 20 and 40 g per liter. The corrosion rate has been calculated on the basis that the corrosion is uniform and takes place only in the high-pressure system in which the surface area is about 100 ft<sup>2</sup>. It is also assumed that the corrosion occurs only while the fuel solution is circulating at temperatures above 100°C. The results are summarized in Table 1 for operation of the reactor with normal uranium and with enriched uranium at low power. Because of the uncertainty in the nickel analyses and the relatively

# HRP QUARTERLY PROGRESS REPORT

TABLE 1. CORROSION OF THE HRE FUEL SYSTEM

DATE	URANIUM IN FUEL SOLUTION	FUEL CIRCULATING TIME (hr)		NICKEL REMOVED (g)	CORROSION RATE (mpy)
		Under 100°C	Between 100 and 250°C		
January 22 to April 8	Normal	23	452	12	1.5
April 8 to May 22	Enriched	140	-	2.1	0.3
June 12 to July 23	Enriched	-	466		
October 10 to November 10	Enriched	76	118	0.9	0.5

short running times, the calculated corrosion rates may be indicative only of the order of magnitude. Also, the possibility of localized attack in the equipment cannot be ruled out, even though such attack was not evident at locations accessible for visual inspection.

## HRE SIMULATOR

The electronic analogue computer is described in a report (to be issued) by J. P. Palmer, D. M. Collier, and L. A. Meeks of the ORNL Instrument Department. On a 1:1 time scale, it simulates a reactor with a negative temperature coefficient and delayed neutrons with parameters corresponding to the HRE at 250°C. Considerable data on the temperature and power response to step increases in reactivity will be included in the report.

The simulator was moved to the HRE area for the purpose of obtaining further information on the kinetic behavior of the reactor prior to actual tests on the reactor. Several minor modifications were made to approximate more closely the temperature coefficient of reactivity and the heat capacity of the heat exchanger and to improve operating flexibility. In addition, the potentiometer that controls reactivity has been fitted with a motor drive to allow the introduction of linear rises in  $k$ .

About 200 runs have been made with various rates of reactivity change, to simulate those available on the HRE,

and at various temperatures and power rates. A useful parameter in this work is  $\delta$ , the excess  $k_{eff}$  under external control, which is defined by

$$k_{eff} - 1 = \delta + \alpha(\theta - \theta_0),$$

where  $\alpha$  is the temperature coefficient of reactivity,  $\theta$  is the instantaneous core temperature, and  $\theta_0$  is the initial core temperature. At constant temperature, or in the absence of a temperature coefficient,  $\delta = k_{eff} - 1$ . The results have not been completely analyzed, but the indications are that a useful approximation to the observed behavior, for rates of  $\delta$  increase up to  $0.005 k_{eff} \text{ sec}^{-1}$ , is obtained by assuming that the reactor core generates whatever power is necessary to maintain itself at the required critical temperature. As a result, the core temperature increases uniformly with the added reactivity.

Figures 1a, b, c, and d are typical power and temperature plots obtained from the simulator. The machine was set for a temperature coefficient of  $1.6 \times 10^{-3} k_{eff}/^\circ\text{C}$ , a total power extraction of 0.6 megawatt, and a total input in  $\delta$  of 0.031. The rate of rise of  $\delta$  in Figs. 1a and 1b was  $0.00069 \text{ sec}^{-1}$ , which corresponds to injecting fuel solution into the core at a rate of 1 gpm from the dump tanks where the fuel concentration has been increased to a value three times that in the core. In Figs. 1c and 1d, the rate was  $0.0048 \text{ sec}^{-1}$ , which corresponds to the situation of running the

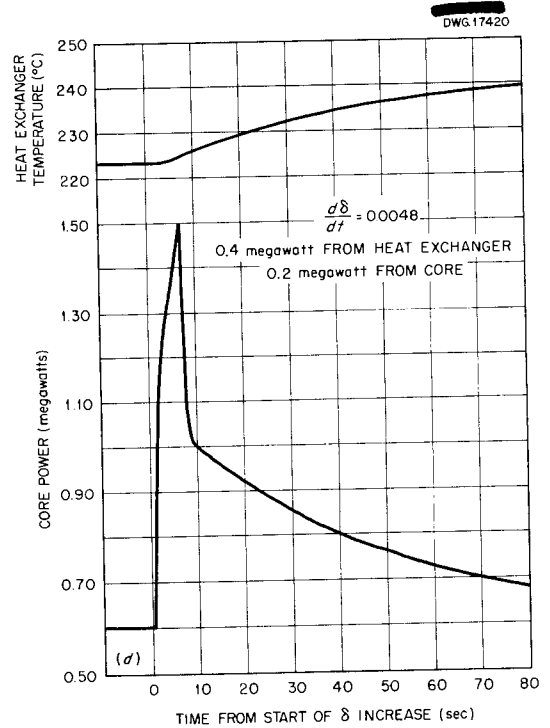
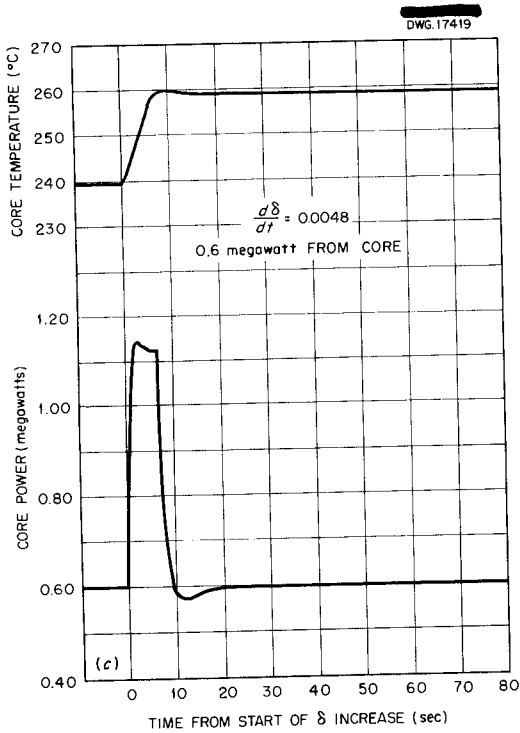
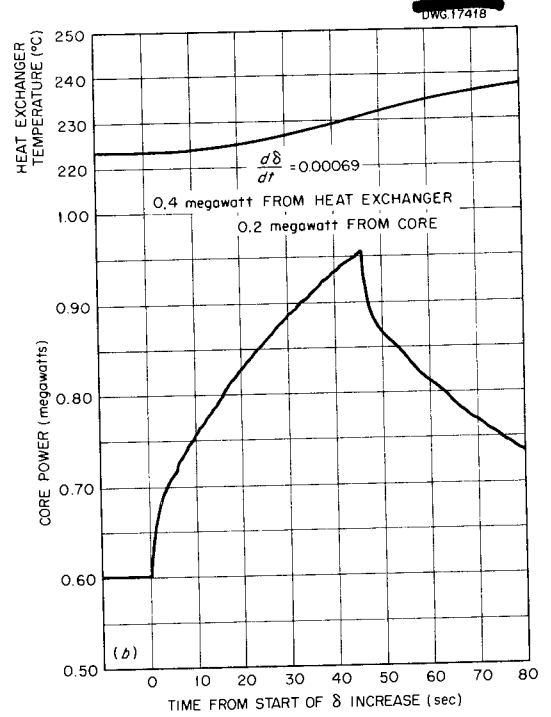
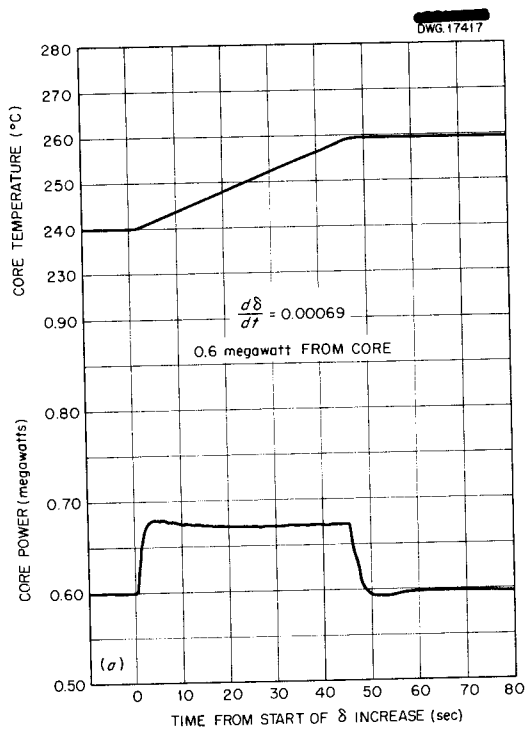


Fig. 1. Power and Temperature Response of the HRE Simulator of Constant  $\partial\delta/\partial t [k_{eff} - 1 = \delta + \alpha (\theta - \theta_0)]$ .

reactor steadily with a larger than normal gas vortex which is then collapsed by opening wide the let-down valve. It should be pointed out that neither of these situations is anticipated for normal operation of the HRE, but they should be considered as part of the test program on the kinetic behavior of the reactor. The curves illustrate the uniform rise of core temperature with constant core power for the case where power is extracted directly from the core at a constant rate of 0.6 megawatt. This type of operation of the HRE is, of course, not normal but might be achieved by maintaining a constant difference in temperature between the core and heat exchanger.

For Figs. 1b and 1d, it was postulated that 0.2 megawatt was extracted directly from the core and 0.4 megawatt was taken directly from the heat exchanger. Heat conduction to the reflector of the HRE should produce a constant heat extraction from the core of 0.05 megawatt; however, because of limitations in the circuitry of the simulator, this value was set at 0.2 megawatt. The core temperature, not shown, behaves as before, but the core power continues to rise as long

as the driving force,  $\delta$ , is applied, since the rate of heat removal from the core is not constant but is proportional to the difference in temperatures between core and heat exchanger. The exponential portions of the curves have a period given by the ratio of the liquid mass in the heat exchanger, including coolant, to the mass flow rate in the fuel-circulating loop.

Estimates of power behavior, based on previous work,<sup>(3)</sup> in which delayed neutrons are neglected, yield, for constant heat extraction of 0.6 megawatt from the core and a rate of change of  $\delta$  of  $0.0048 \text{ sec}^{-1}$ , an oscillation with a peak power of 1.9 megawatts. This is compared with the steady value of 1.1 observed on the simulator, where a slight indication of a peak is apparent without any indication of oscillation.

Since the maximum rise in power for the four cases analyzed with the simulator is only 0.9 megawatt, no difficulty is anticipated should the assumed conditions materialize when the reactor is operating at high power levels.

<sup>(3)</sup> *Homogeneous Reactor Experiment Feasibility Report, ORNL-730, p. 76 (Aug. 15, 1950).*

**Part II**

**BOILING REACTOR RESEARCH**



## BOILING REACTOR RESEARCH

R. N. Lyon, Section Chief

### OVER-ALL PROGRAM CHANGE

During the past quarter the increased emphasis on the ISHR design has greatly reduced the design effort that could be placed on the boiling reactor program. As a result, construction of the Reactor Experiment Building has been postponed for at least one year, and the immediate objective of the program has changed from the construction of an operating experiment to the development of a mockup of the Teapot for more complete testing of alternate components.

Considerably more emphasis is now being placed on a study of solution stability in boiling reactors, since this may become a controlling problem in high-pressure boiling reactor operation.

### BUILDING DESIGN

J. R. McWherter	R. L. Cauble
R. E. Aven <sup>(1)</sup>	A. R. Eckels
J. B. Brown	P. N. Haubenreich <sup>(1)</sup>
C. W. Day <sup>(1)</sup>	W. Terry

A review of the building and shield design for the boiling reactor experiments was made in early October. At that time the following suggestions and decisions were made and have since been incorporated in the design.

1. The cells will be no less than 8 ft in any dimension.
2. No underwater storage pool will be provided in the building.
3. Permanent facilities will be provided in the building for preparing and handling solutions.
4. The control room will be located on the south side of the building and adjacent to the service room so that access from the two rooms to the reactor cells can be through a common service tunnel.

<sup>(1)</sup>Part time.

5. A layout of the present HRE reactor system in the proposed cells will be made to establish the flexibility of the shield.

The building as now proposed is still similar to the HRE structure, and the underground shield (Fig. 2), which has a removable cover, is approximately 35 ft square and 30 ft deep. There are six cells that are separated by 3-ft-thick concrete walls to reduce induced activity in all but the cells surrounding the core cell. These walls will also permit flooding of the individual cells. A 10-ft-wide, open, operating gallery outside the east face of the shield permits access to unshielded equipment during operation.

In making the HRE layout in the boiling reactor shield, a 4-ft-dia core in a 6-ft-dia reflector vessel was used for comparison with the proposed 6-ft-dia boiling reactor experiment. All other equipment was scaled up from HRE size to accommodate the increased core volume at 2-megawatt operation. The blown-up HRE system fitted well in the shield, with ample room for maintenance.

Shielding calculations<sup>(2)</sup> have been made for the proposed experiments. Approximately 6½ ft of barytes concrete or 13 ft of ordinary concrete would be required to shield the proposed experiments. The relatively poor shielding provided by ordinary concrete is due to the high-energy (7.63 Mev) capture gammas from the iron in the reactor vessel. Figures 3 and 4 give the attenuation of the primary and total gamma radiation from the reactors through barytes and ordinary concrete shielding. If a safety margin of 6 in. is allowed, the fast-neutron

<sup>(2)</sup>R. E. Aven, A. R. Eckels, and P. N. Haubenreich, *Some Calculations for the Boiling Reactor Shield*, ORNL-CF-52-12-118.

# HRP QUARTERLY PROGRESS REPORT

DWG.17812

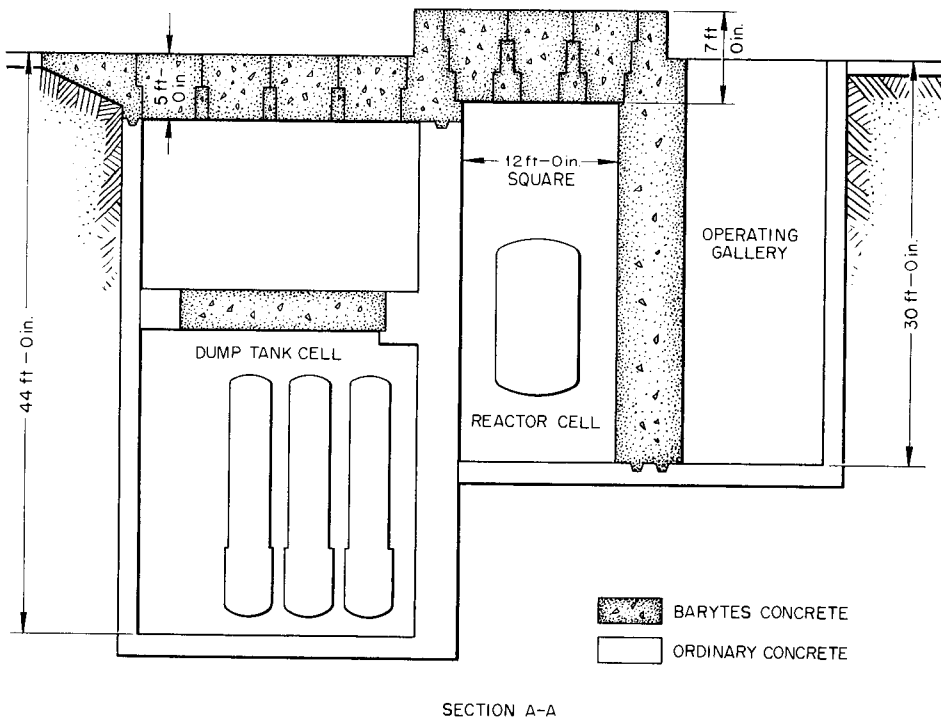
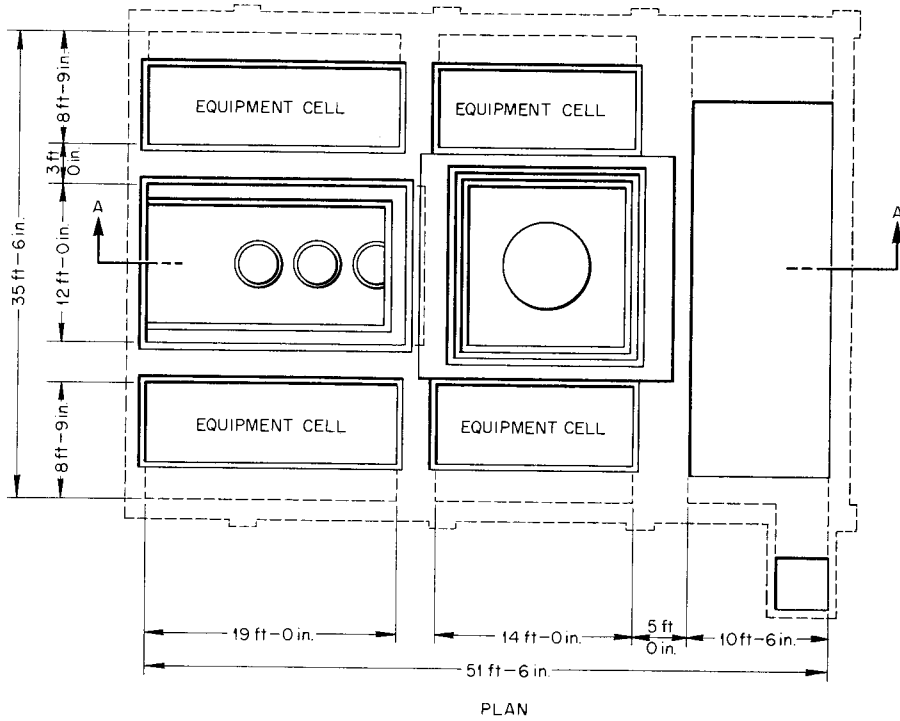
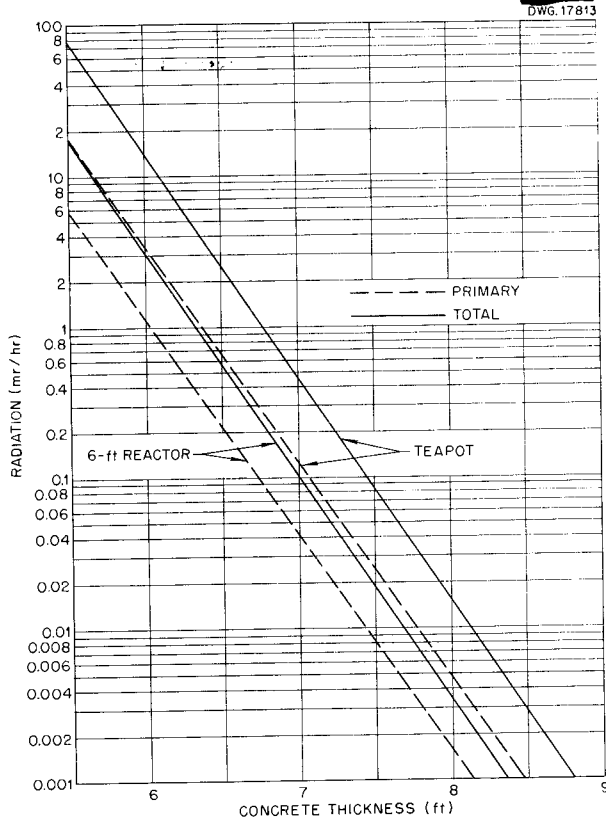


Fig. 2. BRE Shield Proposal.



**Fig. 3. Gamma Radiation Through Top Shield Plug of Barytes Concrete.**

current at the outside of the 7 ft of barytes concrete would be  $0.0237$  neutrons/cm<sup>2</sup>.sec. Beyond the  $13\frac{1}{2}$  ft of ordinary concrete, the neutron current would be less than  $10^{-5}$  neutrons/cm<sup>2</sup>.sec.

A report has been written on the shield proposal and will be issued in the near future.

**TEAPOT DESIGN**

R. L. Cauble      J. R. McWherter

Along with the building postponement, the Teapot experiment will be delayed until additional studies of components and characteristics of a Teapot mockup can be made.

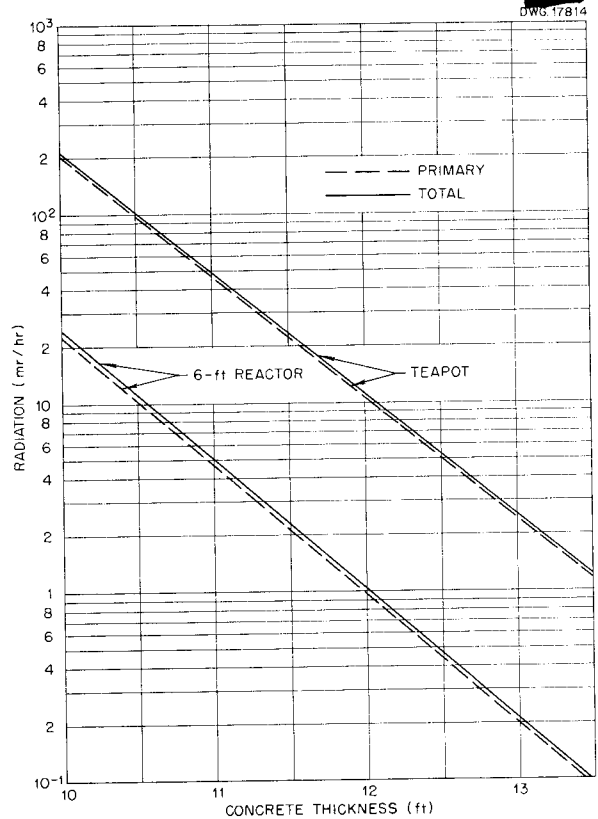


**Fig. 4. Gamma Radiation Through Top Shield Plug of Ordinary Concrete.**

Present plans call for construction of a mockup in the northeast corner of the main experimental area of Building 9204-1. The initial setup will be designed to use available 150-psi building steam, which will be fed directly to the core tank and condensed. This will give information on the operation of the main condenser, the various feed proposals, and the after condenser. At a later date, a high-pressure core tank will be installed, and electric heat will be used to operate the system at 600 psi for additional studies. The recombiner can be tested either by hydrogen and oxygen supplied from outside the core or by electrolytic generation of the gases directly in the core. A piping drawing of the proposed experiment is shown in Fig. 5.

# HRP QUARTERLY PROGRESS REPORT

DWG. 17815

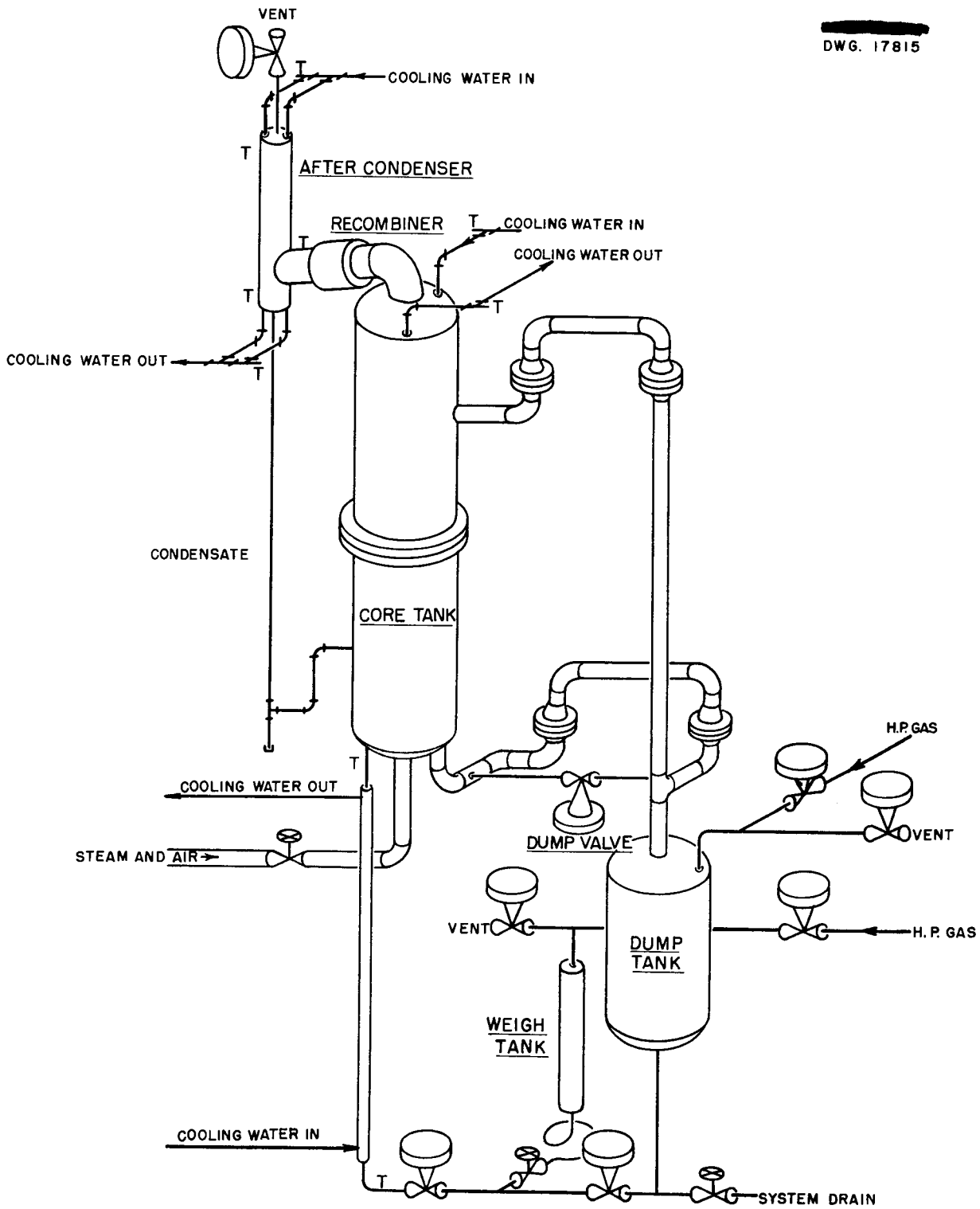


Fig. 5. Teapot Mockup.

STABILITY OF BOILING  $UO_2SO_4$  SOLUTIONS

C. G. Lawson

It has definitely been established by the HRP corrosion groups that unless an oxidizing condition is maintained in high-temperature uranyl sulfate solution in contact with metals such as stainless steel, some of the uranium is reduced and precipitates as  $UO_2$  or  $U_3O_8$ . In this reaction, the pH of the remaining solution is reduced, and the tendency toward further reduction and precipitation of the uranium is increased. In the present HRE, oxygen gas is dissolved in the solution and is effective in preventing reduction of the uranium, but in a boiling reactor system, it would be extremely difficult to dissolve more than a few parts per million of oxygen in the system because of the stripping action of the steam. Some oxygen is produced in the solution by decomposition of the water, but it is not clear whether this will be sufficient to prevent reduction of the uranium.

The first problem is to determine the minimum oxygen content required for solution stability. An experimental apparatus to study this problem is being designed. It is expected that the design will be completed and submitted for fabrication during the coming quarter. The apparatus will permit control of the bomb temperature, the power density in the bomb solution, and the pressure and oxygen concentration within the bomb. The apparatus is to be constructed of type 347 stainless steel.

In solution stability experiments it would, in general, be desirable to have a high-temperature and high-pressure electrode system that would determine a change in solution condition. In connection with this problem, some time has been spent with M. H. Lietzke of the Chemistry Division in studying the feasibility of such a system. This work will be reported in detail in the Chemistry Division

quarterly progress report for the period ending December 31, 1952.

NUCLEAR STABILITY STUDIES

P. R. Kasten

To supplement the knowledge that the Los Alamos Supo and the LITR can both be boiled safely, it would be desirable to know how rapidly changes in the density of the liquid will compensate for suddenly impressed changes in reactivity. Two methods of investigating this question with boiling homogeneous reactors have been studied. Both methods involve adding reactivity in a known manner and observing the resultant neutron-flux variation; the difference between the methods lies in the time variation of reactivity additions and the manner of interpreting the data. In the first method, a sudden reactivity change is made by quickly removing or inserting an absorbing rod in the core region. The reactor stability can then be determined by combining the imposed reactivity change with the resultant neutron-flux variations. In the second method, the core reactivity is varied continuously by means of an oscillating poison rod. From the resultant flux changes, the phase lag between input reactivity and output flux can be determined. Association of this phase lag with the power coefficient of reactivity leads to an evaluation of the reactor stability.

The better method to use depends upon the accuracy desired and to a lesser degree upon the ease of fabrication, installation, and operation of the required apparatus. Both the above methods are complicated by the erratic "steady-state" operation of boiling reactors, which results in flux deviations of  $\pm 20\%$  about the average value. These deviations are undoubtedly due to the transient condition of the fluid density at any particular point within the reactor. Because of these

## HRP QUARTERLY PROGRESS REPORT

flux deviations, the first method seems preferable.

In order to obtain rapid reactivity increases that will over-ride any natural flux deviations, a mechanism has been developed at KAPL that will provide a 3-g acceleration to a control rod, the distance of rod travel being limited to about 25 inches. This rod mechanism can be obtained as an integral unit, and one unit has been ordered for use in stability experiments. Present plans are to perform the first boiling reactor stability experiments on the Los Alamos Water Boiler in cooperation with L. D. P. King and his staff.

### BUBBLE NUCLEATION BY FISSION FRAGMENTS

R. J. Goldstein

An experiment is in progress to attempt to resolve an apparent conflict between data on the rate of bubble initiation in nuclear reactors and the data on bubble formation outside of nuclear reactors.

Experiences at Los Alamos<sup>(3)</sup> and Hanford<sup>(4)</sup> indicate that bubbles will form almost instantly in chain reacting water solutions at atmospheric pressure in a reactor, whereas results at UCLA<sup>(5)</sup> indicate that in the absence of radiation, about 250 msec elapse before the appearance of heat in the form of vapor in a boiling solution. In addition, the experiments made by Ghormley (cf., "Related Basic Chemistry Research," this report) show that considerable superheat is required before fission recoils will form stable bubble nuclei.

In the experiment now under way, hydrogen gas is bubbled through a sample of uranyl sulfate solution at known pressure and temperature. After

(3) L. D. P. King, private communication.

(4) B. R. Leonard, Jr., *A Study of the Radiation Burst in the Hanford Homogeneous Reactor*, HW-24327 (May 2, 1952).

(5) Private communications, W. L. Martin to C. E. Winters et al.

a sufficient period of time has passed to ensure saturation, the liquid is allowed to fill a small capillary. The pressure on the liquid is then reduced to get the desired superheat and supersaturation; all the events take place at constant temperature. The sample may then be irradiated by neutrons and any macroscopic bubbles formed can be observed.

It is believed that gas bubble nuclei may be produced by fission recoils in a liquid supersaturated with gas. These bubbles are probably quite small unless the liquid is very highly supersaturated. However, if the liquid is also superheated, the gas bubble may form a nucleus for a vapor bubble.

### POWER REMOVAL FROM VOLUME BOILING SYSTEMS

P. C. Zmola            H. A. MacColl  
W. S. Brown           M. Richardson

In the last quarterly report,<sup>(6)</sup> the general problem of power removal from boiling homogeneous reactors was reviewed. These considerations indicated that two problems for which experimental evidence is required in order to test the realism of the analytical work are:

1. For large boiling reactors having a free surface, will internal circulation materially improve vapor removal for a given mean fluid density, and can internal circulation be maintained by natural convection?

2. What are the growth rate and the drag coefficient of bubbles formed in a simple volume boiling system, and what power density can be maintained as a function of mean fluid density in such a system?

Information on the first problem will permit evaluation of the possible operating modes of a large reactor; that is, it will permit a determination

(6) R. V. Bailey, E. N. Lawson, H. A. MacColl, and P. C. Zmola, *HRP Quar. Prog. Rep. Oct. 1, 1952*, ORNL-1424, p. 14-20.

of whether steam separation devices or forced circulation will be necessary to obtain satisfactory power densities from large reactors. Information on the second problem would apply to small systems, such as the Teapot, in which power removal depends only upon bubble growth and natural rise. This information would be particularly helpful in interpreting experimental results obtained from a small boiling reactor.

Two experiments have been designed to obtain at least semiquantitative information on each of the above problems. Apparatus for both experiments is being constructed.

To obtain information on large-scale systems, a vertical, 6-ft-dia tank 12 ft high and open at the top is being set up so that it can be filled with water to some initial height and air can be bubbled through canvas sheeting on the tank bottom to simulate a boiling system. Fluid mean density values will be obtained from liquid level measurements, and the air throughput will be measured by means of an orifice meter. The objectives of the experiment are:

1. to determine air throughput as a function of mean fluid density,
2. to determine the influence of internal circulation on the mean density for a given air throughput,
3. to determine whether natural internal circulation can be established or maintained in this geometry.

To achieve the second objective, the air-water mixture will be forced into circulation by propeller mixers. To achieve the third objective, the canvas sheeting will be painted over part of its area so that a number of bubble distributions can be tested. The apparatus can be easily adapted to further simple experiments.

Although the results will not be directly applicable to vapor-liquid mixtures, it appears that this study can yield information on the behavior of large-scale, two-phase systems.

The apparatus for the small-scale experiment has a test section 4 ft high and 6 in. square in which a dilute acid or salt solution can be boiled by electrical-resistance heating of the liquid. The electrodes form two sides of the test section; the other sides are of Lucite. Vapor leaving the top of the test section is condensed and returned to the test section at the bottom. The temperature difference between the boiling liquid and the vapor above it will be measured by a differential thermocouple. Operation will be at atmospheric pressure. Mean fluid density values will be determined from measurements of the liquid level. Motion pictures will be taken at sufficiently high speed to obtain measurements of growth and rise rates of a number of individual bubbles. Rough maps of bubble population can also be obtained from the motion-picture photographs. The objectives of the experiment are:

1. to determine mean fluid density as a function of power input for a small system of simple geometry,
2. to obtain the heat transferred to a bubble and the drag coefficient for a bubble as characterized by bubble growth and rise rates,
3. to determine the contribution of surface evaporation to heat removed from a volume boiling system with a free surface.

#### UNSTEADY-STATE VAPOR REMOVAL TESTS

W. S. Brown

In addition to the program listed above, an experiment is in progress to determine the amount of entrained liquid in vapor from a boiling liquid at various power densities and liquid levels. Water is heated in a closed container up to pressures of 2000 psia. At the desired pressure, the pressure is released and the steam is allowed to escape through a small orifice. The temperature downstream from the orifice and the pressure in the container are recorded. By making a heat

## HRP QUARTERLY PROGRESS REPORT

balance on the container, it is possible to determine the power density. The amount of entrained liquid in the vapor will be determined by making use of the principle of a throttling calorimeter.

Several test runs have been made, and the equipment is presently being modified to make better temperature measurements possible.

### RESPONSE OF A BOILING HOMOGENEOUS REACTOR TO CHANGES IN STEAM DEMAND

P. R. Kasten

The characteristics of a boiling reactor system operating under variable power demand conditions have been investigated. In general, if no special provisions are made, only under very special conditions will it be possible to operate under power demand control. Addition of a system control will allow the reactor to meet various power demands.

In this study it was assumed that the reactor will always be just critical and that the over-all density of the reactor fluid is the primary factor in determining reactor criticality. Also, the heat energy produced by the reactor core was considered as

$$P = \frac{h_{fg} \rho_v f_v V_r}{t_{avg}}, \quad (1)$$

where

$P$  = reactor power,

$h_{fg}$  = latent heat of vaporization of liquid,

$\rho_v$  = density of generated vapor,

$f_v$  = average vapor fraction within reactor core region,

$V_r$  = volume of reactor fluid (liquid plus vapor),

$t_{avg}$  = average time vapor remains within the core region.

Under the assumptions of this study,  $V_r$  is constant regardless of temperature, pressure, or power level. In addition,  $t_{avg}$  is assumed to be constant. With reference to some steady-state power,  $P_0$ ,

$$\frac{P}{P_0} = \frac{h_{fg} \rho_v f_v}{(h_{fg} \rho_v f_v)_0}. \quad (2)$$

For a given average fluid density,  $f_v$  and  $h_{fg} \rho_v$  will be functions of pressure, as determined from the thermodynamic relations of the fluid.  $P/P_0$  is therefore a function of pressure alone. In Fig. 6 are some typical  $P/P_0$  vs. pressure curves for various initial pressures and vapor fractions within the core region. It is emphasized that for each curve the value of  $f_v$  will decrease with pressure from that of  $(f_v)_0$  to zero, at which point no power is produced. In Fig. 7, the plot of relative heat content per cubic foot of vapor vs. pressure reveals that the total reactor power always increases with pressure at a given vapor fraction.

From Fig. 6 it is noted that to obtain large negative power changes in response to small positive pressure changes, operation should be confined to a small vapor fraction within the core and to low pressures.

To determine whether there is any range of a particular  $P/P_0$  vs.  $p$  curve that is more favorable than another for power demand operation of boiling reactors, the reactor system shown in Fig. 8 was studied. In this system, the generated steam is used to drive a turbine that converts heat energy into shaft power. The power demand therefore controls the rate at which steam is required by the turbine. An increase in demand power will therefore lower the pressure within the reactor steam chest, whereas a decrease in demand power will increase the pressure. The reactor should therefore produce more power as the pressure decreases and less power as the pressure increases; also, the pressure range necessary to follow reasonable power demands should be small enough that the turbine efficiency would not be greatly affected. This dictates

UNCLASSIFIED  
DWG. 17816

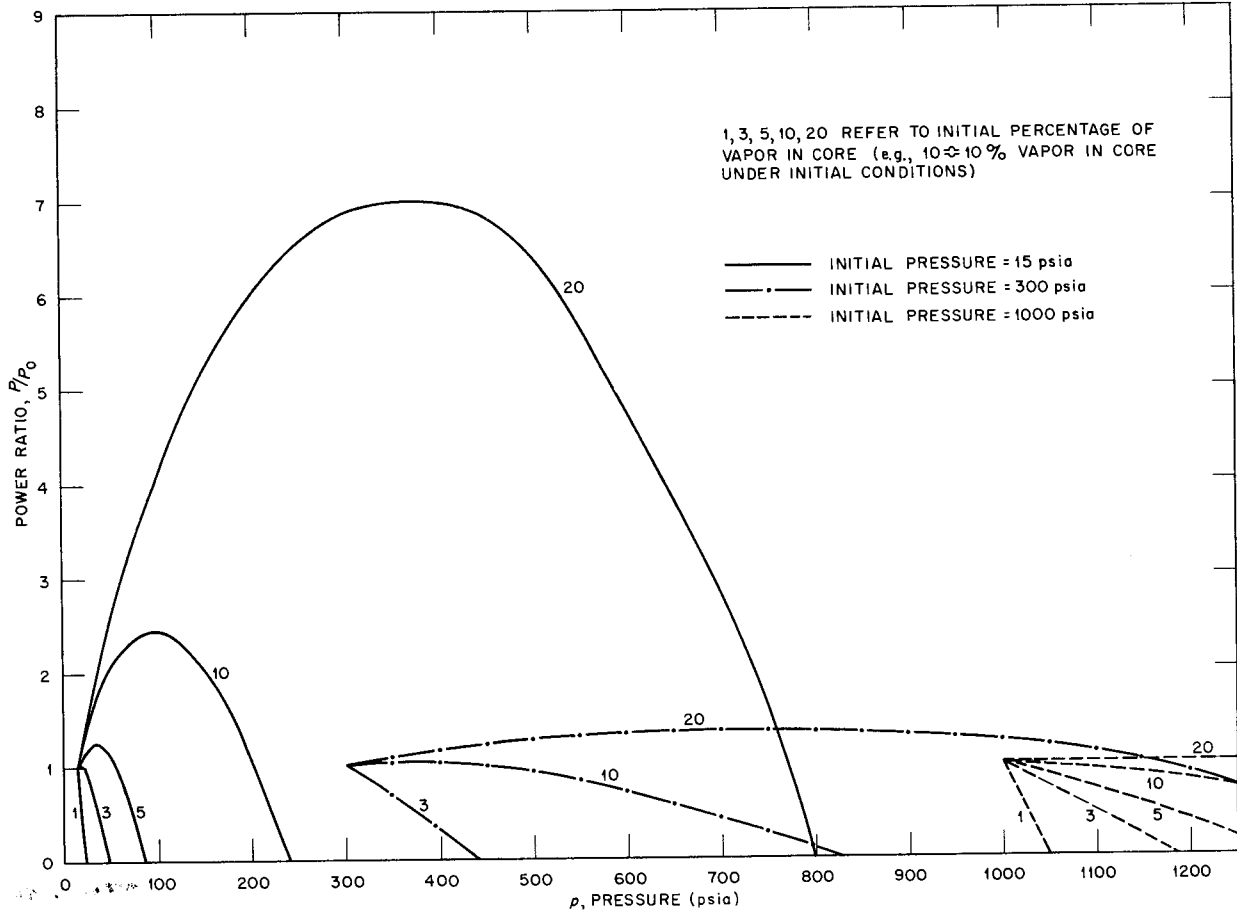


Fig. 6. Power Ratio vs. Operating Pressure for Various Initial Vapor Fractions.

reactor operation over that portion of the  $P/P_0$  vs.  $p$  curves that has a highly negative slope. This limits  $f_v$  to such an extent as to make operation under these conditions impractical.

To operate at higher  $f_v$ , it is necessary to install a system that will control the reactor power level as a function of power demand. Several such control systems are feasible. For example, if the reactor core is connected to a fuel reservoir that is held at constant pressure, an increase in the pressure of the reactor will force fuel into the reservoir

and reduce the permissible  $f_v$ , and hence the power production at the just-critical condition.

Another proposal is to control the turbine by dumping a portion of the steam directly to a condenser instead of throttling the steam flow to the turbine. It is conceivable that a direct control arrangement could be made between the turbine governor and control rods or the solution supply system, so that small variations in reactivity would be made to maintain the desired power output. In future studies, some of these possible control systems will be investigated.

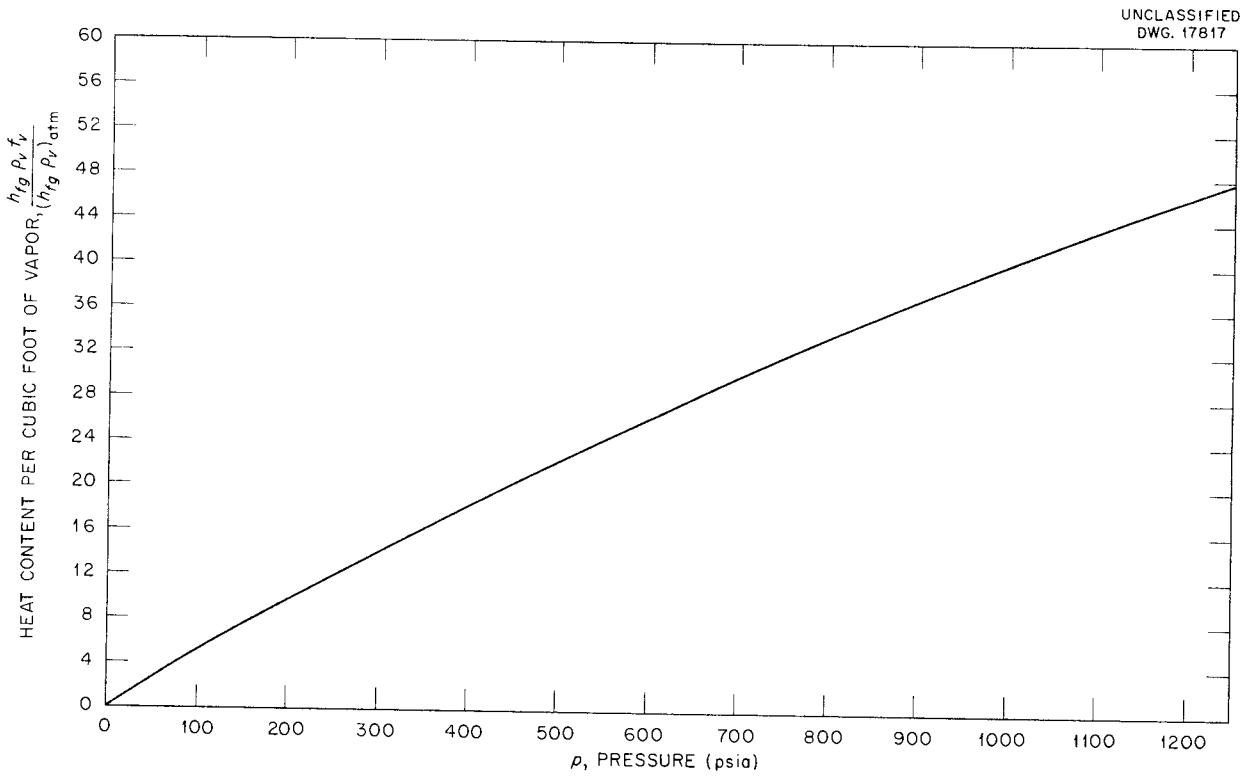


**Fig. 7. Variation with Pressure of Heat Content Per Cubic Foot of Vapor.**

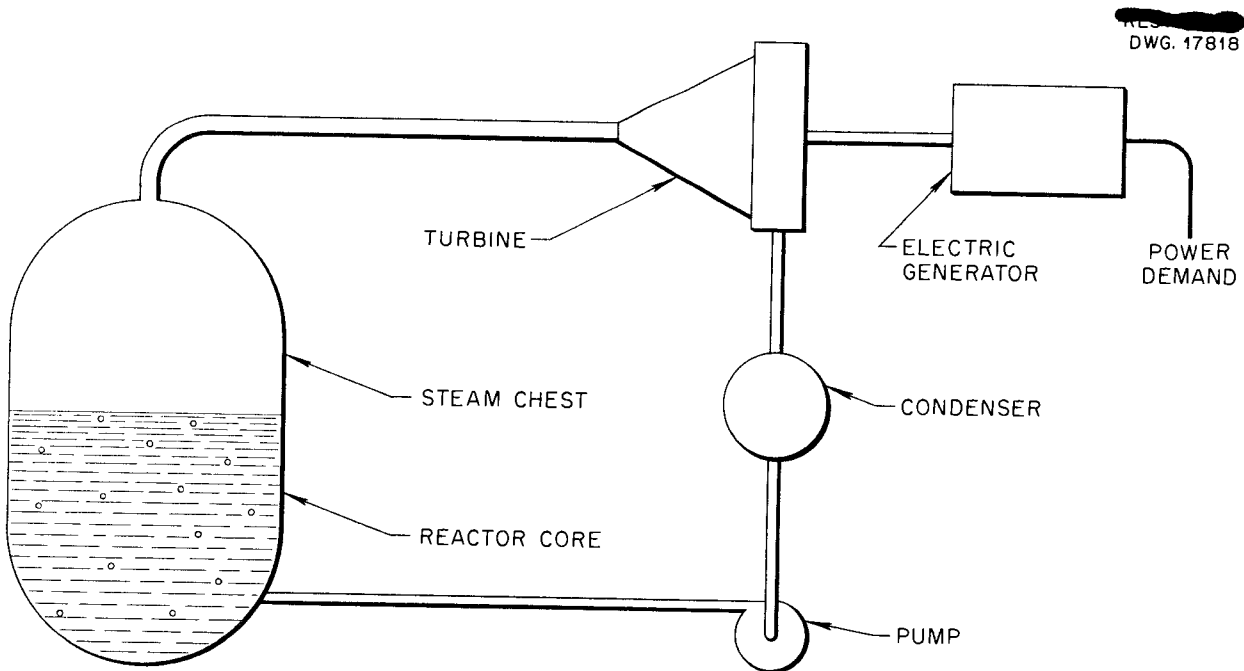


**Fig. 8. Schematic Diagram of a Boiling Reactor System for Producing Power.**

**Part III**

**GENERAL HOMOGENEOUS REACTOR STUDIES**



## INTERMEDIATE-SCALE HOMOGENEOUS REACTOR DESIGN

R. B. Briggs, Section Chief

W. R. Gall	J. D. Maloney	R. E. Aven
C. L. Segaser	W. L. DeRieux	L. Cooper
F. C. Zapp	P. N. Haubenreich	R. C. Robertson
R. H. Chapman	M. Tobias	W. Terry
D. K. Taylor	C. H. Barkelew	J. P. Sanders

In previous reports,<sup>(1,2,3)</sup> the design studies for an intermediate-scale, homogeneous, plutonium and power producing reactor have been discussed. In ORNL-1424,<sup>(3)</sup> some preliminary design data for a two-region reactor were introduced. Several alternate core designs were presented, along with a stress analysis of the core vessel and estimates of criticality and neutron balance for eight separate conversion arrangements. It was suggested that a dilute solution (approx. 5 g of uranium per liter) of  $\text{UO}_2\text{SO}_4$  in  $\text{D}_2\text{O}$  be used as the fuel in the core and that the blanket contain either thorium for producing  $\text{U}^{233}$  or lithium for making tritium. Operating conditions were to be  $250^\circ\text{C}$  and 1000 psi in both the core and the blanket. Type 347 stainless steel was chosen as the construction material.

The major interest of the Homogeneous Reactor Project is now focussed on the development of this type of reactor for converting thorium into  $\text{U}^{233}$ . The design has been extended to include more details, many of which are identical with those originally proposed for the plutonium and power producing reactor. The developmental work on the blanket system has been only preliminary, and the design is very indefinite at present. Most of the work reported here has been on the fuel system, which is similar to that of the plutonium and power producing reactor.

(1) R. B. Briggs et al., *HRP Quar. Prog. Rep.* Mar. 15, 1952, ORNL-1280, p. 113 ff.

(2) R. B. Briggs et al., *HRP Quar. Prog. Rep.* July 1, 1952, ORNL-1318, p. 95 ff.

(3) R. B. Briggs et al., *HRP Quar. Prog. Rep.* Oct 1, 1952, ORNL-1424, p. 43 ff.

### FUEL SYSTEM FLOW SHEET

Figure 9 is a preliminary flow sheet of the fuel system. It differs from that given previously<sup>(2)</sup> for the plutonium and power producing reactor in the following ways:

1. There is no core by-pass line in the main circulating loop.
2. A condenser, or "steam killer," is used instead of the turbine-condenser previously shown.
3. The fuel feed system is vented separately and is independent of the other systems.
4. The pressures of the fuel and blanket gas systems are balanced against each other by means of two weighted check valves.
5. The condensate-storage and concentrate-storage tanks are independently vented to the gas-separator effluent gas line.
6. The high-pressure storage tank and the evaporator system operate at the same pressure.
7. No provision is made to return oxygen from the fission-product absorbers to the high-pressure system.
8. A dump line to the high-pressure storage tank is provided.
9. A low-pressure condenser has been added to the fuel-dump off-gas system.

The components of the system are discussed separately in the following paragraphs.

### DESIGN DATA

The principal design data are given in the following tabulation. Most of these data are tentative, but they form the present basis of design.

# HRP QUARTERLY PROGRESS REPORT

	CORE SYSTEM	BLANKET SYSTEM
Power level, megawatts	48	9.6
Fluid	UO <sub>2</sub> SO <sub>4</sub> -D <sub>2</sub> O solution	ThO <sub>2</sub> -D <sub>2</sub> O slurry
Concentration	4.8 g of U per liter	1000 g of Th per liter
Fuel enrichment	93.5% U <sup>235</sup>	
System pressure, psia	1000	1000
System temperature, °C	250	250
Vessel diameter, ft	4	8
Heat capacity at 250°C, Btu/lb·°F	1.15	0.60
Density at 250°C, g/cm <sup>3</sup>	0.89	1.65
Thermal conductivity, Btu/hr·ft <sup>2</sup> ·(°F/ft)	~0.35	
Viscosity, lb/ft·hr	0.29	36.3
Vapor pressure of D <sub>2</sub> O over fuel solution at 250°C, psia	576	
Heat of recombination of D <sub>2</sub> and O <sub>2</sub> , Btu/lb-mole	105,000	
Heat of vaporization of D <sub>2</sub> O at 250°C, Btu/lb-mole	13,300	
Nuclear constants at 250°C		
Per cent voids assumed	3	0
Fermi age, $\tau$ , cm <sup>2</sup>	208	186
Diffusion length squared, L <sup>2</sup> , cm <sup>2</sup>	238	85
Diffusion constant		
Fast, cm	1.714	1.4
Slow, cm	1.286	1.15
Thermal utilization, $f = \frac{\sum_a(U)}{\sum_a(\text{total})}$	0.993	
Infinite multiplication constant, $k_{\infty}$	2.10	
Thermal-neutron cross sections, cm <sup>-1</sup>		
$\sum_f$	0.0045	
$\sum_a$	0.0054	0.0135
$\sum_s$	0.348	0.370
Thermal-neutron flux, neutrons/cm <sup>2</sup> ·sec		
$\phi_{\text{avg}}$	$3.7 \times 10^{14}$	$1.2 \times 10^{13}$
$\phi_{\text{max}}$	$9.04 \times 10^{14}$	$1.1 \times 10^{14}$
Fast-neutron flux, neutrons/cm <sup>2</sup> ·sec		
$\phi_{\text{avg}}$	$3.8 \times 10^{14}$	$1.3 \times 10^{13}$
$\phi_{\text{max}}$	$8.8 \times 10^{14}$	$1.4 \times 10^{14}$
Fast-(resonance)-neutron cross section, cm <sup>-1</sup>		
$\sum_r$		0.00482
Neutron balance for initial operation		
Absorptions in core		
U <sup>235</sup>		0.00000
U <sup>238</sup>		0.00029
S		0.00082
D <sub>2</sub> O		0.0065

PERIOD ENDING JANUARY 1, 1953

Absorptions in blanket		
Th (resonance)		0.21
Th (thermal)		0.58
Absorptions in shell (1/4 in. thick)		0.31
Losses from leakage		
Fast neutrons		0.0073
Slow neutrons		<u>0.0087</u>
Total absorptions and losses		2.12
Conversion ratio, atoms U <sup>233</sup> produced per atoms U <sup>235</sup> consumed		0.79
Estimated volume of system, liters	3860	7550
Material of construction	Type 347 stainless steel	Type 347 stainless steel
Maximum fluid velocity, fps	22.3	12.3
Friction losses at 250°C, psi/100 ft of pipe	6.7	7.6
Estimated total loop pressure drop, psi	39	36
Pumping requirements		
Capacity, gpm	5000	1000
Type proposed	Canned rotor	Canned rotor
Estimated pump efficiency, %	57	57
Estimated power requirement, hp	197	37
Reactor vessel effective volume, liters	950	6540
Specific power in vessel, kw/liter	50.6	1.47
Shell thickness, in.	0.25	3.0
Flow rate of solution, lb/sec	620	230
Heat removed by solution, Btu/sec	43,700	9100
Temperature of fluid entering reactor, °F	421	416
Temperature of fluid leaving reactor, °F	482	482
Gas separator		
Type	Pipe-line centrifugal	Pipe-line centrifugal
Void volume, ft <sup>3</sup>	3.35	0.91
Length of void, ft	6.0	4.0
Diameter of void, ft	0.84	0.54
Axial velocity, fps	12	4.5
Inside diameter, in.	16.5	11.5
Heat exchangers		
Type	Two-pass, horizontal, shell-and-tube exchangers, with water and steam in shell	
Steam pressure, psia	215	215
Steam temperature, °F	388	388
Feedwater inlet temperature, °F	100	100
Steam generated, lb/sec	38.7	8.0

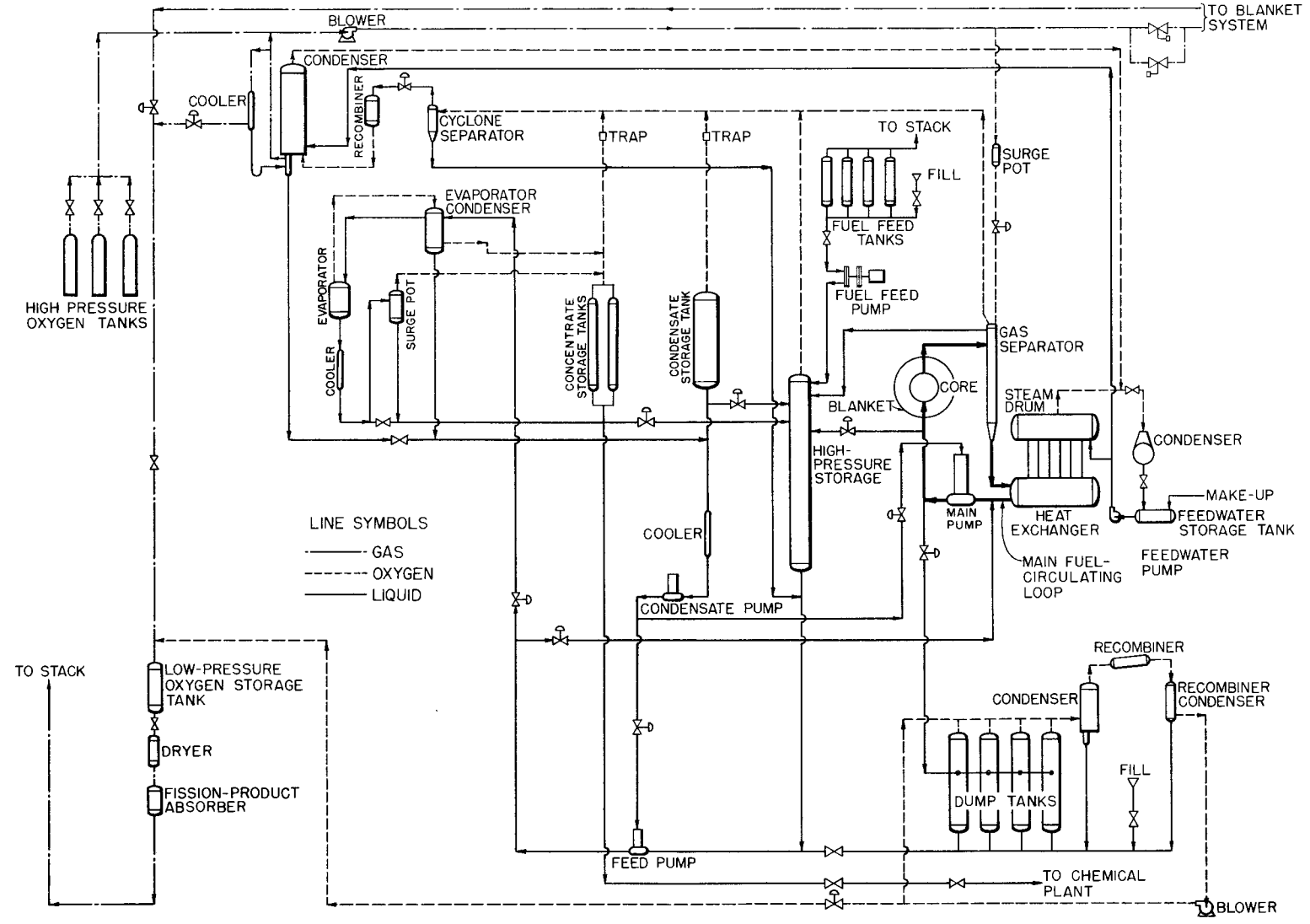


Fig. 9. Preliminary Flow Sheet of Fuel System for Intermediate-Scale, Two-Region, Homogeneous Converter.

**CORE VESSEL**

The design proposed for the core vessel is a modification of one given in ORNL-1424<sup>(4)</sup> and is presented here in Fig. 10. The design shown is for a reactor without a mechanical control element.

**HEAT EXCHANGER**

The results of a survey to obtain heat transfer data for the design of a heat exchanger for the ISHR were presented in ORNL-1424,<sup>(5)</sup> and the general design specifications for two design studies of vertical units were tabulated by using these data. It was shown that the coefficients for boiling heat transfer from horizontal tubes are substantially greater than those from vertical tubes for the same temperature difference between the metal surface and the boiling fluid. Preliminary layouts of the proposed equipment and shielding arrangement indicate that horizontal units may effect considerable saving in space, with resultant economy in construction. Hence, design studies have been completed for this type of unit.

Figure 11 is a schematic drawing of a unit that, apparently, is suitable as a steam generator for the ISHR. This unit consists of a vaporizer drum that contains the tube bundle and a steam drum connected to the vaporizer drum by a downcomer pipe and risers. The tube bundle contains a large number of U tubes attached to a single tube sheet so that the fuel solution enters and leaves the unit through the same header. Boiler water circulates by natural convection through the downcomer pipe to the bottom of the vaporizer drum. Heat is transferred to the water by nucleate boiling from the tube surface, and the resultant mixture of vapor and water rises to the upper steam drum at a rate determined by the difference between the

densities of the liquids in the vaporizer and in the downcomer pipe and the total resistance to flow through the unit. Steam is separated from the mixture in the upper steam drum by a simple baffle and dry-pipe arrangement, as shown.

If the feed were completely vaporized in the lower shell, it would emerge as a vapor and any dirt that was originally present would be left behind on the tube surface over which vaporization occurred. Since this exchanger will be very difficult to service, it is important that the design be such as to ensure adequate circulation to minimize excessive fouling of the tubes. Recirculation ratios equal to or in excess of 4:1 are required. Hence, the shells and piping of the unit are arranged to present a minimum of resistance to flow.

Table 2 presents the results of calculations of surface areas and pressure drops through the tubes of a horizontal evaporator with 1/2-in.-OD, 16-Ga (0.065-in. wall thickness) tubes and one with 3/8-in.-OD, 18-Ga (0.049-in. wall thickness) tubes. These tube-wall thicknesses were chosen to provide a corrosion allowance of 0.030 inch. The table shows that for equal pressure drop and flow rates the exchanger with 3/8-in. tubes will have less surface area and less holdup than the exchanger with 1/2-in. tubes. However, the 3/8-in. tubes will require many more connections to the tube sheet and there will be a greater possibility of leakage. Both tube bundles may be inserted in the same diameter shell.

An estimate has been made of the recirculation ratio that may be achieved with an exchanger similar to that shown in Fig. 11. For the estimate it was assumed that drum spacing was 16 ft, center to center. With this arrangement, the hydrostatic driving force of liquid in the cold leg was

<sup>(4)</sup> *Ibid.*, p. 54.

<sup>(5)</sup> *Ibid.*, p. 44-48.

DWG. 17787

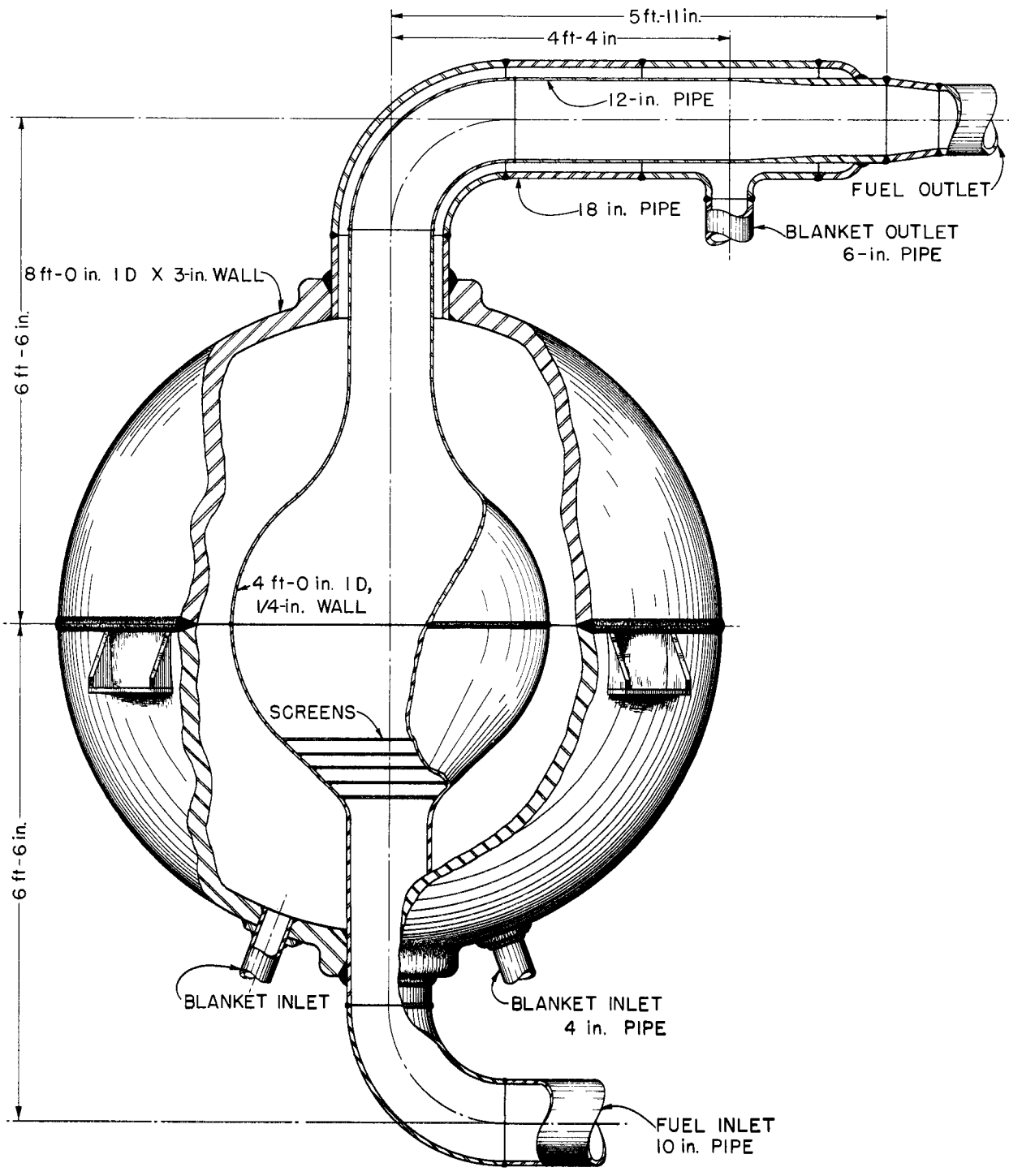


Fig. 10. Proposed Core Vessel Design for Intermediate-Scale, Two-Region, Homogeneous Converter.

DWG.17788

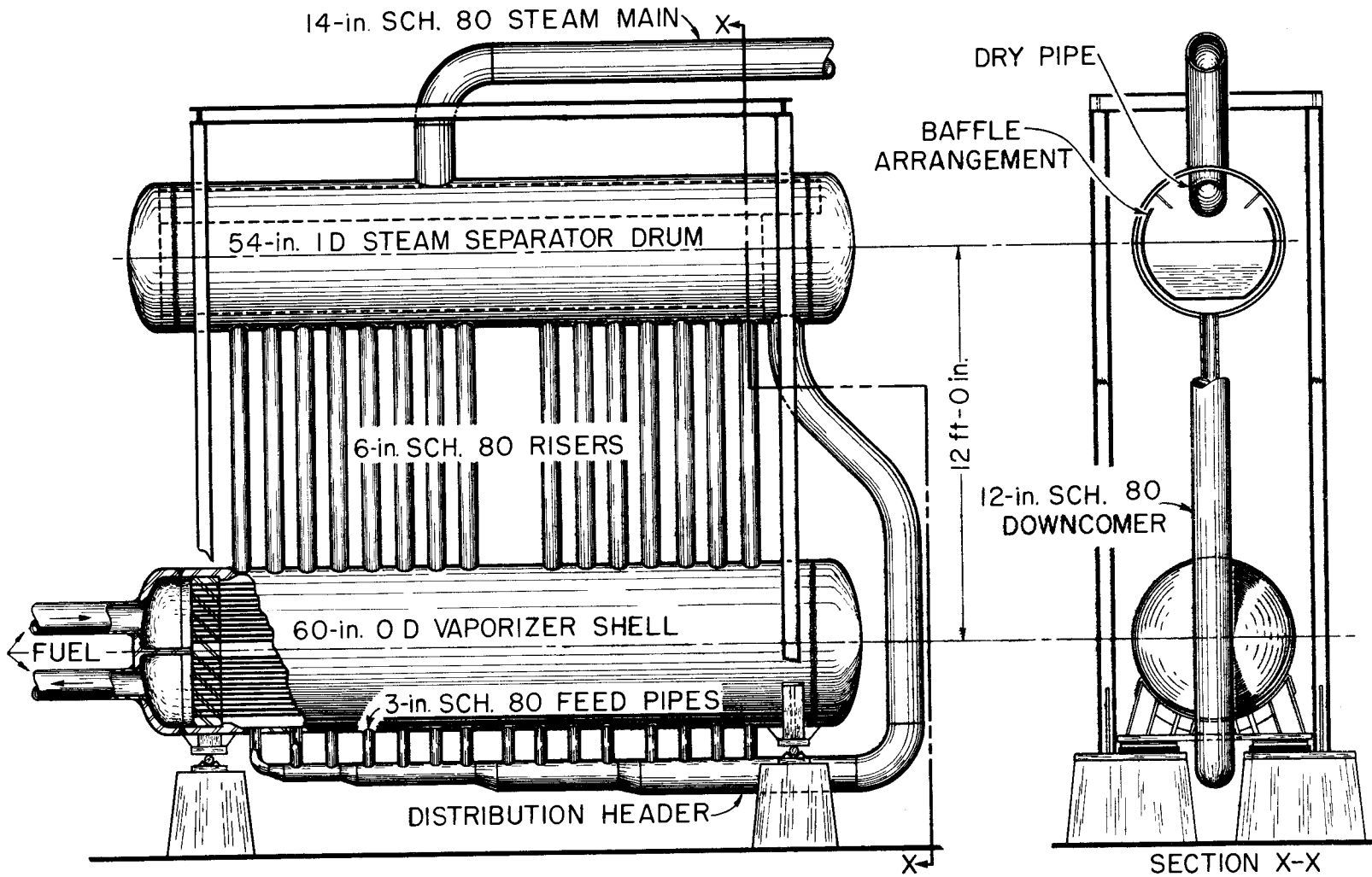


Fig. 11. Intermediate-Scale, Homogeneous-Reactor, 50-Megawatt Heat Exchanger.

PERIOD ENDING JANUARY 1, 1953

# HRP QUARTERLY PROGRESS REPORT

calculated to be 6.65 psi. The equilibrium recirculation ratio is attained when the sum of resistances in the vaporization circuit equals the hydrostatic driving force on the vaporizing fluid. Table 3 lists the estimated flow resistances in the system for circulation ratios of 4:1, 8:1, and 12:1. By plotting and extrapolating the results, the system was found to be capable of a recirculation ratio of greater than 20:1. This ratio is much higher than that needed for cleanliness.

The only requirement is that the resultant recirculation ratio shall be 4:1 or greater. Hence, the drum separation has been decreased to 12 ft, as shown in Fig. 11.

This design and several alternate designs were discussed with manufacturers of heat exchanger equipment. All designs submitted were considered to be practical, but a preference for the proposal of Fig. 11 was indicated, mainly because of the manufacturer's better background of commercial

**TABLE 2. COMPARISON OF SURFACE AREAS AND PRESSURE DROPS FOR 1/2-in., 16-Ga AND 3/8-in., 18-Ga STAINLESS STEEL TUBES**

TUBE DATA			FLOW RATE (fps)	NUMBER OF TUBES	AREA OF TUBES (ft <sup>2</sup> )	AVERAGE LENGTH OF TUBES (ft)	PRESSURE DROP (psi)	HOLDUP (ft <sup>3</sup> )
Outside Diameter (in.)	Wall							
	BW Gage	Thickness (in.)						
0.375	18	0.049	10	2650	5960	22.7	11	25.4
			12	2200	5810	26.6	18	24.8
0.500	16	0.065	10	1490	7140	36.0	13	40.0
			12	1230	6870	42.0	20	39.2

**TABLE 3. RESISTANCES IN CIRCULATORY SYSTEM OF HEAT EXCHANGER**

ELEMENT OF RESISTANCE	RESISTANCE (psi)		
	Recirculation Ratio		
	4:1	8:1	12:1
Pressure of leg in evaporator	0.263	0.388	0.487
Pressure of leg in vertical risers	0.177	0.310	0.432
Friction loss through 12-in. downcomer	0.126	0.406	0.842
Friction loss through 3-in. bottom nipples	0.010	0.033	0.068
Expansion loss through evaporator	0.002	0.007	0.007
Friction loss through evaporator shell	0.036	0.093	0.105
Friction loss through 6-in. risers	0.099	0.185	0.277
Total	0.713	1.322	2.218

experience. A single-drum design was also considered to be practical, although its performance would be somewhat more difficult to predict.

A memorandum discussing a preliminary single-drum design will be issued in the near future.

**GAS SEPARATOR**

In the present design proposal for the gas separator, Fig. 12, the liquid-gas mixture from the core enters the separator through a volute casing. The volute imparts a large tangential velocity component to the stream and causes the gas to move toward the void at the center of the separator. A mixture of oxygen and  $D_2O$  vapor is brought in through the central gas inlet pipe to the vortex void to dilute the gas from the core so that the gas leaving the separator will contain only about 2 mole % of deuterium. Greater percentages of  $D_2$  might present an explosion hazard and, also, might cause excessive temperatures in the recombiner.

Excess liquid is spilled over into the section immediately above the volute and is drawn off. The gases are withdrawn through a pipe annulus around the inlet gas pipe into the topmost section of the separator. In this section, baffles remove some of the entrained liquid. The gas then passes through the gas outlet to the cyclone separator, where the remaining liquid mist is removed.

At the bottom of the separator, a baffle is provided to define the length of the vortex void. Around this baffle is a set of straightening vanes to destroy the rotation of the liquid before it is discharged into the circulating line. The baffle and straightening vanes are placed in the concentric reducer at the bottom of the separator to provide, as nearly as possible, a constant cross section for the flow of the liquid as it passes from the separator into the circulating line.

DWG. 17789

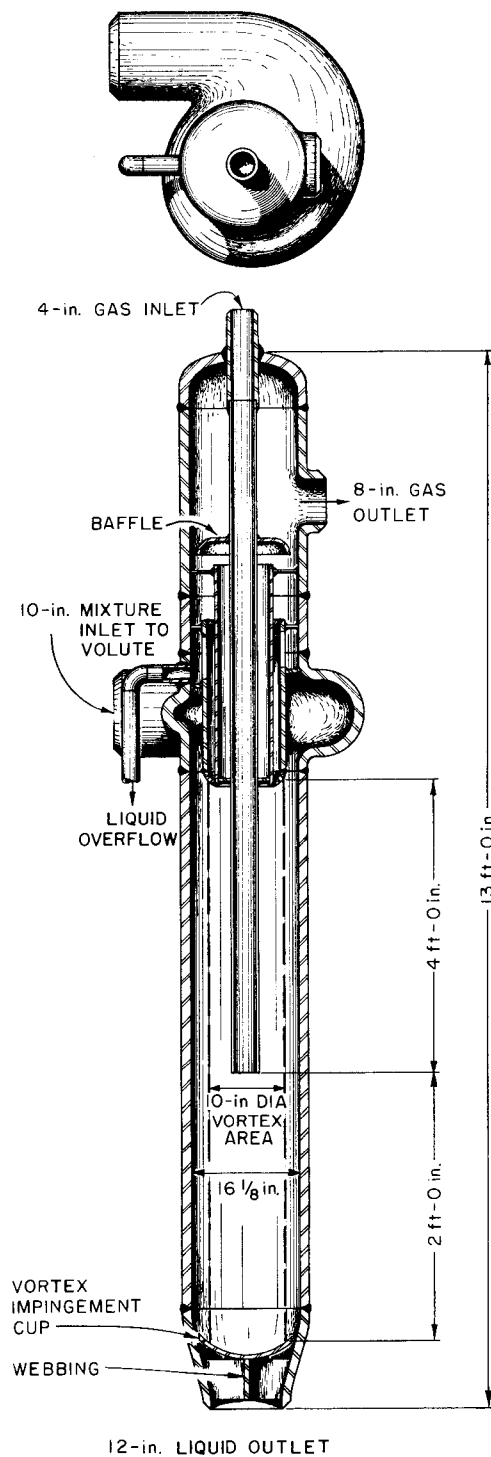


**Fig. 12. Intermediate-Scale, Homogeneous-Reactor, Gas Separator for 5000 gpm of Fuel.**

## HRP QUARTERLY PROGRESS REPORT

The static pressure and tangential velocity profiles of the liquid at the top of the vortex section of the separator are shown as a function of radius in Fig. 13. The assumptions involved are:<sup>(6)</sup>

1. A free vortex is formed; that is,

$$v_t(r) = \frac{R}{r} v_t(R) .$$

2. The axial velocity is given by

$$v_a(r) = j \left( \frac{R-r}{R} \right)^s ,$$

where  $s$  and  $j$  are constants.

3. The static pressure at any distance  $r$  from the center of the vortex is given by

$$\frac{dp(r)}{dr} = \frac{\rho [v_t(r)]^2}{r} .$$

4. The pressure in the circulating line where it enters the separator is 1000 psi.

By writing an energy and material balance between a point "1" in the liquid-gas mixture just before it enters the volute and a point "2" in the liquid just after it leaves the volute and solving for  $p(r_2)$ , the static pressure equation becomes

$$p(r_2) = -\frac{\rho [v_t(R)]^2}{2} \left( \frac{R}{r} \right)^2 + p_1 + \frac{\rho V^2}{4\pi^2 R^4} \left\{ \frac{\left[ \frac{1}{2s+1} - \frac{1}{2s+2} \right]}{\left[ \frac{1}{s+1} - \frac{1}{s+2} \right]^2} - \frac{1}{(1-X_2^2)(1-X_2)} \frac{\left[ \frac{1}{2s+1} - \frac{1-X_2}{2s+2} \right]}{\left[ \frac{1}{s+1} - \frac{1-X_2}{s+2} \right]^2} \right\} + \rho g [Z_1 - Z_2] - \frac{\rho \eta [v_t(R)]^2}{(1-X_2^2)} \ln \left( \frac{R}{r_v} \right) \dots , \quad (1)$$

where

- $v_t$  = tangential velocity of the liquid ( $LT^{-1}$ ),
- $v_a$  = axial velocity of the liquid ( $LT^{-1}$ ),

<sup>(6)</sup>J. O. Bradfute, *ISHR Gas Separator*, ORNL CF-52-5-235, p. 13 ff.

$Z$  = height of any point above a datum plane ( $L$ ),

$\rho$  = density of the liquid ( $ML^{-3}$ ),

$p$  = pressure at any point ( $ML^{-1}T^{-2}$ ),

$R$  = inside radius of separator ( $L$ ),

$r_v$  = radius of vortex void ( $L$ ),

$V$  = volumetric flow rate ( $L^3T^{-1}$ ),

$X = r_v/R$ ,

$\eta$  = proportionality constant = 0.2 for the vertical separator,

$v_t(R) = 20$  fps (assumed),

$s = 1/7$  (assumed).

For the fluid properties of the ISHR fuel solution, Eq. 1 reduces to

$$p(r_2) = 4.628 \times 10^6 - 11,100 \left( \frac{R}{r} \right)^2 ,$$

where  $p(r_2)$  has the units  $lb/ft \cdot sec^2$ .

So many assumptions are involved that the values shown in Fig. 13 should be considered as estimates until experimental data are available. Experiments are being performed by the development groups to study the feasibility of substituting rotational vanes for the volute casing. It is hoped that this will result in lower pressure drop and lower initial cost than with the volute type of separator.

### GAS PRODUCTION IN THE REACTOR CORE

Calculations of the gas production in the ISHR core, made by using a value for  $G$  of 1.67, show that 1.03 lb-moles of  $D_2$  and 0.51 lb-moles of  $O_2$  are formed each minute. Under the conditions of reactor operation, the

recombination rate of these two gases may be neglected. The D<sub>2</sub>O vapor contained in the evolved gas is 2.22 lb-moles per minute. The liquid-gas mixture leaving the core contains 4.9 vol % saturated gas.

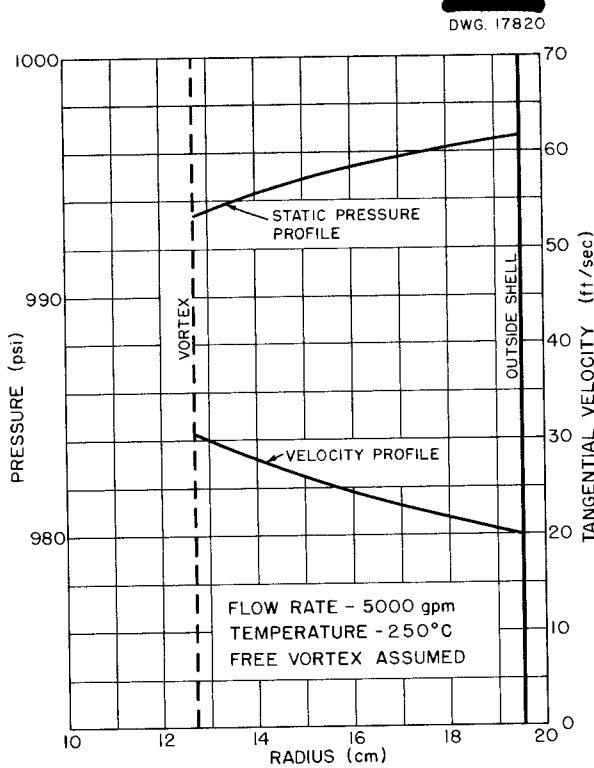


Fig. 13. Velocity and Pressure Profiles of Liquid in Separator.

In the gas separator, the gas from the core was assumed to be diluted with O<sub>2</sub> to about 2% D<sub>2</sub> content. The average total pressure in this unit is 990 psi, and the partial pressures of the components are 576 psi for D<sub>2</sub>O, 20 psi for D<sub>2</sub>, and 394 psi for O<sub>2</sub>.

The steady-state concentrations of dissolved gases in the liquid entering and leaving the core were calculated. It was assumed that the liquid leaving the core is in equilibrium with the gas in the bubbles and that all undissolved gases are separated in the gas separator. It was found that a small amount of O<sub>2</sub> is dissolved in the gas separator and that it is evolved in the core. The steady-state concentrations of dissolved gases, together with equilibrium concentrations, are given in Table 4.

The calculated flow rates and compositions in the core and gas separator are shown in Fig. 14.

RECOMBINER SYSTEM

Gas-vapor mixture from the gas separator goes through the cyclone separator for removal of entrained moisture before it passes through the catalytic recombiner. The gas stream then passes through the recombiner condenser for condensation of the D<sub>2</sub>O before being pumped back to the gas

TABLE 4. DISSOLVED GASES AT 250°C

	CONCENTRATION OF D <sub>2</sub> (lb-moles/lb-soln.)	CONCENTRATION OF O <sub>2</sub> (lb-moles/lb-soln.)
In equilibrium with a gas of partial pressure 282 psi D <sub>2</sub> + 142 psi O <sub>2</sub> + 576 psi D <sub>2</sub> O	4.95 × 10 <sup>-5</sup>	2.24 × 10 <sup>-5</sup>
In equilibrium with a gas of partial pressure 576 psi D <sub>2</sub> O + 20 psi D <sub>2</sub> + 394 psi O <sub>2</sub>	0.03 × 10 <sup>-5</sup>	6.77 × 10 <sup>-5</sup>
In liquid entering core	4.59 × 10 <sup>-5</sup>	2.40 × 10 <sup>-5</sup>
In liquid leaving core	4.60 × 10 <sup>-5</sup>	2.39 × 10 <sup>-5</sup>

# HRP QUARTERLY PROGRESS REPORT

DWG. 17821

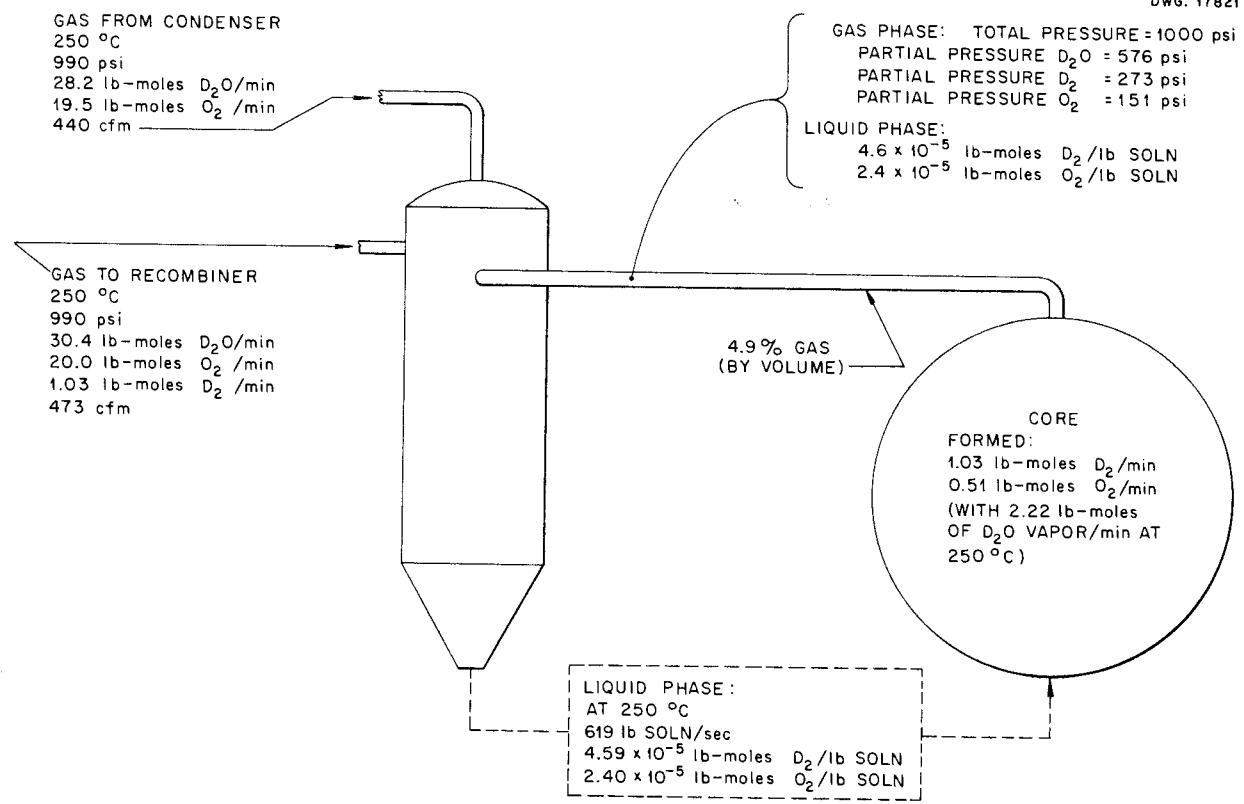


Fig. 14. Gas Production and Flow Rates in the ISHR.

separator. Condensate from the re-combiner condenser is drained to the condensate storage tank. Since this is a high-pressure condenser, the heat removed is used to generate steam, which goes into the main header from the steam drum. Details of equipment for this system have not been developed. If the use of a homogeneous catalyst in this reactor proves feasible, it should be possible to eliminate the recombiner system.

### EVAPORATOR SYSTEM

The canned-rotor pumps proposed for circulation of the fuel and blanket fluids require a flow of cool, distilled water into the motor end to provide satisfactory operating conditions for the bearings. In order to provide this flow without dilution of the fuel solution, an evaporator system is to

be provided for continuously distilling a small amount of solution. The condensate from this system will be supplied to the circulating-pump motor by a small, canned-rotor pump, such as the Westinghouse model 30-A. Components of the system are the evaporator, condenser, and the condensate-storage and concentrate-storage tanks. The details of the evaporator system have not been worked out.

### FUEL DUMP SYSTEM

The fuel dump system is necessary as a subcritical storage place for the fuel. It is intended that the dump tanks will be operated at atmospheric pressure during normal operation of the reactor so that fuel can be dumped in as short a time as practical. Thus, the losses from a leak in the high-pressure system can be minimized.

However, because of the high pressure drop, gas and vapor are released from the solution that is dumped; so a recombiner and a condenser are required. A blower is provided to circulate the gases through the recombiner and the condenser and to return the excess gas to the off-gas system. The problems to be solved are: selection of optimum line size, design of the dump valve, and design of the condenser, recombiner, and blower.

The dump tanks will be fabricated from 24-in. stainless steel pipe 26 ft long. They will contain sufficient boron in the form of boral-stainless steel sandwich plates to ensure non-criticality under all conditions. The volume thus provided, 272 ft<sup>3</sup>, is approximately twice the volume of the high-pressure fuel system.

#### FUEL FEED SYSTEM

With an operating core-fluid concentration of 5 g of uranium per liter and a feed concentration of 250 g of uranium per liter, the total required feed volume is 100 liters or 26.4 gallons. A pulsafeeder pump is proposed for pumping the concentrated feed solution, but a multistage centrifugal pump may be substituted. The maximum flow rate will be approximately 1 1/2 gpm, and therefore the feed could be added to the system in 18 minutes.

The tentative design calls for four, vertical, stainless steel vessels 8 ft long, made of 5-in. schedule-40 pipe and joined by 1 1/2-in. headers on both ends. A 1/2-in. vent line and a 1-in. fill line, with appropriate valving, will be connected to the top header. All pump-head lines are to be flanged and valved to permit removal with a minimum loss of time and effort.

Concentrated feed solution is pumped into the high-pressure storage tank that is mounted in the cell that contains the blanket system dump tanks. The feed tanks are located above the storage tanks, and the feed pump and

associated heads are located at the bottom of the cell or at an intermediate level.

#### CONTROL ROD CALCULATIONS

Studies have indicated that aqueous, homogeneous reactors should be operable without control rods. There may be occasions when a control element would be convenient, however, and the design of a rod is being studied for the ISHR. The primary function of the control rod would be to aid in startup and shutdown of the reactor.

The ISHR will operate normally at 250°C with about 3% voids in the core and the rod withdrawn. It is desired that the rod be sufficiently effective so that when it is fully inserted the reactor will be subcritical at any temperature above about 100°C. Two types of rod are being considered. The first is a pipe containing borated D<sub>2</sub>O. The second is a cylinder of absorber material through which fuel solution may flow freely. The required rod diameters have been calculated by two-group methods in which the reactor is treated as a bare cylinder with the same geometric buckling as the ISHR. The borated D<sub>2</sub>O rod is assumed to be a region with the same diffusion properties for fast neutrons as the core material but black to slow neutrons. Except for the source of fast neutrons in the fuel solution inside the cylinder, the two cases are essentially the same. Since the slow flux, and hence the fast-neutron source inside the cylinder, is small, there is actually very little difference in the effectiveness of the two schemes. This has been checked by a perturbation type of calculation, which indicates that the presence of fuel solution in the interior of the rod is equivalent to approximately 0.12% in reactivity. The calculated diameter for criticality at 100°C is about 9.5 in. in either case. It should be pointed out that there is some uncertainty in the

## HRP QUARTERLY PROGRESS REPORT

results because of the simplification of the geometry that may lead to an overestimate of the value of the rod.

### CONTROL ROD OPERATOR

An operator for the ISHR control rod needs to meet fewer requirements than those for most reactors. The rod will be in use only during startup and shutdown, and it will ordinarily be fully up or fully down. The rate at which the rod can be withdrawn must be limited, but precise positioning at intermediate points is not imperative. Therefore a hydraulically operated rod, such as shown in Fig. 15, is proposed for which only the completely up or down points are stable positions. It is intended that the differential pressure across the main circulating pump be used for supplying the effort necessary to move the piston. Because of the location of the reactor relative to the pump, a much larger force can be obtained for holding the rod in the up position than that which is available for lowering it. On the area of a 10-in.-dia piston, the force would amount to about 2500 lb up and 200 lb down. The lower downward force will be partly compensated by the weight of the control rod.

### STEAM SYSTEM

The design of the steam and condensate system for the ISHR will provide for the utilization of conventional equipment, and developmental work will not be required. A flow diagram of the steam system is shown in Fig. 16.

The steam generated in the steam drum may be used in a steam turbine to generate about 10,000 kw (at full power level), but during the initial stages of reactor operation a heat dumping condenser, or steam "killer," will be used. Installation of the relatively expensive turbine-generator and power condenser, although provided in the design, will be deferred until continuous operation is assured. The

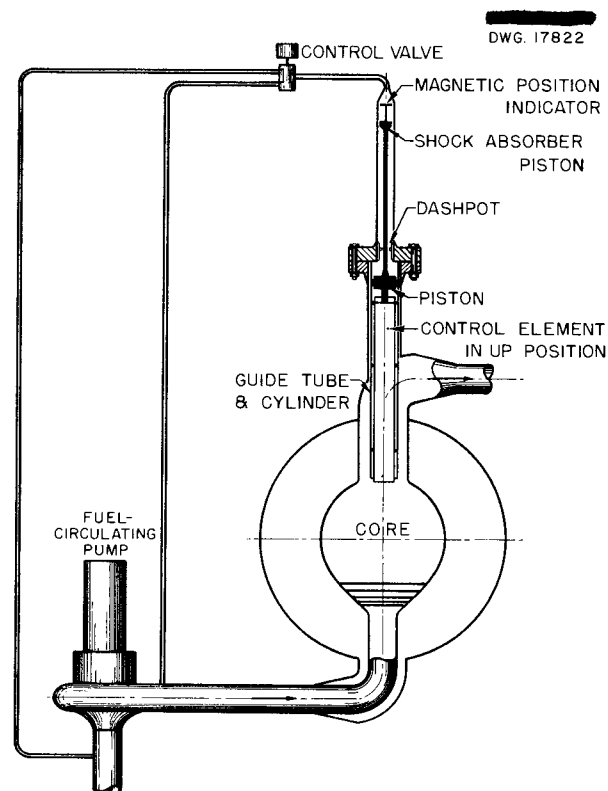


Fig. 15. Schematic Layout of Control Rod System.

steam and condensate systems will be designed with connections that are easily accessible for future connection of the steam turbine.

The steam pressure from the drum will vary from about 215 psia at full power output to over 400 psia at low output. Control of the steam flow to either the turbine or the steam-dumping condenser will be accomplished by employing a pressure reducing valve to maintain a constant 215 psia on the downstream side. Loss of availability of energy by this throttling during turbine operation is not great for turbine loadings over one half of rated output.

When heat is being dumped, a turbine load can be simulated by using a flow-control valve in the steam line to the dumping condenser. The steam piping from the drum to the future turbine

DWG. 17823

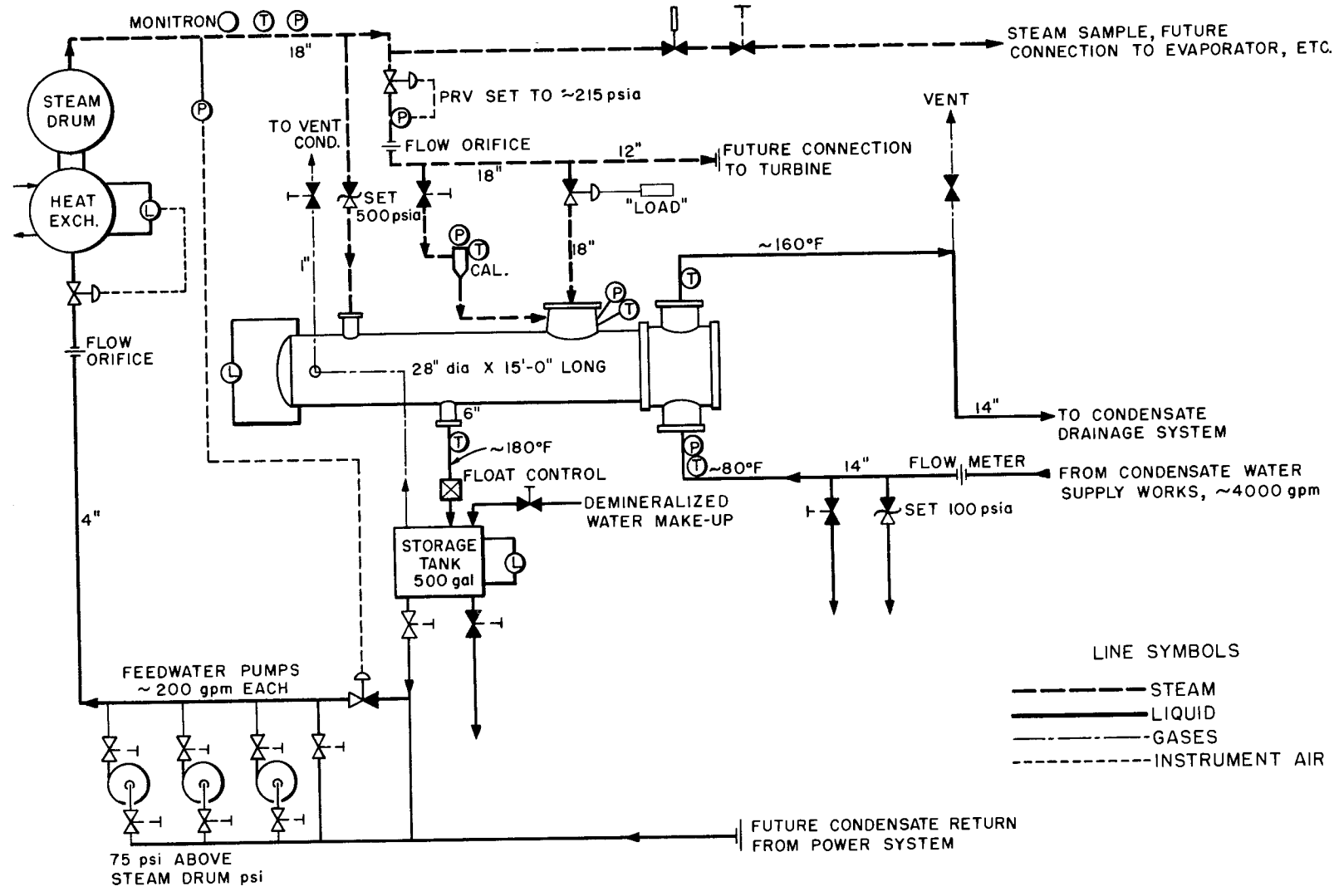


Fig. 16. Flow Diagram of Steam System for the ISHR.

PERIOD ENDING JANUARY 1, 1953

## HRP QUARTERLY PROGRESS REPORT

probably will be 12 in. in diameter, but from the drum to the dumping condenser it will be 18 in. in diameter to accommodate the large specific volume of steam at the low pressures that may be generated during initial phases of operation.

The steam-dumping condenser will be similar in most respects to the conventional U tube, horizontal, closed, feedwater heaters used in steam power plants. It can be obtained through adaptation of one of these units for about \$10,000 (not including fittings, piping, and foundations). The condensate will be drained to a storage tank, which will also receive the demineralized water from makeup and the drainage from the feedwater pump glands, etc.

The centrifugal feedwater pumps for returning the condensed steam to the steam drum can serve either the dumping condenser or the power condenser; they will probably consist of multiple units to supply a maximum requirement of about 400 gpm and be arranged to give standby protection, as well as stepwise capacity control. A flow-control valve in a by-pass around the pump will regulate pump-discharge pressure, and a level controller in the steam drum will regulate flow.

A supply of approximately 4000 gpm of 60 to 80°F, relatively clean, cooling water is needed for the steam-dumping condenser. The condenser will

use a condensing-water supply system consisting of intake structure, screens, pumps, 14-in. piping, and a discharge drainage system. Further planning of the circulating water system awaits selection of a site.

### EQUIPMENT LAYOUT

Equipment layouts for the two-region reactor system are similar to those reported previously<sup>(2)</sup> for the plutonium and power producing reactor. It is still planned to design the shield to withstand an internal pressure of 50 psig in the event of a major leak from the high-pressure system. This has been found to be structurally feasible. The shield will also be compartmented for accessibility for maintenance work, and flooding of the compartments will be possible.

### CRITICAL CONCENTRATION AND NEUTRON BALANCE

Additional calculations of the critical concentration and the neutron balance, similar to those described in the previous report,<sup>(7)</sup> have been performed or are under way. Calculations have been completed for the reactor with 4218 g of thorium per liter in the blanket as ThO<sub>2</sub> pellets in D<sub>2</sub>O. The reactor with 7000 g of thorium per liter as thorium metal balls in D<sub>2</sub>O is currently being studied. The results of the calculations for two-region thorium converters with 4218 g of thorium per liter in the blanket are presented in the following tabulation.

(7) R. B. Briggs *et al.*, *HRP Quar. Prog. Rep.* Oct. 1, 1952, ORNL-1424, p. 47 and 58.

Temperature, °C	250
Core solution	UO <sub>2</sub> SO <sub>4</sub>
Core tank	Type 347 stainless steel
Core diameter, ft	4
Blanket thickness, ft	2
Fuel enrichment	93.5% U <sup>235</sup>
Poisons in core	None

PERIOD ENDING JANUARY 1, 1953

Poisons in blanket		None
Blanket		4218 g of thorium per liter as oxide pellets in D <sub>2</sub> O
Voids		3% voids in core
Core tank thickness, in.	1/8	1/4
Critical concentration, g of uranium per liter	5.15	5.30
Neutron balance		
Core, U <sup>235</sup>	1.0000	1.0000
Other	0.0071	0.0069
Blanket	1.00	0.92
Shell	0.11	0.19
Slow leakage	0.00007	0.00007
Fast leakage	0.00069	0.00068
U <sup>233</sup> atoms produced per U <sup>235</sup> atom destroyed	1.00	0.92

CONVERSION RATIO AS A FUNCTION OF RADIUS

In an attempt to estimate the effectiveness in conversion of various regions of the thorium-bearing blanket, calculations have been made concerning the variation of conversion ratio (U<sup>233</sup> atoms produced per U<sup>235</sup> atom destroyed) with radius in two-region thorium converters with 2-ft-thick blankets. The conversion ratio was calculated for four distances into the blanket measured from the core-tank wall.

Calculations were performed for the cases of 1000 g of thorium per liter and 4218 g of thorium per liter as ThO<sub>2</sub> in D<sub>2</sub>O. The methods outlined by S. Visner<sup>(8)</sup> were employed. Calculations for the case of 7000 g of thorium per liter as thorium metal are now being made. The geometry, dimensions, and materials are the same as those given in the preceding paragraph. The results obtained thus far are given in Table 5.

(8)S. Visner, *Nuclear Calculations for Homogeneous Reactors Producing U<sup>233</sup>*, ORNL CF-51-10-110.

TABLE 5. CONVERSION RATIO AS A FUNCTION OF RADIUS IN TWO-REGION THORIUM CONVERTERS

RADIUS (cm)	DISTANCE FROM CORE WALL INTO BLANKET (in.)	CONVERSION RATIO			
		With 1000 g of Thorium per Liter		With 4218 g of Thorium per Liter	
		1/8-in. Shell	1/4-in. Shell	1/8-in. Shell	1/4-in. Shell
60.96	0	0	0	0	0
76.20	6	0.61	0.52	0.89	0.81
91.44	12	0.82	0.71	0.98	0.91
106.68	18	0.88	0.78	1.00	0.92
121.92	24	0.90	0.79	1.00	0.92

# HRP QUARTERLY PROGRESS REPORT

## HEATING OF PELLETS IN THE BLANKET

The temperature and the thermal stresses have been estimated for pellets of metallic thorium and of fused thorium oxide in the blanket of the ISHR. Only those pellets in the highest radiation next to the core wall were studied. The results for 100-megawatt operation are shown in Table 6.

Table 6 shows that unstressed pellets of thorium oxide larger than 1/2 in. in diameter are likely to crack under the conditions assumed. It should be remembered, however, that a pellet is likely to have a large residual internal stress as a result

of firing operations during manufacture. This stress would be in the opposite sense to that caused by radiation; hence the pellets are likely to be more durable than the calculations would indicate.

## PRODUCTION OF TRITIUM IN A THREE-REGION REACTOR

The conversion ratios for three possible three-region arrangements of an intermediate-scale lithium converter have been computed by the standard two-group procedure. In each case, the core is a 4-ft-dia, spherical, stainless steel tank containing a solution

TABLE 6. EFFECTS OF RADIATION ON BLANKET PELLETS

MATERIAL	EXPOSURE (days)	POWER DISSIPATION (watts/cm <sup>3</sup> )	PELLET DIAMETER (in.)	TEMPERATURE ABOVE COOLANT		SURFACE STRESS ABOVE ALLOWABLE
				Surface (°C)	Center (°C)	
ThO <sub>2</sub>	0	20	1/8	1	5	No
			1/4	2	18	No
			1/2	6	72	Yes
			3/4	11	155	Yes
Th	0	29	1/8	1	2	No
			1/4	1	5	No
			1/2	10	14	No
			3/4	16	27	No
ThO <sub>2</sub>	10	26	1/8	1	6	No
			1/4	3	22	No
			1/2	8	90	Yes
			3/4	13	190	Yes
Th	10	36	1/8	2	2	No
			1/4	4	6	No
			1/2	11	17	No
			3/4	20	33	No
ThO <sub>2</sub>	50	96	1/8	5	24	No
			1/4	12	79	Yes
			1/2	30	340	Yes
			3/4	50	730	Yes
Th	50	125	1/8	6	8	No
			1/4	15	20	No
			1/2	40	59	No
			3/4	65	111	No

PERIOD ENDING JANUARY 1, 1953

of uranyl sulfate in  $D_2O$ , with the uranium enriched to 93.5%  $U^{235}$ . The core is surrounded by a 3-cm layer of molten lithium, which, in turn, is

surrounded by a beryllium oxide reflector. The results of the calculations are summarized in the following tabulation.

Reflector thickness, cm	58	58	28
Reflector material	60% BeO-40% Li	BeO	BeO
Critical concentration, g of uranium per liter	4.81	4.78	4.78
Neutron balance			
$U^{235}$	1.000	1.000	1.000
Remainder in core	0.007	0.007	0.007
BeO in reflector	0.000	0.033	0.016
Fast leakage	0.037	0.004	0.062
Slow leakage	0.000	0.031	0.051
1/8-in. shell			
Shell	0.085	0.086	0.086
Lithium	0.99	0.96	0.90
1/4-in. shell			
Shell	0.17	0.17	0.17
Lithium	0.90	0.87	0.81



## CONTROLS AND INSTRUMENTATION

W. M. Breazeale, Section Chief  
 A. M. Billings                      C. A. Mossman  
 D. G. Davis                         D. S. Toomb  
 C. G. Heisig                         W. P. Walker

During the past quarter this group has worked on the instrument layout of the ISHR and Boiling Reactor designs and on the development of valves, operators, and instruments for aqueous homogeneous reactor application.

### VALVES

A test loop is being built to provide a facility for testing various sample valves with flowing uranyl sulfate solution at temperatures up to 250°C and pressures up to 1000 psi. A flow sheet for this loop is shown in Fig. 17. The design of the loop is similar to that of the corrosion loops now operating, and it provides for the addition of oxygen to the solution. A Milton Roy positive-

displacement pump is provided that will circulate uranyl sulfate solution at a rate of 65 gph against pressure heads up to 1000 psi. Valve-trim materials, high-pressure seals, valve operators, etc. will be investigated under conditions similar to those of actual homogeneous reactors (except for the presence of radiation).

Testing of the thermal oxygen valve continues. Two such valves have been installed in Westinghouse Model 100-A pump loops and have performed satisfactorily for about 100 hours. This valve was described in the last quarterly report. (1)

(1) W. M. Breazeale et al., *HRP Quar. Prog. Rep.* Oct. 1, 1952, ORNL-1424, p. 9.

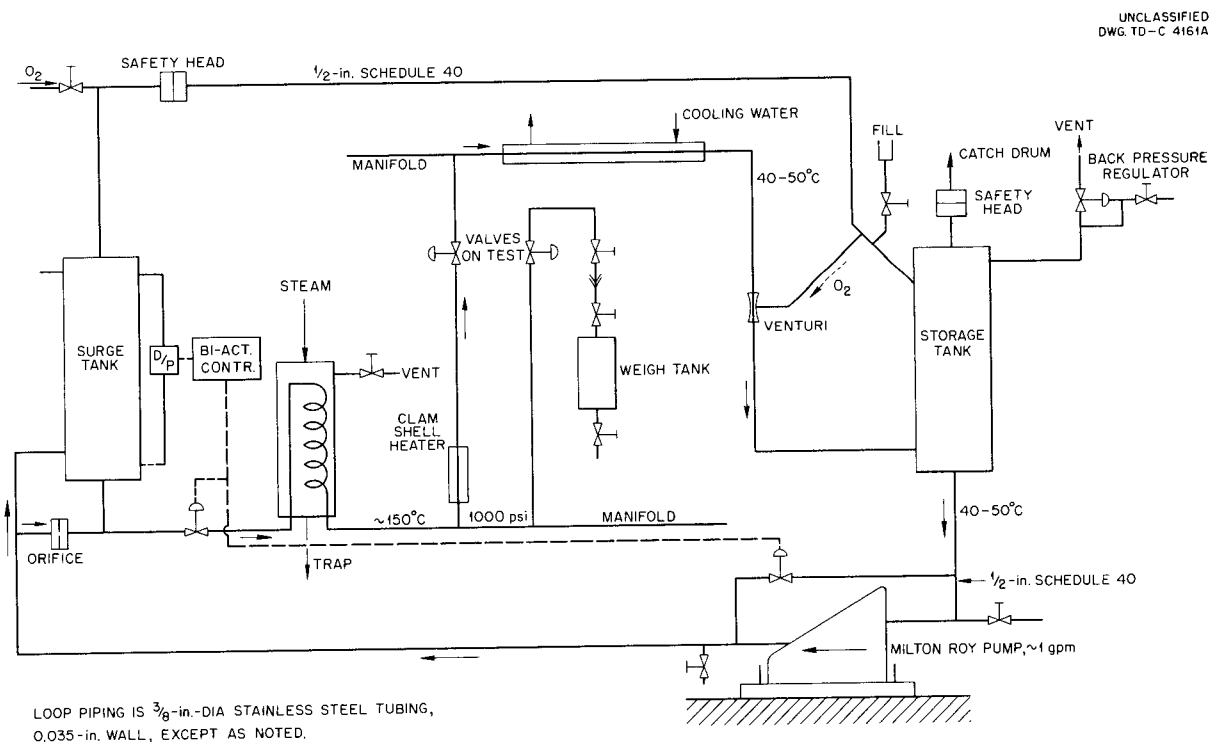


**Fig. 17. Valve Test Loop Flow Sheet.**

## HRP QUARTERLY PROGRESS REPORT

Life testing of the Fulton-Sylphon type of bellows-valve-stem seals continues. When sufficient test data are accumulated to provide for the formulation of statistical conclusions, the results will be published.

### CONCENTRATION INDICATOR

Design of the equipment for the radiation testing of synthetic gems, which it is hoped can be used in the spectrophotometer for uranyl sulfate solution monitoring, has been the subject of several conferences with the reactor operations staff. A general design has been agreed upon, and detailed drawings are now being completed. The plastic model of the cell to contain the flowing uranyl sulfate solution has been fabricated and tested, and the flow pattern has been determined. The time constant with the flow rate of 0.1 gpm is 20 sec; with 0.3 gpm, it is 5 seconds. This indicates that at the higher flow rate the cell design will be satisfactory.

Two Densichron photocell amplifiers have been procured, and a circuit to compare their outputs has been built and tested. One Densichron will measure the intensity of the light beam transmitted by the cell containing the uranyl sulfate solution, and the other Densichron will measure the intensity of a direct beam from the same light source. With the use of the comparison circuit, the effect of fluctuations of the light intensity of the source is cancelled.

### LIQUID LEVEL INDICATOR

Ultrasonic liquid level indicators are being investigated. The advantage of this type of indicator is that internal floats are eliminated. It is also hoped that better accuracy of indication will be obtained.

Two schemes have been tried. The first method involves transmitting an ultrasonic wave through the bottom of the vessel and measuring the time for the wave reflected from the surface of the liquid to return to the transducer. In the other method, the transducer is placed on the side of the vessel, and the change in signal is noted when the liquid level moves from above to below the point opposite the transducer. This scheme will be applied to tall vessels of small diameter and will probably involve vertical adjustment of the transducer. The tests thus far have been made with 5-megacycle shock-excited waves and a quartz crystal transducer, and the results are very encouraging. However, before this method can be judged as successful, the equipment must be made to work in the presence of higher temperatures and radiation.

### DENSITROL

Little work has been done on the Densitrol during the past quarter. Two titanium plummets have been machined and are awaiting welding and pressurizing. It is planned to install and test these during the coming quarter.

ENGINEERING DEVELOPMENT

C. B. Graham, Section Chief

CORE AND GAS-SEPARATOR DEVELOPMENT

J. A. Hafford            I. Spiewak  
L. B. Lesem              R. H. Wilson

The recent decision to design the intermediate-scale homogeneous reactor in the form of a two-region converter or breeder directly affects the problem of fuel flow through the core, since it is necessary to operate the inner core at considerably higher power densities than were visualized for single-core reactors. The ISHR core will operate at about 50 kw/liter, and industrial breeders are visualized as operating up to 200 kw/liter.

Of the two types of flow considered for single-core reactors, only the straight-through flow appears promising when applied to the inner core of a high-power-density reactor. The pressure drop in rotating flow becomes prohibitive and the structural details more complicated when applied to high liquid throughputs.

Therefore the present investigations of the rotating type of flow are being de-emphasized. Small-scale experimental work was completed, and only a limited amount of intermediate-scale testing is planned.

**Core Development for Straight-Through Flow.** The optimum flow arrangement for a high-power-density reactor is slug flow, with equal temperature rise in each stream line. In addition to the orderly removal of heat, this core has significant advantages in that it can be built with low pressure drop and low gas holdup. Low pressure drop results in pump-power saving, and the lower velocities required in the pump reduce the amount of corrosion. Low gas holdup, which can be accomplished by upward slug flow, results in improved controllability of core power.

The model shown in Fig. 18 has five screens mounted in the inlet to provide smooth expansion from pipe to sphere, and it has slug flow through the sphere. It is an 18-in. model of the ISHR core proposed in an ORNL memorandum.<sup>(1)</sup> Preliminary tests of flow pattern, pressure drop, and gas behavior indicate that the requirements of the ISHR core are met.

(1) I. Spiewak, *Preliminary Design of Screens for the Inlet of the ISHR Core*, ORNL CF-52-10-181.

UNCLASSIFIED  
DWG. 17824

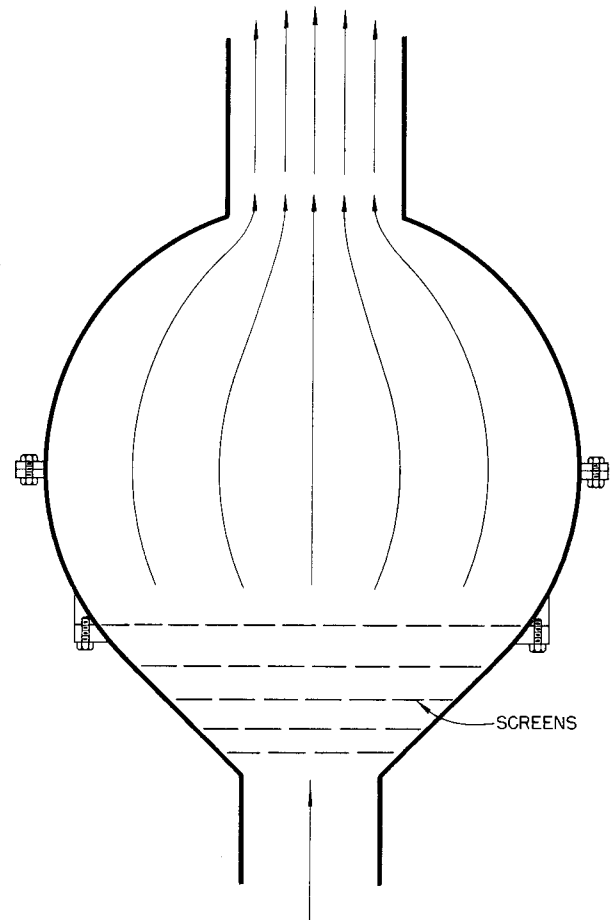


Fig. 18. Straight-Through Flow Model with Screens in the Inlet Diffuser.

## HRP QUARTERLY PROGRESS REPORT

Three sets of screens have been tried in this model: (1) five 8-mesh screens with a solidity ratio of 0.446 (solidity ratio is the ratio of metal area to total screen area), (2) five 4-mesh screens with a solidity ratio of 0.440, (3) four 8-mesh screens similar to sets 1 and 2, except that the upper screen had a higher solidity ratio than the lower screens.

The pressure drop observed across the first set of screens was 1.53 inlet velocity heads, which was close to that measured with the third system. There was a loss of 1.36 velocity heads across the second screen system. The pressure drop in the outlet pipe was less than 0.20 velocity heads. If the observed over-all pressure drop is translated to ISHR conditions and dimensions, the loss expected is about 1.5 psi. This estimate is believed to be quite accurate, since the pressure drop in the model was within 10% of that predicted from the literature data.<sup>(2)</sup>

The flow pattern was examined by means of dye injection, both at the entrance and in the equatorial plane. Quantitative measurements were made of dye residence time when the dye was injected at various points in the equatorial plane.

Slug flow was observed everywhere except near the wall in the southern hemisphere. Furthermore, flow decreased gradually from a maximum at the center to a minimum at the wall, roughly paralleling the neutron-flux distribution.

Because it is desired to eliminate or minimize the flow separation observed in the southern hemisphere, the factors that influence separation were studied qualitatively. They are:

1. *Discontinuities of the Sphere Wall.* The model was constructed from two plastic hemispheres, and originally there was about a 1/2-in. gap at the

equator where the hemispheres were flanged together. When this gap was filled in with putty, the amount of separation was reduced markedly. Further improvement would be expected with a continuous surface.

2. *Discontinuities in the Entrance Diffuser.* The flange joining the conical inlet to the sphere was used also to mount the last screen. Therefore a gap about the same size as the screen thickness existed in the wall of the entrance diffuser. With an 8-mesh screen mounted in the flange, this gap was increased from about 1/16 to 1/8 inch. As a result, the thickness of the separating boundary layer increased from 1 to 2 inches. Since the minimum discontinuity obtainable with a 4-mesh screen in the flange was about 1/8 in., considerable separation was produced by the 4-mesh system.

3. *Solidity Ratio of Top Screen.* The third screen system was tested in an attempt to eliminate separation by going to a higher solidity ratio in the top screen. A 20-mesh screen of 0.51 solidity ratio produced a relatively thin (1/2 in.) separating layer covering only a portion of the southern hemisphere surface. A 16-mesh screen of 0.60 solidity ratio proved quite unsatisfactory from the standpoint of separation.

4. *Velocity Distribution in the Entrance to the Diffuser.* Unbalanced velocity distribution in the entrance to the screens was found to aggravate separation problems. This effect will be investigated further; it may be necessary to provide straightening vanes in the inlet of a reactor core.

The quantitative data on dye residence time are summarized in Fig. 19, which is a plot of temperature rise vs. position of the various stream lines. This plot was obtained by superimposing the neutron-flux distribution of the ISHR core and the flow pattern observed in the model.

<sup>(2)</sup>G. B. Schubauer and W. G. Spangenberg, *Effect of Screens in Wide-Angle Diffusers*, NACA-TN-1610 (June 25, 1947).

The dye residence times were evaluated where no separation existed, except for the 4-mesh screens, which had separation everywhere near the wall. The maximum deviation from the calculated average temperature rise of 40°C was 8% for the 8-mesh system, 25% for the 8-mesh-20-mesh combination, and very large for the separated portion of the 4-mesh system.

The above temperature rises do not include consideration of secondary flow produced by density differences in the fluid, such as would be present in a nonisothermal reactor that produced gas. Preliminary calculations

indicate that density differences cause a very strong damping effect on the deviations from average temperature rise. Since these calculations are difficult, no attempt has yet been made to precisely evaluate the density effect.

Qualitative confirmation of the density influence has been obtained in the model. Methanol colored with methylene blue was injected for a few seconds into the inlet stream and then shut off suddenly. The density difference produced was estimated at 0.15%, but it proved to be sufficient to prevent flow separation. In fact,

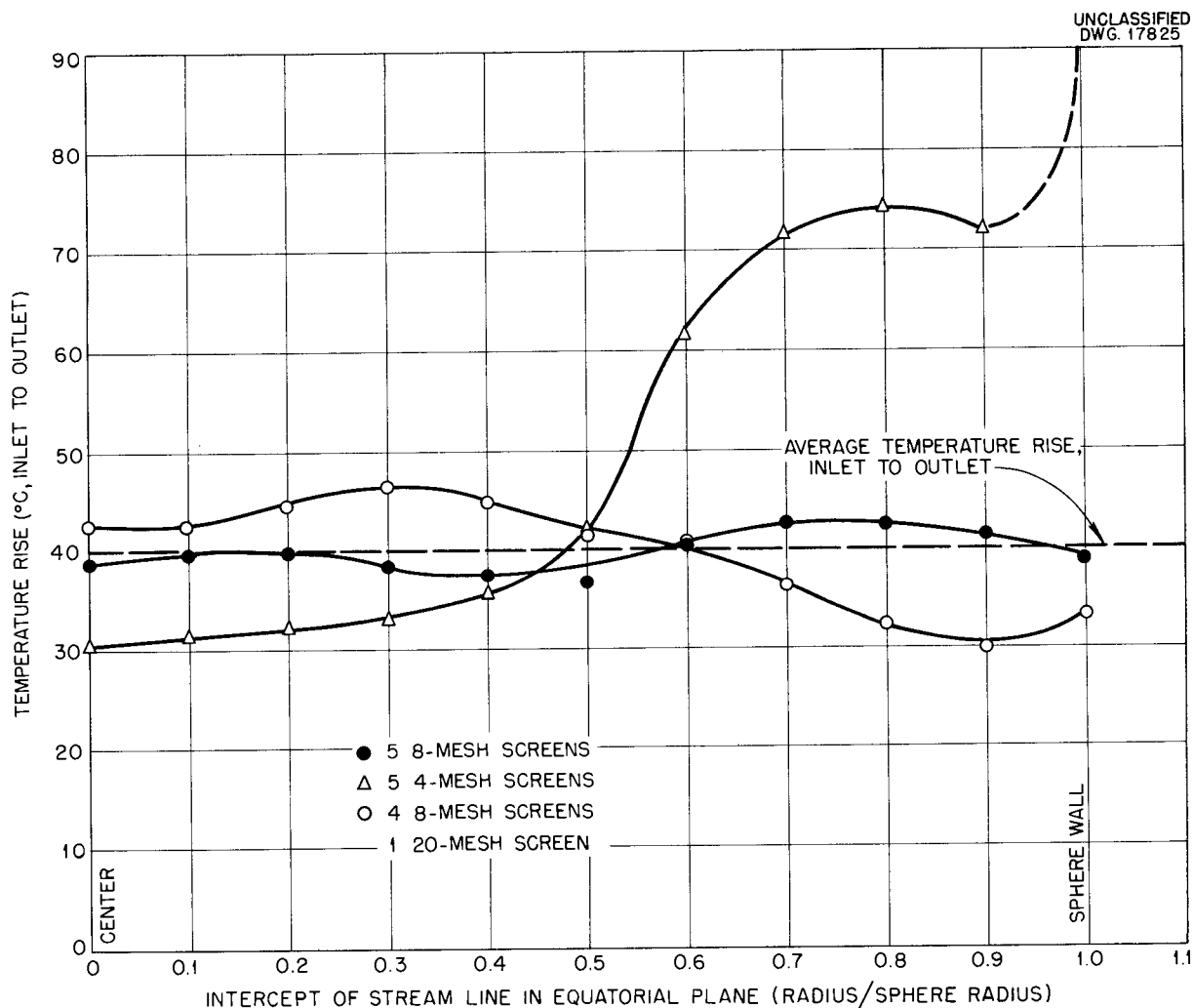


Fig. 19. Temperature Rise of Stream Lines in Straight-Through Flow Model with Screens.

## HRP QUARTERLY PROGRESS REPORT

the lower boundary between the methanol solution and the water rose through the sphere as a plane.

Gas produced in the core of a reactor of this type will rise relative to the liquid because of buoyant forces. The rate of rise will depend on the bubble size. If a bubble diameter of 0.1 in., corresponding to a relative bubble rise of 0.8 fps is assumed, the average gas residence time in the ISHR core is 0.94 sec, as compared with the liquid residence time of 3.00 seconds. For a water decomposition rate of 1 molecule per 60 ev, the gas volume in the core is 1.5%; that in the core exit is 4.9%.

Further development of the proposed ISHR core with straight-through flow is planned, and a full-scale flow model is to be investigated. For the ISHR core, the solidity ratio of the screens will remain the same as for the 18-in. model, but the wire thickness will be increased for greater strength and corrosion resistance. The liquid velocity past the screens is expected to be 10 fps or less, which is in the low-corrosion range.

**Gas Separators.** The use of straight-through flow in the ISHR core necessitates development of a gas separator for the external circulating system. It is desired, also, to combine the functions of gas separation and pressurization in a single piece of equipment. This is to be accomplished, if

possible, with high gas separating efficiency, low pressure drop, and low liquid holdup.

The system believed to be best for meeting these requirements is a pipe-line separator through which the liquid flows in a helical path after passing through a volute or entrance vanes that impart rotation. The gas is centrifuged into a void that forms at the pipe axis; the void is useful also as a pressurizer. Gas withdrawn from the void flows to the recombiner system.

A model of a pipe-line separator, shown in Fig. 20, has been constructed.<sup>(3)</sup> It is made of 5-in.-ID Lucite tubing and can handle up to 600 gpm. Rotation in this device is produced by the vanes shown in the inlet section. The spinning liquid enters the pipe section of the separator, which has been made adjustable in length for experimental purposes. The exit end of the model is a volute in which it is desired to recover some of the rotating kinetic energy. Gas can be removed from the void at either end of the model.

Provisions are made for observing gas separation efficiency, rotational and axial velocity distribution, and static pressure at the wall. From this information, the energy losses

<sup>(3)</sup>C. B. Graham et al., *HRP Quar. Prog. Rep.* Oct. 1, 1952, ORNL-1424, p. 62

UNCLASSIFIED  
DWG. 15753

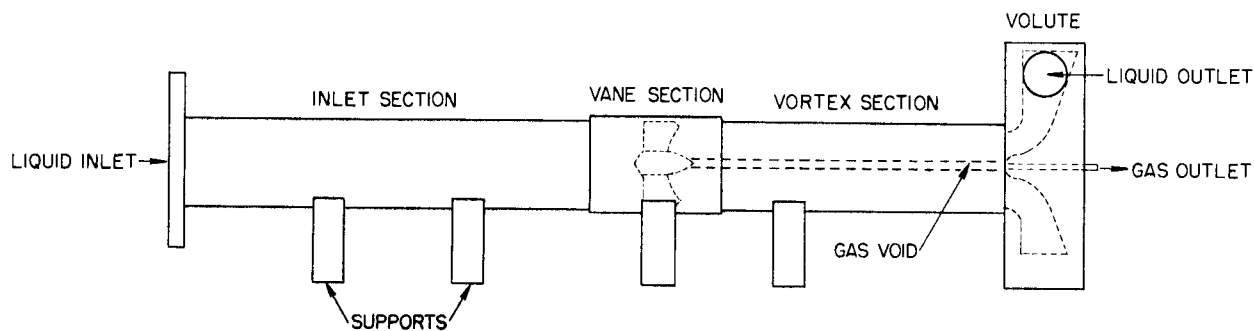


Fig. 20. Test Model of Pipe Gas Separator.

in various parts of the system can be estimated.

Thus far, two sets of vanes have been investigated in the model. The first set was designed to give a tangential velocity distribution that was proportional to the square root of the radius. The actual tangential velocity is shown in Fig. 21. The large deviation from theoretical velocity distribution is believed to be caused by poor vane fabrication.

The excessively complex vane design, together with fabrication difficulties, is believed to cause the low gas separation (80% efficiency) and the cork-screw-shaped void that was observed.

From the energy standpoint, the first set of vanes was quite good. The vane efficiency in converting static energy to rotation was about 80%, which is surprising in view of the turbulent conditions following the vanes. The total head loss measured from vane inlet to volute inlet was 1.33 entrance velocity heads (0.57 psi at 600 gpm). If the exit volute had zero efficiency, loss across the entire separator would be 2.96 velocity heads.

The second set of vanes, which were designed along simpler mechanical lines, had a theoretical tangential velocity distribution that was inversely proportional to the square root of the radius. The actual velocity is shown in Fig. 22. The high theoretical velocities near the center cannot be maintained in practice; so the actual tangential velocity is zero at the center of the pipe.

The second vane system produced a smooth, stable void. Gas separating efficiency, which is influenced by the smoothness of the void, was over 95%. This could probably be improved further by optimization of the gas-removal nozzle.

An analysis of energy losses for this system is under way and will be reported in the future. The losses are believed to be of the same order of magnitude as for the first set of vanes.

Evaluation of energy recovery in the volute of this particular model is more difficult than study of the vanes. The volute was built with a 3-in. discharge so that it could be fabricated from plastic sheet. Acceleration of liquid from the 5-in. separator to the 3-in. discharge produces energy losses that are impossible to distinguish from the energy losses in straightening the flow. Until a

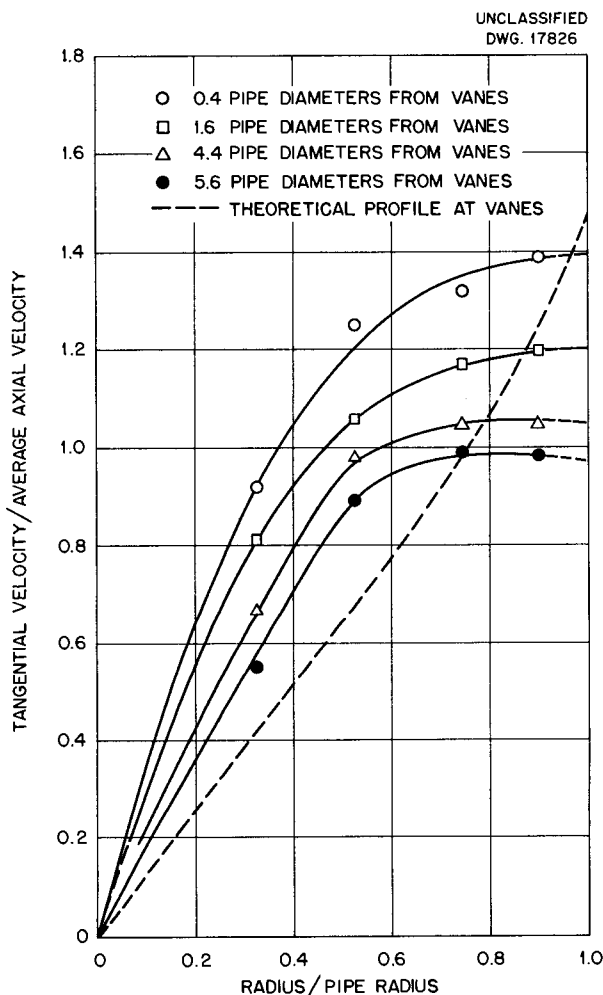
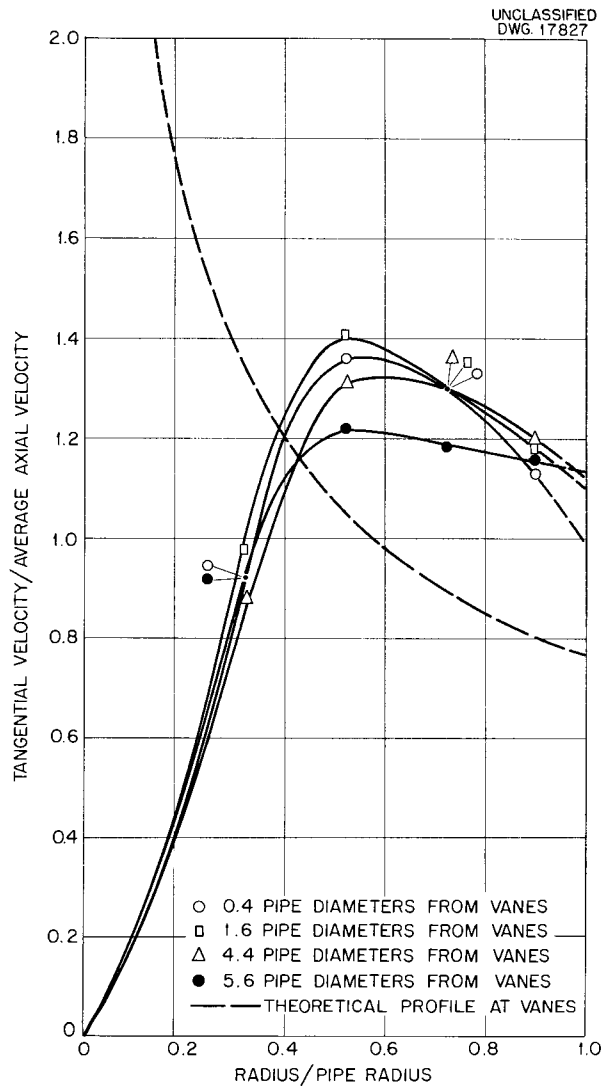


Fig. 21. Tangential Velocity Profiles in Gas Separator, Vane System No. 1.

# HRP QUARTERLY PROGRESS REPORT



**Fig. 22. Tangential Velocity Profiles in Gas Separator, Vane System No. 2.**

volute is built with the same discharge diameter as the separator diameter, the situation cannot be clarified.

Further developmental work planned with this model includes: (1) testing of recovery vanes at the outlet end of the separator to determine whether they will give better performance at lower fabrication cost than for an optimum volute; (2) optimization of gas nozzle design with respect to gas separating efficiency, pressure drop through the nozzle, and liquid

entrainment; and (3) evaluation of the volute as a producer of rotation in comparison with vanes. This information may be required for the design of separators for which there are definite space limitations imposed by other equipment.

The behavior of an acceptable gas separator when coupled to the recombiner system will have to be investigated. In particular, mass transfer of steam to the gas void, liquid entrainment at operating conditions, and transients in gas and liquid throughput will require close observation. Furthermore, since there will be considerable turbulence, corrosion effects must be studied.

**Single-Core Reactor Studies.** A limited amount of work, not related directly to two-region ISHR development, was completed when the single-core ISHR was contemplated. The major portion of this effort has been reported or is in the process of being reported. The following is a summary of these studies:

1. *Twelve-Inch Rotating-Core Model.* A completion report, not yet issued, has been prepared by J. I. Lang. The important conclusions are presented in ORNL-1424.<sup>(4)</sup>

2. *Eight-Foot Rotating-Core Model.* The completion of construction of this system, described in ORNL-1280,<sup>(5)</sup> is expected during the next quarter. The status as of January 1, 1953 is shown in Fig. 23.

3. *Straight-Through Models of Single-Core Reactors.* The investigation of three small glass models has been reported.<sup>(6)</sup> Investigation of models with multiple jet inlets will be reported soon. The information was summarized in ORNL-1424.<sup>(7)</sup>

<sup>(4)</sup> *Ibid.*, p. 59.

<sup>(5)</sup> C. B. Graham *et al.*, *HRP Quar. Prog. Rep. Mar. 15, 1952*, ORNL-1280, p. 151.

<sup>(6)</sup> L. B. Lesem, *Hydrodynamic Studies in Three Glass Models*, ORNL CF-52-10-134.

<sup>(7)</sup> C. B. Graham *et al.*, *HRP Quar. Prog. Rep. Oct. 1, 1952*, ORNL-1424, p. 60.



Fig. 23. Eight-Foot Core and Holdup Tanks for 50,000-gpm Loop, Showing Construction Status as of January 1, 1953.

## HRP QUARTERLY PROGRESS REPORT

4. *Use of Slurry in the HRE Core.*<sup>(8)</sup> Room-temperature circulation of slurry through the plastic model of the HRE indicates that slurry can probably be used with the present HRE core. This will be ascertained in the Y-12 mockup.

5. *Thermal Stress in a Single-Core ISHR.*<sup>(9)</sup> Two methods for reducing thermal stress in the outer pressure vessel of a reactor are suggested - borated water thermal shielding and controlled cooling of the outside of the vessel. The methods have general applicability where thermal stress is a problem.

### TEST LOOP FOR 4000-gpm-PUMP

W. L. Ross

A description of the loop design was given in a previous quarterly report.<sup>(10)</sup> The loop was designed for operation at 250°C with uranyl sulfate solution. Some changes in loop design will be necessary to attain satisfactory performance if it should become desirable to operate the loop with a slurry or cold liquids.

A Byron Jackson 4000-gpm canned-rotor pump is available for use in the loop. All major items of equipment for the loop have been ordered, and approximately 25% of the major components and auxiliary equipment have been received. Completion of delivery of the remaining items is anticipated by January 1953.

### LARGE HEAT EXCHANGERS

L. F. Goode      W. L. Ross

A memorandum covering the investigation of large, 200-megawatt, heat exchangers is currently being prepared. The preliminary design data presented

<sup>(8)</sup> I. Spiewak, *Use of Slurry in HRE Mockup Core*, ORNL CF-52-9-171.

<sup>(9)</sup> I. Spiewak, *Thermal Stress in the ISHR Pressure Vessel*, ORNL CF-52-10-81.

<sup>(10)</sup> J. R. McWhorter, *HRP Quar. Prog. Rep.* Nov. 15, 1951, ORNL-1221, p. 18.

in the last quarterly report<sup>(11)</sup> have been modified and revised, with emphasis on the 3/8-in.-OD, 18-BW-Ga tube system. The major designs that have been considered are: (1) a unit consisting of a horizontal tube bundle and exchanger with an elevated horizontal steam drum connected by risers and downcomers that is semiconventional and, at present, looks promising; (2) a unit consisting of a horizontal tube bundle within a horizontal steam drum that is quite compact and possesses a minimum of expansion problems; (3) a unit consisting of vertical exchangers connected by headers to an elevated horizontal steam drum that is somewhat unwieldy and has quite a few drawbacks. Although type 3 is still considered as a workable possibility, it is felt that types 1 and 2 represent a considerable improvement over type 3.

The horizontal, single-drum exchanger (type 2) was selected for further study of the water-side pressure drop, tube pitch, recirculation rates, header problems, and separation and expansion problems, and a more detailed analysis of sizes, weights, etc. In order that this design may be available for consideration in the current ISHR heat exchanger program, a scaled-down preliminary design of the ISHR size (50,000 kw) is being prepared. A memorandum covering this study will be available shortly. Much of the information obtained from the large heat exchanger study has been used in the development and evaluation of possible ISHR exchanger designs.

Discussion of the preliminary designs with various manufacturers has resulted in the following opinions. All three basic designs are feasible and can be manufactured. Exchangers similar to types 1 and 3, with a steam drum above the tube bundle, are more widely used and thus subject to precise heat transfer analysis. A sufficient

<sup>(11)</sup> C. B. Graham et al., *HRP Quar. Prog. Rep.* Oct. 1, 1952, ORNL-1424, p. 67.

number of exchangers similar to type 2, with a single drum, has *probably* been built to permit reasonably accurate analysis, if considerations such as compactness, cost, and freedom from expansion problems warrant its use.

With respect to the use of smaller tube size to reduce the fuel holdup in the tubes, it must be remembered that as the tube diameter decreases, the number of tubes required and the possibility of a faulty tube joint increase. At present, one of the most pressing needs in the reactor heat exchanger field is the development of a reliable tube joint. In the large exchangers with complex headers and tube systems, one leaking connection could easily necessitate the scrapping of the entire exchanger if radioactive contamination prevented repair. Several designs for expanded tube connections have been proposed, and in view of the seriousness of the problem it appears that considerable developmental work in perfecting a reliable tube joint would be justified. Also, the method of welding the tubes needs to be studied. An automatic or semi-automatic method, such as "flash" welding or cone-arc welding, would be very useful.

#### PULSAFEEDER PUMP DEVELOPMENT

V. S. Culver	C. D. Zerby
P. N. Stevens	W. L. Ross

As discussed in previous reports, some difficulties have been experienced with the pulsafeder pumps in the HRE; however, a number of changes has been made and operation has been improved. A survey of alternate types of pumps has not revealed any obviously desirable substitutes. It appears that the use of pulsafeders, or variations of this design, may be desirable in future reactors, if operating reliability can be established. For these reasons, developmental work on the pulsafeder has continued. Several

further improvements, some of which have not been explored to date, are anticipated.

The developmental progress made since the first pump was received is summarized in the following paragraphs. The changes noted have produced a smoothly running pump that has operated satisfactorily for 1100 hr without serious trouble and with no failure of the reagent head. A comprehensive report is being prepared on all pulsafeder work to date.

**Recontouring of Head Flanges.** All head flanges have been recontoured to the Lapp design curve. The original contours were at considerable variance with the design curve, and there was question as to the effect of contour on diaphragm life. The long life obtained to date would suggest that although the Lapp design may not be optimum, it will be satisfactory until more fundamental information suggests a change.

**Strainers in the Pumping Heads.** Examination of early heads in which the diaphragm failed invariably revealed an area in which severe distortion of the diaphragm occurred as a result of foreign material. The life of the present fuel pump head has already been twice the usual diaphragm life of some previously recontoured heads. This would indicate that the strainers built into the present head design are valuable.

**Reduction in Speed.** Tests conducted both on the HRE mockup and on the reactor pumps show that an improvement has been made by reducing the speed of the pumps. Progressive reductions in speed from 78 to 60 to 52 rpm all reduced the check-valve chatter without reducing output below an acceptable level. The fuel pump in the HRE is now equipped with a two-speed motor that will give 50 and 25 strokes per minute. Operation at the lower speed produces an output of 0.6 to 0.8 gpm, which is considered adequate for the reactor at moderate power.

## HRP QUARTERLY PROGRESS REPORT

An additional advantage gained at the lower speed is a great reduction in the amount of air leakage into the oil system through the packing in the oil pump. A daily bleeding of air is normally adequate and can be done without affecting operation.

**Reduction in Oil Line Length.** Moving the oil pumps close to the shielded pits where the heads are installed has added to the output of the fuel pump by eliminating the large compressibility loss previously experienced. In the case of the D<sub>2</sub>O pump for the reflector, the length of the lines carrying the fluorocarbon oil was reduced from 30 to 1½ ft, and thus the inertia effects and compressibility were greatly reduced. Here again the air leakage problem was greatly reduced, although not entirely eliminated. Some improvement was noted when "O" rings were installed in the oil-pump packing gland. Tests are being conducted on a modification of the Chevron seal supplied in the drive pump to exclude air.

**Check Valve Development.** Earlier, check valves supplied by the manufacturer had 1/16-in. diametral clearance between the balls and their cages. The clearance in the cages was increased for ease of welding before installation in previous assemblies. Tests showed that valve chatter could be reduced by using closer-fitting cages, and, accordingly, the design was revised to provide 1/64-in. diametral clearance. The manufacturer simultaneously discovered the importance of this clearance, apparently, and supplied a spare pair of check valves with 1/32-in. diametral clearance. These 1/32-in. cages are now installed in the fuel pump head.

**Fundamental Studies.** Further significant improvement requires a more thorough understanding of the fundamental characteristics of the numerous components of the pump. Accordingly, some components are receiving special study. The thickness of the diaphragm

could be increased to provide an increased factor of safety in corrosion or puncturing, but the increased diaphragm thickness would probably require a shorter stroke, which would result in a decrease in capacity per head. Fatigue failure in the present heads does not appear to be likely, but this must be confirmed. An improvement in contouring may result in reduced stresses. Theoretical analyses of stresses, strain gage tests, and fatigue tests are being made to establish design criteria for further improvements.

**Stress Analysis.** An attempt is being made to calculate the theoretical stresses in a diaphragm and then to compare these values with the stresses as determined by strain gage measurements. Unfortunately, there are no readily applicable stress equations that are valid for these particular conditions. The exact solution for a circular diaphragm with clamped edges and free deflection has been calculated from an established theory<sup>(12)</sup> for deflections up to twice the thickness of the diaphragm. An attempt is being made to extend this analysis to include large deflections that conform to fixed contours.

To substantiate the theoretical analysis and to obtain a better understanding of the stress condition existing in the diaphragm, an experimental determination of the stress was made by using strain gages. Both free deflection and deflection conforming to the pump head design contour were considered. Some correlation between the experimental and calculated stresses was obtained from the first tests. Preliminary results show that the maximum stress is approximately 20,000 psi.

The theoretical analyses of the contour design and the diaphragm thickness will be continued in an attempt to reduce to a minimum the

(12) S. Way, *Trans. Am. Soc. Mech. Engrs.* 56, 627 (1934).

possibilities of a diaphragm failure. When an optimum theoretical contour has been calculated, further experimental strain gage tests will be needed.

**Diaphragm Endurance Tests.** An apparatus has been constructed and is currently operating to determine the fatigue limit of a 0.019-in. type 347 stainless steel diaphragm mounted in the standard HRE pulsafeder head. Failures brought about by other than the repeated flexures are virtually eliminated by using an air-operated cycle with a gasket-free assembly. More than five million cycles have been run to date and there has been no detectable leakage. If failure does not occur before ten million cycles, the diaphragm will be removed and examined for evidence of fatigue cracking.

A previous water-operated cycle with a gasket-sealed diaphragm had operated about one million cycles before failure. Examination of the ruptured diaphragm indicated that failure could have occurred from flexure, dirt in the water, misaligned gaskets, or some combination of the three. No firm determination could be made as to a single cause for the rupture.

Further evidence of expected diaphragm life is being accumulated on the HRE. The reagent head on the 1-gpm fuel pump has 1100 hr of operation, which represents almost four million cycles, without failure. This head is equipped with built-in strainers to exclude foreign material, and the flanges were recontoured to conform to the Lapp design. Since this head has operated over twice as long as most previous assemblies, the importance of excluding dirt and chips from the diaphragm region is again emphasized.

(13) C. B. Graham and L. F. Goode, *HRP Quar. Prog. Rep. Oct. 1, 1952*, ORNL-1424, p. 7.

#### SEAL WELDED HEAD FOR THE 1-gph PULSAFEEDER PUMP

A 1-gph pulsafeder pump head has been designed in which all external gaskets are eliminated. The design incorporates the diaphragm seal weld used in the larger pulsafeders but retains the bolts to overcome the hydrostatic pressure. The check valve housing has been incorporated in one of the flanges for simplicity of assembly and also for minimizing welding. The original Lapp check-valve assemblies are retained to minimize construction time; however, the internal Teflon gaskets will be replaced with annealed stainless steel gaskets.

#### POSITIVE-DISPLACEMENT TRIPLEX PUMP DEVELOPMENT

Modification of the Union Triplex pump head and frame for the test program outlined previously<sup>(13)</sup> has been completed. The actual test work has been delayed pending delivery of the nylon test packing. However, Neoprene Chevron-type packing has recently been obtained in sufficient quantity for testing, and, in order to expedite the program, it will be tested in the apparatus until the nylon packing is received. The Union Steam Pump Co. has submitted a quotation for a pump head that incorporates the desired design changes. The head is fabricated from Stellite, stainless steel and chrome-plated components. The quotation has been reviewed, but no action will be taken until testing indicates satisfactory operation of the design and packing material.

#### DEVELOPMENT OF 1-gpm PUMP WITH A STELLITE PISTON

V. S. Culver

An alternate pump design was prepared by Angel and Welch of the HR Design Department during the period in which the pulsafeder pumps in the

## HRP QUARTERLY PROGRESS REPORT

HRE were giving a great deal of trouble. This pump, described in a previous report,<sup>(14)</sup> utilizes a Stellite piston in a Stellite cylinder driven by an oil cylinder. Original specifications required that the piston and cylinder be made of type 98M2 Stellite, but the manufacturer requested that grade 3 be substituted so that the assembly could be successfully cast. These parts have been received and installed in an apparatus to test the piston and cylinder for wear, galling, etc.

Upon receipt, the parts were carefully measured to determine the clearance between piston and cylinder and the effect of temperature change. The diameters of the piston and the cylinder at 70 and 120°F are given in the following:

Piston diameter, in.	
Design	2.4997 to 2.4995
Measured	
at 70°F	2.4997
at 120°F	2.5003
Cylinder diameter, in.	
Design	2.5000 to 2.5004
Measured	
at 70°F	2.5010
at 120°F	2.5016

It can be seen from these figures that the cylinder is 0.0006 in. above maximum tolerance, which gives a diametral clearance of 0.0013 inch. This is more than the designers anticipated and will increase leakage, since there are no seals other than the fit of the piston in the cylinder.

Before assembling the actual pump, it was agreed that the piston and cylinder should be given a thorough test under ideal conditions to determine whether the combination of the Stellite No. 3 piston and cylinder would have reasonable life under service conditions. The apparatus

shown schematically in Fig. 24 was built for this test.

In operation, distilled water is forced out of vessel (1) through the ports in the piston and cylinder and forces the piston (2) up until the ports are closed. The pressure switch then shifts the solenoid valve to vent, and the piston returns to its original position, aided by the 5 psi air pressure above it. This cycle repeats itself indefinitely, and leakage past the piston upward is accumulated until it spills over into vessel (4). Since the pressure difference across the piston skirt is similar to the expected dump-tank pressures, the leakage should give some idea of what may be expected in the pump.

Since it was expected that the wear would be small, the piston was photographed before testing and again after 50,000 cycles at room temperature. No serious wear or galling was evident.

The leakage rate observed is not reliable because of the short operating time (15 hr); however, about 100 cm<sup>3</sup> of water was pumped over in 8 hours. Adding a larger leakage volume and a drain valve after the initial run will make it possible to obtain more reliable data in the future. The apparatus will be run until approximately one-half million cycles have been accumulated in the vertical position with distilled water in the system. Future plans call for rotating the cylinder axis to a horizontal position to provide some side-thrust effect. Since the system is made entirely of standard pyrex glass fittings, geometry changes and the addition of uranyl sulfate solutions will not involve any problems. If the piston and cylinder assembly stand up under the corrosive effect of cold uranyl sulfate solution and the solution at 65°C, they will be assembled as a pump and tested under service conditions.

<sup>(14)</sup> R. B. Briggs, C. L. Segaser, and F. C. Zapp, *HRP Quar. Prog. Rep. Mar. 15, 1952*, ORNL-1280, p. 25.

DWG. 17828

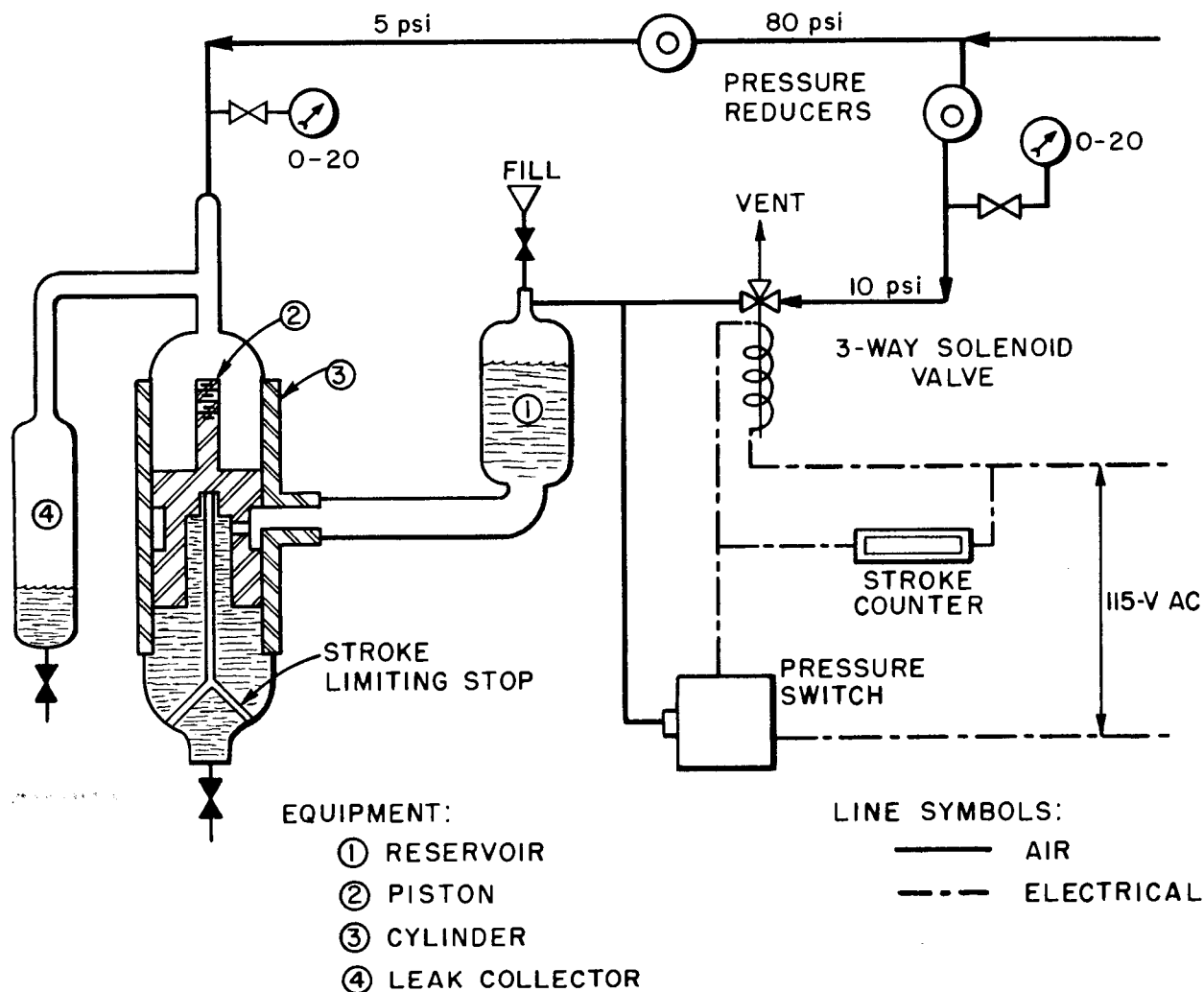


Fig. 24. Stellite Piston and Cylinder Test Apparatus.

**SMALL CANNED-ROTOR PUMP DEVELOPMENT**

Allis-Chalmers 5-gpm Pump (R. J. Kedl and W. L. Ross). As stated in the last progress report,<sup>(15)</sup> it has been found that slurry is centrifuged out in the rotor and bearing chamber of the Allis-Chalmers, 5-gpm, canned-rotor pump. When this occurs, the pump will not start once it is stopped.

<sup>(15)</sup> C. B. Graham et al., *HRP Quar. Prog. Rep.* Oct. 1, 1952, ORNL-1424, p. 66.

Attempts were made to rectify this condition by running the pump in a vertical position with the rotor-bearing chamber above the pump impeller and by increasing the starting torque with a starting capacitor; however, none of these changes were successful. This pump is satisfactory for circulating water, and it possibly will operate satisfactorily with dilute solution. A seal between the impeller and motor housings should be provided

## HRP QUARTERLY PROGRESS REPORT

for applications in which welding is undesirable.

**ORNL Small Canned-Rotor Pump Development** (R. J. Kedl, T. H. Mauney, C. B. Graham, and W. L. Ross). A small canned-rotor pump (Fig. 25) is being designed by ORNL. It is designed for approximately 10-gpm flow against a head of 30 ft when pumping solution at 250°C and 1000 psi. All parts that operate at the temperature of the circulated fluid will be fabricated of type 347 stainless steel. These parts are designed for easy replacement with titanium or some other material. The rotor, bearings, can, etc. operate at low temperature to reduce corrosion. The pump is therefore expected to be operable with many corrosive solutions or slurries, and will be used for in-reactor loops, corrosion test loops, and similar applications. In this design, emphasis is being placed on "minimum cost" so that the pump can be discarded if it becomes radioactive or in some other way unserviceable. The cost is being minimized by using as many standard

parts as possible and by careful design.

The bearings consist of two Graphitar sleeves that are identical to those now used in the Westinghouse model 100-A pump. The shaft will be fabricated of type 347 stainless steel and will be chrome plated where it runs on the bearings. This type of bearing assembly has been used in a Westinghouse model 30-A pump that has operated satisfactorily in low-temperature fuel solutions. The bearing chamber of the pump will be cooled by a water jacket. It is estimated that the temperature of the bearing and rotor chamber will be about 120°C when the system is at 250°C. The axial thrust is carried by the rotor, which runs on the edge of the rear radial bearing. The rotor, as shown, will be machined from a solid rod of type 410 stainless steel. When the first experimental pump is built, a canned rotor will also be provided because the type 410 stainless steel rotor may not provide sufficient driving force. A secondary impeller is machined on the rear of the

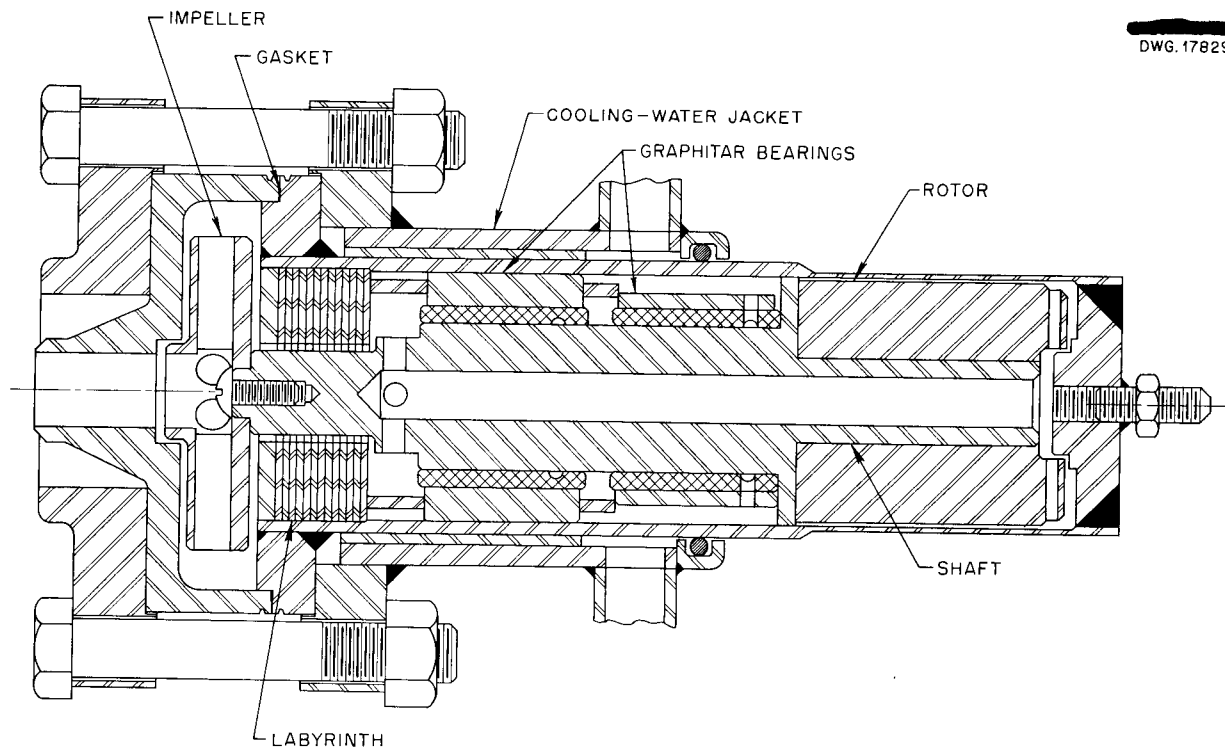


Fig. 25. ORNL Centrifugal Pump, 10 gpm, 30-ft Head.

the rotor to provide circulation in the bearing chamber. This circulation cools the bearings, rotor, and can.

The pump volute is closed by means of a high-pressure flange and a type 347 stainless steel gasket; provisions have been made for a seal weld. The impeller is a type 347 stainless steel disk with six radial holes.

A standard, capacitor-run, 3600-rpm, 1/2-hp stator will be used. The stator will probably be cooled by passing water through tubes that will be expanded into the present air holes in the stator laminations. If overheating occurs, a high-temperature winding or air cooling may be required.

The fluid connection between the volute and the rotor chamber is through a close-clearance labyrinth that prevents free circulation between the two chambers and also serves as a heat barrier.

#### CONVERSION OF THE HRE MOCKUP TO OPERATE WITH URANIUM OXIDE SLURRY

C. D. Zerby

Component tests are now being planned or are in progress to determine the necessary changes for converting the HRE Mockup to one suitable for operation with uranium oxide slurry. The let-down system and pulsafeeder pump, the dump tanks, dump line and valve, and the pressurizer and level controller are the components most likely to be troublesome when the HRE mockup is converted; these will be mocked up separately to determine whether they will operate satisfactorily with slurry prior to the conversion of the mockup of the HRE. The criteria for satisfactory operation of the components are that under normal operating conditions the slurry concentration will remain constant in the circulating system, no fissionable material will gather as a result of the slurry settling or caking on container walls, and each component

will operate satisfactorily in a mechanical sense.

The first component test consisted of pumping slurry through a low-pressure loop with a 1-gpm Lapp pulsafeeder pump. Continuous pumping of a slurry containing 50 g of uranium per liter for 24 hr was achieved with no apparent effect on the pump or pumping rate. In subsequent tests, pumping of slurries containing 150 and 300 g of uranium per liter caused no change in the pump characteristics. The slurry containing 300 g of uranium per liter was allowed to settle in all parts of the loop for 66½ hours. Resumption of circulation was achieved immediately upon starting the pump. Examination of the diaphragm in the pump gave no indication of unusual wear or surface deformation as a result of the test.

The low-pressure pulsafeeder pump loop has been converted for high-pressure operation, and it now includes a let-down heat exchanger and a let-down valve to mockup the let-down system of the HRE. Seven hours of intermittent operation at atmospheric pressure and at 1000 psi pressure have been logged with slurry containing 50 g of uranium per liter. Indications are that the  $UO_3 \cdot H_2O$  rod crystals are rapidly being broken into particles, small relative to the diameter of an original rod (1 to 5  $\mu$ ), in passing through the system. At present there is no indication that the small particle size will cause unsatisfactory operation of the system.

#### RECOMBINER DEVELOPMENT

J. A. Ransohoff

Preparatory to completing the recombiner design for the ISHR, a small (< 2 scfm  $2H_2 + O_2$ ) recombiner test unit has been built at Y-12 for studying quantitatively the effects of temperature, pressure, and  $I_2$  poisoning on both packed-bed and "tube-and-shell" recombiner units. The packed-bed unit uses alumina as its catalyst

## HRP QUARTERLY PROGRESS REPORT

support, and the tube-and-shell unit uses sputtered stainless steel tubing. In both cases, the catalyst used will be platinum reduced from chloroplatinic acid either by heating or by electrolysis.

Two groups of MIT Practice School students have made a study of the effect of  $O_2$  concentration on the catalytic reaction during the past

---

(16) T. W. Costikyan, C. B. Hanford, and D. L. Johnson, *The Catalytic Recombination of Hydrogen and Oxygen*, KT-130 (June 2, 1952).

year.<sup>(16,17)</sup> Using percentage recombination vs. space velocity as a criterion for recombining effectiveness, it was shown that recombining efficiency improved with higher  $O_2$  concentration. This indicates that diffusion of the gas is perhaps the controlling factor in the recombination process, since  $O_2$  has a much lower diffusion coefficient than  $H_2$ .

---

(17) J. V. Gaven, R. B. Bacastow, and A. C. Herrington, *Catalytic Recombination of  $H_2$  and  $O_2$  - II*, KT-134 (Aug. 29, 1952).

CORROSION

E. G. Bohlmann, Section Chief

DYNAMIC CORROSION TESTS

H. C. Savage      R. A. Lorenz  
D. Schwartz

**Westinghouse Model 100-A Pumps.** Ten pump loops are now in operation for studying the dynamic corrosion of various metals and alloys by uranyl sulfate and uranyl fluoride solutions. The Westinghouse model 100-A pumps used in these circulating loops have been described previously.<sup>(1)</sup> Twenty model 100-A and two model 30-A pumps have been received to date. These pumps are being used in the circulating test loops and in the HRE.

During the past quarter two pump failures occurred and brought the total number of pump failures to ten; four were due to leakage of uranyl sulfate through the 0.040-in.-thick Inconel diaphragm into the motor windings, which resulted in a breakdown of the electrical insulation. These leaks appeared to be unrelated to uranyl sulfate concentration and temperature, since failure occurred in pumps that circulated uranyl sulfate solutions at concentrations of 5, 40, and 100 g of uranium per liter and at temperatures up to 250°C. One pump has been in operation with uranyl sulfate solutions containing up to 700 g of uranium per liter with no apparent damage to the Inconel diaphragm. Metallurgical examination of the diaphragms that leaked has shown that the inferior material used in these diaphragms was the principal cause of failure.

Five pumps failed as a direct result of electrical insulation breakdown and subsequent short circuiting of the stator windings. This type of failure has occurred even though the cooling-oil circulation through the

stator windings was considered as adequate.

One pump failure was a direct result of improper operation. This pump was inadvertently operated in the HRE with no bearing lubrication and bearing seizure resulted; electrical insulation breakdown occurred as a result of current overload.

When it first became evident that pump failures might curtail the dynamic corrosion program, plans were initiated for the repair of pumps in the local shops. The pump repair program has been established, and model 100-A and model 30-A pumps can be completely rebuilt in a relatively short time. The Inconel diaphragms can be removed and new diaphragms, usually types 347 or 321 stainless steel, installed. The substitution of stainless steel for Inconel has resulted in very little loss in electrical efficiency and was made to improve the corrosion resistance of the diaphragm. When an electrical failure occurs, the pump stator is removed and rewound. At some points in the stator windings, the amount of insulation has been increased.

To date ten Westinghouse (nine model 100-A and one model 30-A) pumps have been repaired and returned to service. A cumulative operating time of approximately 8500 hr has been attained on the pumps repaired in the local shops with no failures to date.

A survey of the operating service of all pumps used in this program shows that the maximum time on one pump is about 9000 hr, and the pump is still in operation. A pump on a life test at Westinghouse Electric Corp. ran for about 14,000 hr before electrical failure occurred.<sup>(2)</sup> In

(1) H. C. Savage et al., *HRP Quar. Prog. Rep.* Mar. 15, 1952, ORNL-1280, p. 42.

(2) Private communication from A. J. Mei, Westinghouse Electric Corp., Atomic Power Div., Pittsburgh, Penna.

## HRP QUARTERLY PROGRESS REPORT

general, the pump bearings (Stellite 98M2 journals with Graphitar No. 14 bearings) are giving excellent service.

Pump thrust balance can be maintained for extended periods if corrosion does not occur around the impeller hubs, seal rings, or welded balance pads. One pump operating with uranyl sulfate solutions containing 300 g of uranium per liter at 100°C or 15 g of uranium per liter at 250°C has maintained thrust balance for more than 4000 hr, and bearing wear has been negligible. The pump with a titanium impeller and seal rings, installed in loop A, has been operated for more than 800 hr in uranyl sulfate solution containing 300 g of uranium per liter at 250°C. A mixture of hydrogen and oxygen was maintained in solution. The impeller and seal rings were not attacked by the solution, and pump thrust balance was maintained. The only noticeable effect of the solution was that a thin, black film deposited on the impeller surfaces. A type 347 stainless steel impeller would have been corroded beyond use in the same environment after 300 to 400 hr of operation.

The Westinghouse model 100-A pump with the flanges seal welded has been in service in the HRE for approximately 800 hr and appears to be operating satisfactorily. A second pump was seal welded, tested, and sent to the HRE Site as a spare for the present pump.

**Pump Loops.** One additional circulating loop, identified as loop I, was completed during the past quarter. This loop is of 1-in. type 347 stainless steel pipe with various types of welded and forged fittings and is now operating with uranyl sulfate solution. An all-titanium loop, identified as loop G, is still under construction and should be completed during the next quarter. Loop F, which has operated for more than 2000 hr at 250°C with uranyl sulfate solutions containing from 100 to 750 g of uranium per

liter, will be replaced with a new loop in the near future. The very great corrosion in this loop has been due to the high uranyl sulfate concentrations and temperatures used. Therefore a cross sectional examination of the entire loop will be made to evaluate qualitatively the areas of the loop most susceptible to corrosion and/or erosion attack.

**Heat Exchanger Tests.** A heat exchanger test assembly has been installed on loop H in a by-pass line. This assembly consists of a 1/4-in.-OD by 0.049-in.-wall type 347 stainless steel tube that is passed through a water jacket, as shown in Fig. 26. Two seal welds at one end of the test assembly simulate the entrance and exit welds of the heat exchanger now in use in the HRE. The tubing used in the test assembly is identical to that used in the tube bundle in the HRE heat exchanger.

The purposes of the test are to determine the effect on the over-all heat transfer coefficient of any corrosion scale or film formed after prolonged operation and to obtain an estimate of the over-all heat transfer coefficient under operating conditions of the HRE.

The temperature difference across the length of tubing is obtained by measuring the potential between couples 1 and 2, Fig. 26. These couples are constantan-type 347 stainless steel made by fusion welding constantan thermocouple wire to the type 347 stainless steel tube. A Leeds & Northrup microvoltmeter is used for this measurement. A calibration of the constantan-type 347 stainless steel couple had previously been made by the Instrument Department. Temperatures in the water jacket are obtained from three thermocouple wells, one of which is shown in Fig. 26. Here iron-constantan and constantan-type 347 stainless steel couples are used to measure both the absolute temperature and the temperature difference between

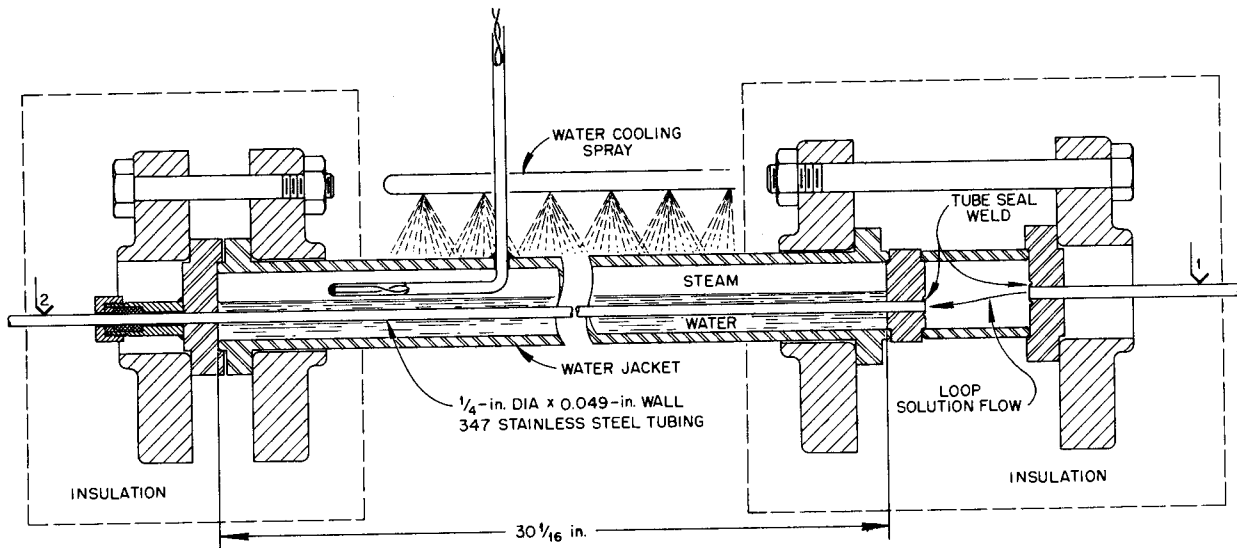


Fig. 26. Heat Exchanger Test Assembly.

the water or steam and the solution in the tube.

The present test procedure is to add sufficient distilled water to the water jacket to cover the tube. The water jacket chamber is sealed off after it is evacuated to about 25 in. Hg. The flow of uranyl sulfate solution through the 1/4-in. tube can be adjusted up to more than 40 fps for any given run in the present assembly. Heat flow is from the hot solution inside the tube to the water in the jacket. Heat is removed from the outside of the water jacket by means of a water spray, as shown in Fig. 26.

To date, some data have been obtained with uranyl sulfate solutions containing 40 g of uranium per liter and temperatures of steam and uranyl sulfate solution of about 200 and 250°C, respectively.

Results to date indicate that an over-all heat transfer coefficient at least as large as design calculations ( $\sim 1000 \text{ Btu/hr} \cdot \text{°F} \cdot \text{ft}^2$ ) at HRE operating conditions may be expected. These results and the effects of long-term operation are still being tested, and additional data are necessary

before detailed results can be reported. A report will be issued upon completion of the test.

#### PUMP LOOP CORROSION RESULTS

J. C. Griess      J. M. Ruth  
R. E. Wacker

A number of different systems were investigated in the circulating loops during the past quarter. In addition to the usual data obtained on the pin type of corrosion specimens, some preliminary data have been obtained on the effect of velocity on the corrosion rate of type 347 stainless steel. Included also in this report is a complete summary of all the pin data obtained to date. This summary will be brought up to date in subsequent quarterly reports.

**Solution Stability.** Most of the solutions tested during the past quarter were uranyl sulfate solutions containing various concentrations of uranium. In one case, a dilute solution of uranyl fluoride (5 g of uranium per liter) was run, and a series of short runs with a solution of uranyl fluoride (300 g of uranium

## HRP QUARTERLY PROGRESS REPORT

per liter) and 0.2M lithium hydroxide, pH ~ 3.9, has been completed. This last solution was suggested by W. L. Marshall.

All solutions investigated have shown adequate stability, with the following exceptions:

1. In the runs with either uranyl fluoride or uranyl sulfate solutions containing 5 g of uranium per liter, approximately 20% of the uranium always precipitated and the pH always decreased. At the completion of a run, crystals of  $UO_3 \cdot H_2O$  were found deposited on certain areas of the loop. The same general behavior has been observed with uranyl sulfate solutions containing 15 g of uranium per liter. The results have indicated a hydrolysis of uranyl ions accompanied by the formation of an equivalent amount of hydrogen ions.

2. The uranyl fluoride solutions (300 g of uranium per liter) with 0.2 M lithium hydroxide showed a high degree of stability at 250°C when the systems contained even very low oxygen pressures. However, in one run in which no oxygen was added to the solution, a heavy scale developed on all exposed surfaces. Chemical analysis showed that the scale contained

approximately 10% uranium. When oxygen was added, uranium oxides were not present in the film.

It has been known for some time that at least some of the  $UX_1$  (Th) in the natural uranium solutions deposits on the walls of the container during the course of corrosion experiments. To determine the extent of removal of the  $UX_1$ , samples of the solutions from several loops were submitted to S. A. Reynolds of the Analytical Chemistry Division for radiochemical analyses. The results of these analyses are given in Table 7 and show that under a number of conditions nearly complete removal of the  $UX_1$  from solution was obtained.

**Corrosion Data.** A complete summary of all the data collected on the pin type of corrosion specimens<sup>(3)</sup> included in the loops is given in Table 8. The corrosion rates of the systems as a whole (based on nickel determination of the solution) are not given, since generalized rates have little significance when it is considered that most of the attack is localized in areas of severe turbulence - for example, on the pump

<sup>(3)</sup>H. C. Savage et al., *HRP Quar. Prog. Rep.* Mar. 15, 1952, ORNL-1280, p. 46.

TABLE 7. THE PERCENTAGES OF  $UX_1$  REMOVED FROM URANYL SOLUTIONS UNDER VARIOUS CONDITIONS

RUN NO.	SALT	CONCENTRATION OF URANIUM (g/l)	pH	TEMPERATURE (°C)	$UX_1$ REMOVED (%)
B-24	$UO_2SO_4$ *	5	2.2	250	96
C-15	$UO_2SO_4$	300	1.7	150	0
E-8	$UO_2SO_4$	15	2.2	250	95
F-19	$UO_2SO_4$	100	2.4	250	86
H-11	$UO_2SO_4$	40	2.5	250	94
I-1	$UO_2SO_4$ *	40	1.4	250	49
J-20	$UO_2F_2$	5	2.6	250	97
K-11	$UO_2SO_4$	5	2.6	250	97

\*Solutions contained 25 mole % sulfuric acid.

TABLE 8. RESULTS OF PIN CORROSION TESTS

RUN NO.	TEST CONDITIONS						PIN MATERIAL	NO. OF PINS	CORROSION RATE (mpy)									
	Solution	Uranium Concentration (g/l)	Temperature (°C)	Time (hr)	Additions	Flow rate (fps + 10%)			Minimum	Average	Maximum							
K-2 through K-4	UO <sub>2</sub> SO <sub>4</sub>	5	250	1001	200 psi O <sub>2</sub>	15	Type 347 stainless steel	4	0.22	0.26	0.32							
							Type 304 stainless steel	2	0.21	0.22	0.22							
							Type 309 SCb stainless steel	2	0.17	0.20	0.22							
							Type 316 stainless steel	2	0.10	0.13	0.15							
							Type 321 stainless steel	2	0.10	0.11	0.12							
							Carpenter-20 steel	2	0.41	0.49	0.56							
K-5 through K-9	UO <sub>2</sub> SO <sub>4</sub>	5	250	2005	200 psi O <sub>2</sub>	12	Type 347 stainless steel	5	0.08	0.11	0.15							
							Type 347 stainless steel - pre-treated, N <sup>(*)</sup>	3	0.67	0.69	0.74							
							Type 347 stainless steel - pre-treated, C <sup>(*)</sup>	3	0.20	0.22	0.24							
							Type 347 stainless steel - pre-treated, O <sup>(*)</sup>	3	0.05	0.07	0.07							
K-10	UO <sub>2</sub> SO <sub>4</sub>	5	250	1413	200 psi O <sub>2</sub>	12	Type 304 stainless steel	2	0.27	0.29	0.30							
							Type 309 SCb stainless steel	2	0.40	0.49	0.57							
							Type 316 stainless steel	2	0.28	0.43	0.58							
							Type 321 stainless steel	2	0.21	0.22	0.22							
K-10 and K-11	UO <sub>2</sub> SO <sub>4</sub>	5	250	2229	200 psi O <sub>2</sub>	12	Type 347 stainless steel	3	0.23	0.25	0.28							
							K-11	UO <sub>2</sub> SO <sub>4</sub>	5	250	816	200 psi O <sub>2</sub>	12	Zirconium, arc-melted sponge	2 <sup>(*)</sup>			
														Zirconium, crystal bar	2 <sup>(*)</sup>			
								97.5% Zr-2.5% Sn alloy	2 <sup>(*)</sup>									
								95% Zr-5% Sn alloy	2 <sup>(*)</sup>									
L-10 and L-11	UO <sub>2</sub> SO <sub>4</sub>	5	250	1023	200 psi O <sub>2</sub>	15	Type 347 stainless steel	3	0.25	0.32	0.43							
							Type 304 stainless steel	2	0.27	0.27	0.27							
							Type 309 SCb stainless steel	2	0.42	0.42	0.42							
							Type 316 stainless steel	2	0.37	0.40	0.42							
							Type 321 stainless steel	2	0.23	0.25	0.27							
							Carpenter-20 steel	2	0.63	0.66	0.68							
E-7	UO <sub>2</sub> SO <sub>4</sub>	15	250	1065	200 psi O <sub>2</sub>	12 to 18	Worthite	1		0.62								
							Type 347 stainless steel	8	0.21	0.35	0.60							
							Type 347 stainless steel, cast	2	0.78	0.86	0.93							
							Type 304 stainless steel	6	0.19	0.35	0.69							
							Type 304 L stainless steel	4	0.24	0.47	0.70							
							Type 304 stainless steel, cast	2	0.88	0.92	0.96							
							Type 304 L stainless steel, cast	2	0.16	0.31	0.46							
							Type 309 SCb stainless steel	2	0.30	0.39	0.47							
							Type 309 SCb stainless steel, cast	2	0.56	1.1	1.6							
							Type 321 stainless steel	2	0.23	0.26	0.29							
							Stellite 25	2	460	600	730							
							C-7	UO <sub>2</sub> SO <sub>4</sub>	40	250	542	350 psi O <sub>2</sub>	28	Type 347 stainless steel	3	0.31	0.71	1.3
Type 304 stainless steel	2	0.50	0.69	0.88														
Type 309 SCb stainless steel	2	0.69	0.72	0.75														
Type 316 stainless steel	2	0.31	0.35	0.38														
Type 321 stainless steel	2	0.28	0.30	0.31														
Carpenter-20 steel	2	0.75	0.88	1.0														
H-10	UO <sub>2</sub> SO <sub>4</sub>	40	250	351	200 psi O <sub>2</sub>	17	Type 347 stainless steel	3	4.2	4.3	4.5							
							Type 321 stainless steel	3	3.0	3.3	4.4							
J-6	UO <sub>2</sub> SO <sub>4</sub>	40	250	131	200 psi O <sub>2</sub>	15	Type 347 stainless steel	13	9.2	16	24							
							Type 316 stainless steel	1		6.1								
J-7	UO <sub>2</sub> SO <sub>4</sub>	40	250	130	200 psi O <sub>2</sub> <sup>(c)</sup>	13	Type 347 stainless steel	6	3.4	3.8	5.2							
							Type 316 stainless steel	7	1.6	2.0	3.1							
J-8 and J-9	UO <sub>2</sub> SO <sub>4</sub>	40	250	410	200 psi O <sub>2</sub> <sup>(d)</sup>	13	Type 347 stainless steel	5	1.0	1.1	1.2							
							Type 347 stainless steel - pre-treated, O <sup>(*)</sup>	3	0.9	1.1	1.3							
							Type 347 stainless steel - pre-treated, C <sup>(*)</sup>	3	0.5	0.6	0.7							
								Type 347 stainless steel - pre-treated, N <sup>(*)</sup>	3	2.4	2.5	2.7						

PERIOD ENDING JANUARY 1, 1953

TABLE 8. (continued)

RUN NO.	TEST CONDITIONS						PIN MATERIAL	NO. OF PINS	CORROSION RATE (mpy)		
	Solution	Uranium Concentration (g/l)	Temperature (°C)	Time (hr)	Additions	Flow rate (fps + 10%)			Minimum	Average	Maximum
J-10	UO <sub>2</sub> SO <sub>4</sub>	40	250	152	200 psi O <sub>2</sub> , 1 g of SiO <sub>2</sub> /l	13	Type 347 stainless steel Type 304 stainless steel Type 309 SCb stainless steel Type 316 stainless steel Type 321 stainless steel Carpenter-20 steel Titanium (RC-70)	1 2 2 2 1 2 2	91 44 120 81 66 130 0	91 63 130 91 66 160 0	81 140 100 190 0
J-11 through J-14	UO <sub>2</sub> SO <sub>4</sub>	40	250	1048	80 psi O <sub>2</sub> , 150 psi CO <sub>2</sub> , 1 g of SiO <sub>2</sub> /l(*)	13 to 17	Type 347 stainless steel Type 304 stainless steel Type 309 SCb stainless steel Type 316 stainless steel Type 321 stainless steel Carpenter-20 steel Titanium (RC-70)	2 2 2 2 2 2 2	1.4 1.3 2.6 1.6 0.6 6 0	1.8 1.4 2.8 1.8 0.6 9 0	2.2 1.5 2.9 1.9 0.6 11 0
J-15	UO <sub>2</sub> SO <sub>4</sub>	40	250	451	220 psi O <sub>2</sub> , >1 g of SiO <sub>2</sub> /l	13	Type 347 stainless steel Type 304 stainless steel Type 309 SCb stainless steel Type 316 stainless steel Type 321 stainless steel Carpenter-20 steel Titanium (RC-70)	2 2 2 2 2 2 2	15 16 16 110 12 52 0.04	16 17 17 120 13 100 0.08	17 17 17 120 13 140 0.11
L-2 and L-3	UO <sub>2</sub> SO <sub>4</sub>	40	250	487	200 psi O <sub>2</sub> , 6.4 g of Cu/l as CuSO <sub>4</sub>	18	Type 347 stainless steel Type 304 stainless steel Type 309 SCb stainless steel Type 316 stainless steel Type 321 stainless steel Carpenter-20 steel Titanium (Ti-75A)	3 2 2 2 2 2 1	14 10 10 25 5.9 16 0.14	18 12 11 26 6.4 21 0.14	23 13 12 26 6.8 25
L-4 and L-5	UO <sub>2</sub> SO <sub>4</sub>	40	250	465	200 psi O <sub>2</sub> , 6.4 g of Cu/l as CuSO <sub>4</sub>	18	Type 347 stainless steel	12	2.7	3.8	5.1
L-5	UO <sub>2</sub> SO <sub>4</sub>	40	250	261	200 psi O <sub>2</sub> , 6.4 g of Cu/l as CuSO <sub>4</sub>	18	Type 347 stainless steel Type 347 stainless steel - pre- treated, C(*) Type 347 stainless steel - pre- treated, N(*)	5 4 4	1.9 4.1 2.2	2.5 4.3 2.3	3.2 4.5 2.5
C-9 through C-11	UO <sub>2</sub> SO <sub>4</sub>	100	100	1124	180 psi O <sub>2</sub>	20	Type 347 stainless steel	14	0	0.03	0.06
C-12 and C-13	UO <sub>2</sub> SO <sub>4</sub>	100	100	1726	180 psi O <sub>2</sub>	19	Type 347 stainless steel Type 304 stainless steel Type 309 SCb stainless steel Type 316 stainless steel Type 321 stainless steel Type 310 S stainless steel Carpenter-20 steel	3 2 2 2 2 1 2	0.06 0.11 0.06 0.07 0.11 0.03 0.08	0.08 0.13 0.07 0.08 0.13 0.03 0.09	0.09 0.15 0.08 0.09 0.14 0.12 0.10
B-22	UO <sub>2</sub> SO <sub>4</sub>	100	100	444	150 psi O <sub>2</sub>	13	Type 347 stainless steel Type 309 SCb stainless steel Type 316 stainless steel Type 321 stainless steel Type 310 S stainless steel Worthite	8 4 4 4 4 4	0 0 0 0 0 0	0.03 0.01 0.04 0.08 0.03 0.04	0.08 0.04 0.12 0.12 0.12 0.15
B-23	UO <sub>2</sub> SO <sub>4</sub>	100	100	1328	180 psi O <sub>2</sub>	13	Type 347 stainless steel Type 304 stainless steel Type 309 SCb stainless steel Type 316 stainless steel Type 321 stainless steel Type 310 S stainless steel Carpenter-20 steel	6 4 4 4 4 2 4	0 0.08 0 0.03 0.04 0 0.04	0.04 0.16 0.04 0.16 0.08 0.02 0.06	0.06 0.28 0.06 0.31 0.12 0.04 0.08

TABLE 8. (continued)

RUN NO.	TEST CONDITIONS						PIN MATERIAL	NO. OF PINS	CORROSION RATE (mpy)		
	Solution	Uranium Concentration (g/l)	Temperature (°C)	Time (hr)	Additions	Flow rate (fps + 10%)			Minimum	Average	Maximum
F-10	UO <sub>2</sub> SO <sub>4</sub>	100	150	317	225 psi O <sub>2</sub>	13	Type 347 stainless steel	2	2.1	2.3	2.4
							Type 304 stainless steel	2	1.3	1.4	1.4
							Type 309 SCB stainless steel	2	1.2	1.3	1.3
							Type 316 stainless steel	2	3.8	3.9	4.0
							Type 321 stainless steel	2	3.2	4.0	4.8
							Carpenter-20 steel	2	2.3	2.5	2.6
							Titanium (RC-70)	2	0	0	0
F-18	UO <sub>2</sub> SO <sub>4</sub>	100	250	163	200 psi O <sub>2</sub>	13	Type 347 stainless steel	3	27	32	40
							Type 304 stainless steel (f)	1		25	
							Type 304 L stainless steel	1		34	
							Type 309 SCB stainless steel	1		27	
							Type 316 stainless steel	1		44	
							Type 321 stainless steel	3	19	20	21
							Type 430 steel	1		10	
							Type 304 M stainless steel (f)	1		24	
F-18 and F-19	UO <sub>2</sub> SO <sub>4</sub>	100	250	472	200 psi O <sub>2</sub>	10	Type 347 stainless steel	4	9.0	9.6	10
							Type 304 stainless steel (f)	1		9.5	
							Type 304 L stainless steel	1		11	
							Type 309 SCB stainless steel	1		10	
							Type 316 stainless steel	1		15	
							Type 321 stainless steel	4	6.6	7.0	7.4
							Type 430 steel	1		5.8	
							Type 304 M stainless steel (f)	1		8.8	
E-3 through E-6	UO <sub>2</sub> SO <sub>4</sub>	300	100	2882	200 psi O <sub>2</sub>	10	Type 347 stainless steel	4	0.03	0.05	0.07
							Type 304 stainless steel	2	0.12	0.13	0.14
							Type 309 SCB stainless steel	2	0.02	0.03	0.03
							Type 316 stainless steel	2	0.07	0.08	0.08
							Type 321 stainless steel	2	0.15	0.19	0.22
							Carpenter-20 steel	2	0.08	0.18	0.27
C-14	UO <sub>2</sub> SO <sub>4</sub>	300	125	928	180 psi O <sub>2</sub>	17	Type 347 stainless steel	10	0.49	0.67	0.97
							Type 304 stainless steel	6	1.0	1.1	1.3
							Type 304 L stainless steel	4	1.0	1.0	1.1
							Type 304 stainless steel, cast	2	1.2	1.2	1.2
							Type 304 L stainless steel, cast	2	1.0	1.0	1.0
							Type 309 SCB stainless steel	2	0.20	0.26	0.31
							Type 309 SCB stainless steel, cast	2	0.38	0.42	0.46
							Type 321 stainless steel	2	1.0	1.1	1.1
							Stellite 25	2	1.6	1.6	1.6
F-2	UO <sub>2</sub> SO <sub>4</sub>	300	250	130	230 psi O <sub>2</sub>	12	Type 347 stainless steel	3	94	140	180
							Type 304 stainless steel	2	250	440	630
							Type 309 SCB stainless steel	2	430	510	590
							Type 316 stainless steel	2	430	440	440
							Type 321 stainless steel	2	89	100	110
							Carpenter-20 steel	2	440	540	630
							Titanium (Ti-75A)	1		0	
F-9	UO <sub>2</sub> SO <sub>4</sub>	300	250	47	15 psi O <sub>2</sub> , 200 psi He	12	Type 347 stainless steel	14	110	210	270
F-17	UO <sub>2</sub> SO <sub>4</sub>	270	250	209	80 psi O <sub>2</sub> , 150 psi CO <sub>2</sub>	20	Type 347 stainless steel	2	62	66	69
							Type 304 stainless steel	2	72	74	75
							Type 309 SCB stainless steel	2	54	65	75
							Type 316 stainless steel	2	83	120	160
							Type 321 stainless steel	2	56	60	63
							Carpenter-20 steel	2	130	160	180
							Titanium (RC-70)	2	0	0	0
A-28 and A-29	UO <sub>2</sub> SO <sub>4</sub>	300	250	96	100 psi O <sub>2</sub> , 200 psi H <sub>2</sub>	13	Hastelloy C (s)	2			
							Stellite 25	2	580	610	630

PERIOD ENDING JANUARY 1, 1953

TABLE 8. (continued)

RUN NO.	TEST CONDITIONS						PIN MATERIAL	NO. OF PINS	CORROSION RATE (mpy)				
	Solution	Uranium Concentration (g/l)	Temperature (°C)	Time (hr)	Additions	Flow rate (fpa + 10%)					Minimum	Average	Maximum
A-28 through A-30	UO <sub>2</sub> SO <sub>4</sub>	300	250	767	100 psi O <sub>2</sub> , 200 psi H <sub>2</sub>	13	Type 347 stainless steel	2	21	22	23		
							Type 304 stainless steel	2	24	26	27		
							Type 304 L stainless steel	2	23	30	36		
							Type 309 SCB stainless steel	2	15	18	22		
							Type 316 stainless steel	2	20	34	47		
							Type 321 stainless steel	2	10	14	17		
							Carpenter-20 steel	2	29	30	31		
							Titanium (RC-70)	8	0	0.02	0.2		
							Platinum	2	0	0	0		
							Hastelloy F	2	98	110	120		
Hastelloy X	2	28	31	33									
F-11	UO <sub>2</sub> SO <sub>4</sub>	300	250	120	200 psi O <sub>2</sub> , UO <sub>2</sub> U/SO <sub>4</sub> = 1.19	12	Type 347 stainless steel	1		100			
							Type 304 stainless steel	2	220	240	260		
							Type 309 SCB stainless steel	2	110	200	280		
							Type 316 stainless steel	2	400	430	460		
F-12	UO <sub>2</sub> SO <sub>4</sub>	235	250	138	200 psi O <sub>2</sub> , UO <sub>2</sub> , 5 g of Ni/l as NiSO <sub>4</sub> U/SO <sub>4</sub> = 1.09	12	Carpenter-20 steel	2	410	450	480		
							Titanium (RC-70)	2	0.14	0.21	0.28		
							Type 304 stainless steel	2	130	250	360		
							Type 309 SCB stainless steel	2	100	270	430		
F-13	UO <sub>2</sub> SO <sub>4</sub>	240	250	131	200 psi O <sub>2</sub> , 5 g of Ni/l as NiSO <sub>4</sub> U/SO <sub>4</sub> = 0.93	12	Type 316 stainless steel	2	620	660	700		
							Carpenter-20 steel	2	260	300	330		
							Titanium (RC-70)	2	0	0	0		
							Type 347 stainless steel	2	370	440	510		
F-14	UO <sub>2</sub> SO <sub>4</sub>	300	250	116	200 psi O <sub>2</sub> , fission products, etc. <sup>(A)</sup>	20	Type 309 SCB stainless steel	2	590	700	810		
							Type 316 stainless steel	2	520	560	600		
							Type 321 stainless steel	2	310	510	700		
							Carpenter-20 steel	2	520	530	530		
F-16	UO <sub>2</sub> SO <sub>4</sub>	686	100	67	200 psi O <sub>2</sub>	20	Titanium (RC-70)	2	0	0	0		
							Worthite	2	610	720	830		
							Type 347 stainless steel	2	10	320	630		
							Type 309 SCB stainless steel	2	9.5	230	450		
J-16	UO <sub>2</sub> F <sub>2</sub>	5	250	166	200 psi O <sub>2</sub>	15	Type 316 stainless steel	2	560	760	950		
							Type 321 stainless steel	2	9.0	10	11		
							Carpenter-20 steel	2	300	700	1100		
							Titanium (RC-70)	2	0.73	0.73	0.73		
H-1	UO <sub>2</sub> F <sub>2</sub>	300	250	29	200 psi O <sub>2</sub>	17	Worthite	2	480	720	950		
							Type 347 stainless steel	2	0.3	0.7	1.0		
							Type 304 stainless steel	2	0	0.4	0.8		
							Type 309 SCB stainless steel	2	0.8	0.9	1.0		
H-2 and H-3	UO <sub>2</sub> F <sub>2</sub>	300	250	369	200 psi O <sub>2</sub>	17	Type 316 stainless steel	2	0.3	0.7	1.0		
							Type 321 stainless steel	2	1.0	1.0	1.0		
							Carpenter-20 steel	2	0.3	0.4	0.5		
							Titanium (RC-70)	2	0.3	0.4	0.5		
H-1	UO <sub>2</sub> F <sub>2</sub>	300	250	29	200 psi O <sub>2</sub>	17	Type 347 stainless steel	4	0.20	0.66	1.4		
							Type 309 SCB stainless steel	2	1.5	1.7	1.8		
							Type 316 stainless steel	2	0.31	0.66	1.0		
							Type 321 stainless steel	2	1.4	1.6	1.7		
							Type 310 S stainless steel	2	1.5	2.1	2.6		
							Titanium (RC-70)	2	0	0	0		
							Type 304 M stainless steel <sup>(f)</sup>	1	0	0.10			
							Type 310 SM stainless steel <sup>(i)</sup>	2	1.5	2.0	2.4		
							Zirconium and zirconium alloys <sup>(j)</sup>						
							H-2 and H-3	UO <sub>2</sub> F <sub>2</sub>	300	250	369	200 psi O <sub>2</sub>	17
Type 304 stainless steel	2	36	41	45									
Type 309 SCB stainless steel	2	15	17	19									
Type 316 stainless steel	2	72	78	83									
Type 321 stainless steel	2	8.2	22	35									
Type 310 S stainless steel	2	8.2	33	57									
Titanium (RC-70)	2	0	0.3	0.6									
Type 347 stainless steel	2	2.9	3.0	3.0									
Type 316 stainless steel	1		1.9										
Type 321 stainless steel	1		2.2										
Titanium (RC-70)	2	0	0.1	0.2									

TABLE 8. (continued)

RUN NO.	TEST CONDITIONS						PIN MATERIAL	NO. OF PINS	CORROSION RATE (mpy)		
	Solution	Uranium Concentration (g/l)	Temperature (°C)	Time (hr)	Additions	Flow rate (fps ± 10%)			Minimum	Average	Maximum
H-1 through H-3	UO <sub>2</sub> F <sub>2</sub>	300	250	398	200 psi O <sub>2</sub>	17	Type 347 stainless steel	2	2.3	3.3	4.2
							Type 321 stainless steel	1		4.0	
							Titanium (RC-70)	2	0	0.2	0.4
H-5	UO <sub>2</sub> F <sub>2</sub>	300	250	82	150 psi O <sub>2</sub> , 50 psi CO <sub>2</sub>	17	Type 347 stainless steel	3	33	47	61
							Type 304 stainless steel	4	47	59	65
							Type 309 SCB stainless steel	4	24	32	38
							Type 316 stainless steel	4	42	49	54
							Type 321 stainless steel	4	25	30	36
							Type 310 S stainless steel	4	23	30	34
							Titanium (RC-70)	4	0.2	1.8	4.8
H-4(*)	UO <sub>2</sub> F <sub>2</sub>	300	250	133	200 psi O <sub>2</sub> , 1 g of Cu/l as CuF <sub>2</sub> U/2F = 1.05	17	Type 347 stainless steel	2	27	210	390
							Type 304 stainless steel	1		21	
							Type 309 SCB stainless steel	4	99	130	170
							Type 310 S stainless steel	4	30	42	55
H-6	UO <sub>2</sub> F <sub>2</sub>	300	250	49	200 psi He, 0.2 M LiOH <sup>(1)</sup>	17	Type 347 stainless steel	3	9	23	37
							Type 304 stainless steel	4	5.6	9.5	15
							Type 309 SCB stainless steel	3	13	43	67
							Type 316 stainless steel	4	0	6.7	12
							Type 321 stainless steel	3	7.3	7.8	8.7
							Type 310 S stainless steel	3	19	35	54
							Titanium (RC-70)	4	0.4	1.0	1.7
H-7	UO <sub>2</sub> F <sub>2</sub>	300	250	116	200 psi O <sub>2</sub> , 0.2 M LiOH	17	Type 347 stainless steel	2	7	43	80
							Type 304 stainless steel	4	7	41	75
							Type 309 SCB stainless steel	4	71	85	115
							Type 316 stainless steel	3	6	11	16
							Type 321 stainless steel	4	9	32	61
							Type 310 S stainless steel	4	72	80	89
							Titanium (RC-70)	4	0	0.4	0.9
H-8	UO <sub>2</sub> F <sub>2</sub>	300	250	49	5 psi O <sub>2</sub> , 200 psi He, 0.2 M LiOH	17	Type 347 stainless steel	3	65	83	97
							Type 304 stainless steel	4	66	76	80
							Type 309 SCB stainless steel	4	55	63	72
							Type 316 stainless steel	4	17	81	120
							Type 321 stainless steel	4	18	26	32
							Type 310 S stainless steel	4	55	73	87
							Titanium (RC-70)	4	0	0.3	0.7
J-18(*)	UO <sub>2</sub> F <sub>2</sub>	300	250	30	200 psi O <sub>2</sub> , 2.21 M NaF	15	Type 347 stainless steel	6	14	26	37
							Type 304 stainless steel <sup>(f)</sup>	2	14	15	15
							Type 309 SCB stainless steel	2	10	11	12
							Type 316 stainless steel	2	17	23	29
							Type 321 stainless steel	2	37	38	39
							Type 310 S stainless steel	2	22	22	22
							Titanium (RC-70)	2		>6 in./yr	
							Type 304 M stainless steel <sup>(f)</sup>	2	14	22	29
							Type 310 SM stainless steel <sup>(k)</sup>	2	26	29	32
							Type 430 steel	2	21	22	23
							Type 443 steel	2	30	31	31

PERIOD ENDING JANUARY 1, 1953

## Footnotes for Table 8.

(a) The letters N, C, and O refer to various pretreatments given to the type 347 stainless steel specimens: N means pretreated with 1%  $\text{HNO}_3$  for 24 hr at 250°C; C means pretreated with 2%  $\text{CrO}_3$  for 24 hr at 250°C; O means pretreated with 50 psi  $\text{O}_2$  for 24 hr at 250°C. The corrosion rates are based on the total weight loss by the pins as a result of the pretreatment and subsequent exposure to the uranyl sulfate solutions.

(b) To date, the zirconium pins have not been defilmed. Both the 97.5% Zr-2.5% Sn and the 95% Zr-5% Sn alloys showed small weight gains. One of the crystal-bar zirconium pins gained weight, whereas the other lost a small amount. The two arc-melted sponge pins lost substantial amounts.

(c) Run J-7 contained a cast impeller that had, among other inclusions, silica inclusions. The films developed on all specimens were distinctly different from those usually obtained.

(d) Run J-8, which lasted for 252 hr, contained the cast impeller; J-9, which lasted for 158 hr, contained a standard wrought impeller.

(e) The length of runs was as follows: J-11, 249 hr; J-12, 47 hr; J-13, 402 hr; and J-14, 350 hours. Runs J-11, J-12, and J-13 contained 200 psi  $\text{O}_2$  and 0.5 to 1 g of  $\text{SiO}_2$  per liter of solution. Run J-14 contained 80 psi  $\text{O}_2$ , 150 psi  $\text{CO}_2$ , and 1 g of  $\text{SiO}_2$  per liter of solution.

(f) A melt of type 304 stainless steel was split and to one portion was added a small amount of misch metal. The pins made from the portion containing the misch metal are designated 304M, and the pins designated 304 are those from the same melt without the added misch metal.

(g) The Hastelloy C had completely dissolved at the end of 96 hours.

(h) To simulate fission products, 100 ppm of each of the following elements was added: Ru, As, Ce, Ag, Nb, and Sn. In addition, 100 ppm of Ti, Bi, and Pb was also added. The metallic ions were added as either sulfates, nitrates, or oxides.

(i) Type 310 SM stainless steel is a regular melt of type 310 S containing an addition of a small amount of misch metal.

(j) Arc-melted sponge zirconium, crystal-bar zirconium, 97.5% Zr-2.5% Sn alloy, and 95% Zr-5% Sn alloy showed corrosion rates in excess of 2 in. per year.

(k) The corrosion rates given for run H-4 are based on scrubbed (not descaled) weights. The true corrosion rates were higher by an unknown amount.

(l) No oxygen was added. The only oxygen in the system was that dissolved in the solution before introducing it into the loop and that contained in the gas phase at the time the loop was closed.

(m) Run J-18 contained 2 pins of type 416 stainless steel, and both pins had corrosion rates in excess of 19 in. per year.

impeller or at sharp bends. Furthermore, the previous history of the loop has some bearing on its corrosion rate. This effect should be minimized on the pins. The corrosion rates given in Table 8 are expressed in mils per year and are based on the weight loss during the exposure time. The weight loss represents the amount of metal oxidized, since the corrosion products were removed from the surface (after exposure) by an electrolytic descaling method.<sup>(4)</sup> For brevity, in a run where more than two pins of the same alloy were included, only the minimum, maximum, and average rates are given.

Some of the recent loop runs have included coupons held in a tapered titanium holder.<sup>(3)</sup> Each holder contained ten coupons, and the velocity through the holder varied from approximately 10 fps at the entrance end to 70 fps at the exit end. At the end of a run, individual coupons were descaled and weighed. Figure 27 shows the results obtained to date. Each coupon is represented by a line parallel to the velocity axis. The length of this line represents the velocity range over the given coupon. It should be noted that with the solutions containing 100 and 15 g of uranium per liter, velocities above certain minimum values have a significant effect on the corrosion rate.

Experiments with dilute uranyl sulfate solutions (5 g of uranium per liter) to which sulfuric acid has been added in an effort to eliminate precipitation of uranium trioxide from the solution are being made. Although the complete results are not available, the preliminary data indicate that the addition of excess acid prevents the precipitation without greatly increasing the corrosion rate of the system as a whole. In one experiment, also incomplete, with excess sulfuric acid added to a uranyl

sulfate solution (40 g of uranium per liter), the generalized corrosion rate of the system (based on nickel analyses) appears to be somewhat higher than that in the system without sulfuric acid.

Since the chemistry of tetravalent plutonium and thorium exhibit certain similarities, it was thought that the behavior of the  $UX_1$  in the dynamic loops might be of value in predicting whether tetravalent plutonium would precipitate in the system. The results show that under most conditions nearly complete removal of the  $UX_1$  was achieved. The removal of the  $UX_1$  could have been caused by either hydrolysis or adsorption. Although the data do not allow a postulation of the mechanism, it is interesting to note that at least three variables are important: acidity, temperature, and uranyl ion concentration.

The data presented in Table 8, although not completely consistent, give a qualitative indication of how various conditions and additives affect the corrosion resistance of the several alloys tested. Before the data are considered, it should be pointed out that the reported corrosion rates in cases in which the pins accumulated heavy oxide coatings are very much dependent on the length of the run. Runs F-18 and F-19 are good examples of this. Run F-18 contained at least two pins of each of several different alloys; at the conclusion of the run, which lasted for 163 hr, one or more pin of each alloy was descaled and weighed. The other pins were not descaled but were exposed to the same solution for an additional 309 hours. At the end of run F-19, the remaining pins were descaled and weighed. The pins of each alloy lost the same amount of weight, within a few milligrams, regardless of whether they were exposed for 163 or 472 hours. These were the only runs in which this effect has been specifically investigated, but a number of other runs gave

(4) J. L. English and S. H. Wheeler, *HRP Quar. Prog. Rep. Mar. 15, 1952*, ORNL-1280, p. 68.

# HRP QUARTERLY PROGRESS REPORT

DWG. 17830

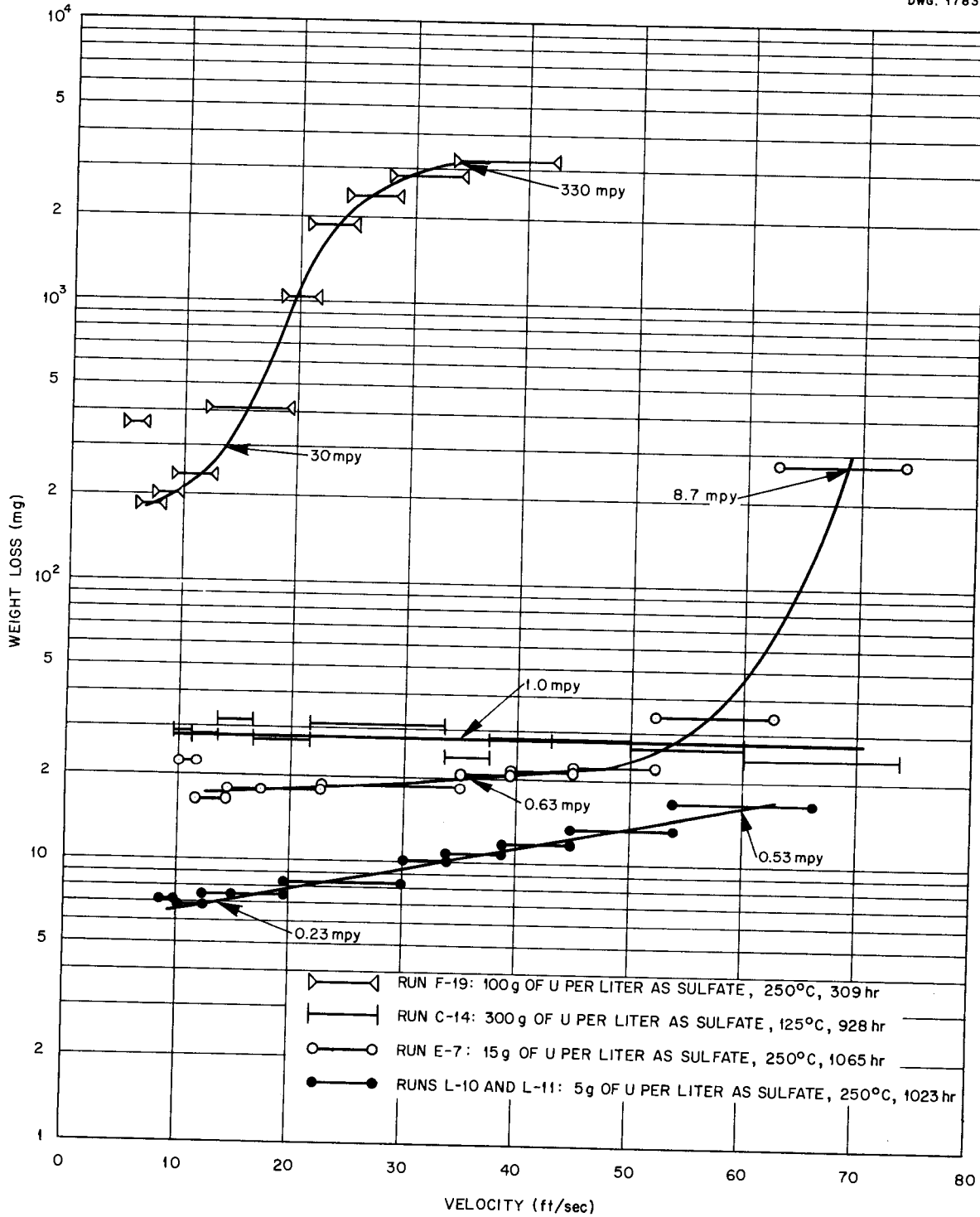


Fig. 27. Effect of Velocity on the Corrosion of Type 347 Stainless Steel Coupons.

## PERIOD ENDING JANUARY 1, 1953

the same indication; that is, the rate of attack is not constant but, in general, decreases with time. Hence, when comparing different conditions in Table 8, runs of similar duration should be compared.

All the runs in which the solutions contained 5 g of uranium per liter of uranyl sulfate showed fairly consistent results from one run to another. All the alloys tested had corrosion rates consistently below 0.5 mpy, with the exception of Carpenter-20. Similarly, low corrosion rates were observed with a low concentration of uranyl fluoride, although the rates appeared to be somewhat higher than with uranyl sulfate. However, on the basis of only one run of short duration, it is impossible to be sure that the observed increase was real.

Only one run in which the solution contained uranyl sulfate at a concentration of 15 g of uranium per liter has been completed to date. In this run (E-7), the corrosion rates appeared to be only very slightly higher than those in the less concentrated solutions. The data also show that, in general, the cast alloys corroded slightly faster than the corresponding wrought materials.

The corrosion rates observed in the solutions containing 40 g of uranium per liter of uranyl sulfate have been inconsistent, and in most cases there is no apparent explanation for such behavior. Additional information is being collected, and it is hoped that a better knowledge of the corrosion rates at this concentration level will be acquired. The effect of silica and cupric sulfate on the corrosion rates at this level is also not clear. Since it is desirable to incorporate a cupric salt in a reactor solution as a homogeneous gas-recombination catalyst, the effect of adding cupric sulfate to uranyl sulfate solutions on the corrosion resistance of several alloys will be reinvestigated.

The effects of additives and temperature on the higher concentrations of

either uranyl sulfate or fluoride are evident from the data in Table 8. In all cases, very low rates were obtained at temperatures between 100 and 125°C, whereas the rates were all high at 250°C. In no case was the effect of additives very significant. Some additions may have resulted in a slight lowering of the corrosion rates at high temperature; but even under the best conditions, the corrosion rates on all steels were too high for steel to be of practical value.

Titanium has shown a very high corrosion resistance to all uranyl sulfate solutions to which it has been exposed. A titanium impeller was used in runs A-28 through A-30, and even at 250°C with solution containing 300 g of uranium per liter, there was no evidence of attack on the impeller. In fluoride systems, titanium has not been so resistant to corrosion as in sulfate solutions but in most tests its resistance appeared to be superior to that of any of the steels investigated. However, it appeared that the addition of excess fluoride ions to uranyl fluoride solutions greatly reduced the corrosion resistance of titanium. This is clearly demonstrated in run J-18 in which the titanium specimens were drastically attacked.

The investigation of zirconium has just begun and will be intensified in the near future. However, run J-16 has clearly indicated that zirconium and its tin alloys are very badly attacked in fluoride systems. In sulfate systems, zirconium has a much higher corrosion resistance than in the fluoride systems, but at present insufficient data have been collected to compare it with other metals and alloys.

As indicated in Table 8, several alloys have shown very poor corrosion resistance to uranyl sulfate solutions at 250°C. Included in this group are Stellite 25, Hastelloy C, and Hastelloy F. Although Hastelloy X has shown somewhat better corrosion resistance

## HRP QUARTERLY PROGRESS REPORT

than the other Hastelloys, its corrosion resistance is inferior to that of most of the stainless steels. In nearly all cases Carpenter-20 and Worthite have been slightly less resistant than have most of the 300 series stainless steels.

The results obtained on the effect of the rate of flow of the solution past flat surfaces on the corrosion rate is apparent from Fig. 27. It is interesting to note that in the uranyl sulfate solutions containing 100 and 15 g of uranium per liter there appeared to be a critical velocity region in excess of which the corrosive attack was greatly accelerated and below which the corrosion rate was not greatly velocity dependent. At 250°C, the critical velocity appeared to be related to the corrosiveness of the solution. For example, in the solution containing 100 g of uranium per liter, the critical velocity appeared to be between 10 and 20 fps; at 15 g/l, between 50 and 60 fps; and at 5 g/l, no critical velocity was evident even at the highest velocity studied. The data obtained at 125°C with uranyl sulfate solution containing 300 g of uranium per liter show no effect of velocity on corrosion, and within experimental error the corrosion rate is the same at 10 fps as at 70 fps. At present, studies of the effect of velocity on corrosion are being continued with the hope of obtaining at least qualitative information of the relation between circulation rates and corrosion.

### SMALL-SCALE DYNAMIC CORROSION TEST PROGRAM

D. Schwartz      G. E. Moore

The effort during this quarter has been devoted to the development of a mechanism for giving the required motion to an assembly of toroids. The mechanical difficulties encountered necessitate further developmental effort.

### STATIC CORROSION STUDIES

J. L. English      S. H. Wheeler

#### Uranyl Sulfate Corrosion Studies.

The effort during the past quarter has been concerned with the initiation of several new corrosion investigations and an evaluation of existing static corrosion data for certain phases of stainless steel corrosion in uranyl sulfate solutions at 250°C. Since these projects are in various stages of completion, a detailed resume of data and results will be withheld for inclusion in the next quarterly progress report. Brief descriptions of the projects now under consideration are presented in the following sections.

*Corrosion Behavior of Synthetic Gems.* In conjunction with the development of a concentration measurement cell requiring a transparent window material for adsorption measurements, static corrosion tests are being run on synthetic sapphires in oxygenated uranyl sulfate solutions containing 40 and 300 g of uranium per liter at 250°C.<sup>(5)</sup> Preliminary test results indicated that synthetic sapphires possess good corrosion resistance in sulfate solutions at 250°C.<sup>(6)</sup> The present tests are concerned with the effect of uranium concentration on the corrosion resistance of the sapphires. Also under examination, with simulated conditions, is the effect on corrosion behavior of fission-product additions to uranyl sulfate solutions.

*Corrosion of Type 347 Stainless Steel at 125°C.* The corrosion behavior of type 347 stainless steel at 125°C as a function of uranium concentration is being studied. The test solutions are uranyl sulfate containing 40, 100, 200, and 300 g of

(5) W. H. Davenport, Jr. and R. H. Powell, *HRP Quar. Prog. Rep. Mar. 15, 1952*, ORNL-1280, p. 74-80.

(6) J. L. English, *Initial Report on the Corrosion of Fused Titania and Synthetic Sapphires in Uranyl Sulfate Solutions at 250°C*, ORNL CF-52-5-33.

## PERIOD ENDING JANUARY 1, 1953

uranium per liter; no excess dissolved oxygen is present in these systems. Chemical analyses of the test solutions at periodic intervals are being used to determine whether the sulfate systems are stable at this temperature in the absence of excess oxygen.

*Crevice Corrosion of Type 347 Stainless Steel.* The susceptibility of type 347 stainless steel to crevice corrosion is being investigated in uranyl sulfate solutions containing 300 g of uranium per liter at 100 and 250°C. Test specimens consist of 1- to 3-in. lengths of 1/4-in.-OD tubing pinched together at one end and 1- by 5-in. strips bent into a U with the open ends bolted together. The test solutions at 100°C are operated under conditions of complete deaeration (helium bubbling into solution), aeration with oxygen gas, and pressurization with 1000 psig of oxygen. The tests at 250°C are run under conditions in which the minimum quantity of dissolved oxygen necessary to ensure solution stability is present and also with pressurization of the solutions with 1000 psig of oxygen.

*Stress Corrosion of Type 347 Stainless Steel.* Stress corrosion studies with type 347 stainless steel are being run at 100°C in deaerated uranyl sulfate solutions containing 5, 40, 100, and 300 g of uranium per liter. The applied stresses being investigated range from 7500 psi in loaded-beam specimens to stresses exceeding the elastic limit for type 347 stainless steel in bent-tube specimens. Similar tests are being conducted with commercial-grade titanium metal.

*Evaluation of Stainless Steel Corrosion Data.* A compilation of existing static corrosion data for approximately 25 stainless steels and related alloys has been started to establish a merit rating based on corrosion behavior for the various materials exposed to closely controlled and similar test conditions. The first phase of this survey will

be confined to uranyl sulfate solutions containing 40 g of uranium per liter at 250°C with the following imposed conditions: (1) specimens pretreated for 24 hr at 250°C in 1% nitric acid prior to exposure and tested with no excess oxygen present, (2) test systems operated with an oxygen partial pressure of 25 psia at 250°C, and (3) test systems operated with an oxygen partial pressure of 500 psia at 250°C.

### **Uranyl Fluoride Corrosion Studies.**

The vapor- and solution-phase corrosion characteristics of type 347 stainless steel were investigated in oxygenated uranyl fluoride solutions at 250°C. The uranium content of the fluoride solutions was approximately 15 g/liter. Corrosion behavior was examined as a function of time over a period of four weeks.

Test specimens were prepared from 0.025-cm-thick cold-rolled, annealed, and pickled type 347 stainless steel sheet. No additional treatment was given the specimens before exposure. Quadruplicate sets of specimens were used for each exposure time of 1, 7, and 28 days in the solution and vapor phases. The tests were run in newly machined type 347 stainless steel autoclaves with 100 ml of test solution. Sufficient 30% hydrogen peroxide was added to the solution at room temperature to produce an estimated oxygen partial pressure of 150 psia at 250°C as a result of thermal decomposition of the peroxide. Specimens were supported in the corrosion environment by means of stainless steel wire hangers. At completion of the tests, the specimens were defilmed electrolytically in inhibited 5% sulfuric acid for 3 min at 75°C. The current density employed was 20 amp/dm<sup>2</sup>.

A summary of the defilmed weight losses and corrosion rates for the specimens appears in Table 9.

Pitting was observed on specimens after an exposure period of one week.

## HRP QUARTERLY PROGRESS REPORT

The magnitude of this attack did not appear to increase materially with time for solution-exposed specimens, but there was a definite increase with time in the frequency of pits on vapor-exposed specimens. The maximum pit depth, measured microscopically, did not exceed 2 mils for the four-week period.

### IN-REACTOR LOOP

G. H. Jenks            R. J. Kedl  
C. B. Graham        W. L. Ross

**In-Reactor Corrosion Studies** (G. H. Jenks). As reported previously, a

program has been undertaken to develop an in-reactor forced-circulation system for use in the study of the effect of irradiation on corrosion in homogeneous reactor systems. The design and development of this system is being carried out by the Engineering and Development group of the HRP under C. B. Graham, and design progress is reported by that group. Some of the more general aspects of the problem of carrying out corrosion studies with the in-reactor system are discussed here.

**General Arrangement of the Circulating System.** The general design of

**TABLE 9. CORROSION OF TYPE 347 STAINLESS STEEL IN OXYGENATED URANYL FLUORIDE CONTAINING 15 g OF URANIUM PER LITER AT 250°C**

EXPOSURE TIME (days)	SPECIMEN POSITION	SPECIMEN NUMBER	WEIGHT LOSS (mg/cm <sup>2</sup> )	CORROSION RATE (mpy)
1	Solution	1	0.15	2.8
		2	0.16	2.9
		3	0.14	2.6
		4	0.14	2.5
1	Vapor	1	0.11	1.9
		2	0.15	2.8
		3	0.07	1.3
		4	0.08	1.4
7	Solution	1	0.17	0.4*
		2	0.12	0.3*
		3	0.18	0.5*
		4	0.20	0.5*
7	Vapor	1	0.17	0.4*
		2	0.14	0.4*
		3	0.11	0.3*
		4	0.09	0.2*
28	Solution	1	0.21	0.1*
		2	0.21	0.1*
		3	0.23	0.2*
		4	0.25	0.2*
28	Vapor	1	0.22	0.1*
		2	0.21	0.1*
		3	0.14	< 0.1*
		4	0.13	< 0.1*

\*Semilocalized corrosion attack observed.

the in-reactor circulating system as it is presently visualized is similar to that outlined in an ORNL memorandum.<sup>(7)</sup> The system is essentially a small loop through which fuel solutions are circulated by a small centrifugal pump. This loop fits within a horizontal hole of the LITR, and the innermost portion is irradiated in a slow-neutron flux of about  $4 \times 10^{12}$  neutrons/cm<sup>2</sup>·sec. The irradiated portion of the loop is enlarged to permit an appreciable fraction of the fuel contained in the system to see the high-neutron flux. The over-all length of the loop, including the pump, is about 6 feet.

The total volume of fuel in the loop is about 1 liter. Of this volume, about 300 ml will be under neutron irradiation in the high-flux region at any instant.

Corrosion specimens are placed in the loop at two sites; one is near the outlet of the core but in the high-neutron-flux region; the other is at some point in the loop outside the high-flux region. With specimens in these positions, the effect on corrosion of fission products plus beta-gamma irradiation can be differentiated from the effect of fission recoils and fast-neutron irradiation plus other short-lived products of slow-neutron irradiation. Shielding for the loop is provided by the reactor shielding.

**Pressure Control.** One very important function that must be carried out with any in-reactor system is that of safely controlling the pressure of hydrogen and oxygen formed in the decomposition of water under irradiation. The solution to this problem in the in-reactor loop is by no means clear as yet, and the problem may be the deciding factor in determining the feasibility of the in-reactor system.

(7) G. H. Jenks, *Consideration of the Feasibility of Corrosion Studies with In-Pile Forced Circulation Systems*, ORNL CF-52-6-105.

The apparently most promising method of pressure control for the in-reactor loop involves the recombination of hydrogen and oxygen over a dry catalyst at the pressure of the system. Gases are circulated over the catalyst by means of a venturi type of pump that discharges into a liquid-gas separator. Gases from the separator are recirculated over the catalyst.

In practice, the system would be pressurized to 1000 psi with oxygen gas and the gas mixture circulated at a rate sufficient to maintain the hydrogen partial pressure at 1% or less, that is, below the explosive limit. Such a system can probably be designed to do this successfully. The problem of detecting a failure of the recombiner system before the partial pressure of hydrogen has reached the explosive limit appears to be more difficult. Studies made at Battelle<sup>(8)</sup> on explosion limits of hydrogen-oxygen-water systems show that such gas mixtures as will exist in the proposed systems may be reactive when the hydrogen partial pressure is 3 to 4% of the total pressure. If these values are accepted and if it is desired to keep the hydrogen pressure below this limit, methods of detecting changes in the performance of the recombiner system must be sensitive, reliable, and rapid. Detection methods are being explored that involve measurements of the pressure in the system, the rate of gas circulation, and the catalyst temperature.

**Handling of System Following Irradiation.** The necessary procedure for handling the system after it has been exposed to irradiation can be generally outlined as follows: the loop will be first drained of hot solution and purged to some extent; it will then be transferred to an appropriate site

(8) H. A. Pray, C. E. Schweickert, and E. F. Stephan, *Explosion Limits of the Hydrogen-Oxygen-Water System at Elevated Temperatures*, BMI-705 (Nov. 1, 1951).

## HRP QUARTERLY PROGRESS REPORT

where the corrosion specimens will be removed and examined. A loop will probably be used for only one in-reactor measurement. The corrosion specimens will be placed inside an all-welded system and will be removed by machining away the section that holds the specimens in position. The specimens will be left intact by this process. The portions of the loop that remain after the specimens are removed, with the possible exception of the pump, will be discarded.

The remote-handling facilities in the Solid State Building are adequate for carrying out most of the operations necessary for removing the corrosion specimens from the hot loop and for their subsequent examination. D. S. Billington and S. E. Dismuke have indicated that these facilities can be made available for this work.

However, the Solid State facilities are not designed to handle activity in a liquid form. Other means that must be provided for removing radioactive solution from the loop before it is moved from its operating position in the reactor and for purging and drying the system are being investigated. It may be feasible to drain and purge through tubes that connect the loop with suitable containers at the shield face. Final drying may be effected by evacuating the system from the shield face. Calculations have indicated that the required containers would not have to be prohibitively large. The principal uncertainty in emptying the loop by this method is the possibility that the connecting tubes may become plugged with corrosion products during operation. This question will be resolved by tests.

As indicated in the preceding paragraphs, some progress has been made in planning for the operation of the in-reactor loop. Planning of this type is prerequisite to the final design of the loop and will be continued.

**Loop Development and Design** (R. J. Kedl, W. L. Ross, C. B. Graham). The major components of the loop will be a centrifugal pump, a catalytic recombiner system, a loop temperature control system, and sample holders. The loop will be fabricated of type 347 stainless steel and will be designed for operating conditions of up to 250°C and 1000 psi. Figure 28 is a preliminary layout drawing of the loop.

The core vessel will probably be cylindrical, with tangential inlet and outlet, to give forced rotational flow. In this manner, the core will also serve as a gas separator for delivering gases to the recombiner and returning liquid to the circulating loop. Plastic models of the core are being built for testing to establish the flow pattern that gives adequate separation of the gas and liquid.

The specimens and sample holders will be designed to give reproducible corrosion data, if possible, and to give a basis for comparison with data being accumulated in the present out-of-reactor corrosion work. Out-of-reactor tests will establish and demonstrate as completely as possible the suitability of the specimen and holder designs without delaying other work with the LITR. Two of these samplers will be present in each loop. One will be adjacent to the outlet of the core where radiation and fission-product concentrations are highest. The other will be located about half way between the pump and the inlet of the core where radiation and fission-product concentrations are much lower because of the distance from the LITR core, fission-particle decay, and recombination of ions. It will probably be desirable to determine whether there is any change of the "critical corrosion velocity" in the presence of radiation and fission products. This can be done with a sample holder that is tapered to increase the fluid velocity.

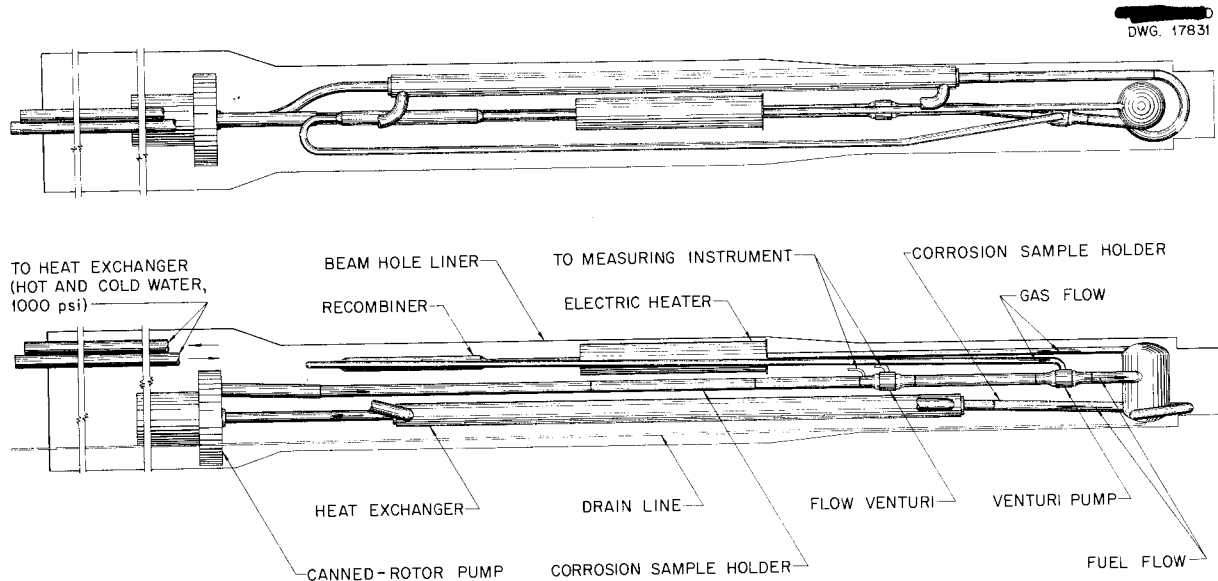


Fig. 28. Preliminary In-Reactor Circulating Loop Layout.

It appears that the Allis-Chalmers 5-gpm pump is not well suited for use with the in-reactor loop because it cannot be used to pump slurry satisfactorily; its chrome-plated hydraulic pressure bearings are subject to corrosion if hot uranyl sulfate solutions are pumped; and its holdup is large. Consequently, ORNL has undertaken the task of designing a pump similar to the Allis-Chalmers pump. This pump is described under "Small Canned-Rotor Pump Development."

The catalytic recombiner is the packed-bed type in which the catalyst is platinum-coated alumina pellets. The gas stream will be taken off the core, passed through the catalyst bed, and returned to the main loop through a venturi pump. One of the major problems involved with the recombiner system is to prevent the foam and entrained liquid, that may come over with the vapor stream, from reducing the efficiency of the catalyst or contaminating it. An arrangement of baffles or an entrainment separator followed by a heater in the gas stream will probably provide sufficient protection for the catalyst.

In the temperature control system it is planned to use an intermediate stream. This stream will be water at high temperature and pressure and can be circulated with an Allis-Chalmers, 5-gpm, canned-rotor pump. The intermediate stream will pass through the circulating loop heat exchanger and then to the outside of the reactor where it will be cooled or heated. The loop heat exchanger will be machined with large square threads on the outside so that the path of the intermediate stream in the exchanger jacket will be that of a helix; this type of flow will increase the heat transfer rate.

Preliminary considerations of the problem of handling the loop after it becomes radioactive indicate that a large amount of shielding will be necessary. Some facilities for remotely cutting out the sample holders are available. Following each run, the most expensive parts of the loop will be cut out and reused if they are not too radioactive. The parts that cannot be decontaminated will be buried. A liner will enclose the loop when it is placed in the LITR to

## HRP QUARTERLY PROGRESS REPORT

contain any fluid that leaks from the system.

Preliminary design of the in-reactor circulating loop is approximately 80% complete. The loop arrangement to fit into a horizontal thimble of the LITR is being studied. The filling, operating, and draining procedures, in-reactor operating conditions, and out-of-reactor service requirements for contaminated loops are being considered, but no definite plans have been formulated.

**Effect of Beta Irradiation on Corrosion** (G. H. Jenks). Another problem of current interest is that of determining the effect of beta irradiation on the corrosion of stainless steel by uranyl sulfate solutions at high temperatures. The results obtained by Sweeton and Yee<sup>(9)</sup> with in-reactor static bombs indicate that corrosion in these systems at 250°C is accelerated during irradiation. If corrosion is indeed influenced by irradiation, it will be of importance

<sup>(9)</sup>F. H. Sweeton, W. C. Yee, W. E. Hill, and H. F. McDuffie, *HRP Quar. Prog. Rep. Oct. 1, 1952*, ORNL-1424, p. 94.

to determine something of the mechanism by which the effect is brought about. A knowledge of the effect of beta irradiation on the corrosion should help to establish whether the ionizing characteristics of the reactor radiations are important in the effect.

Some planning for the experiment has been carried out. The Chemistry Division's Van de Graaff will be used as the source of beta rays in the studies. A cell for the irradiation has been designed and has been constructed by the shops. This cell is essentially a small bomb with a 30-mg stainless steel window through which the electrons enter the cell. The inner surface of the window is in contact with the solution to be tested, and the effect of irradiation on the corrosion of the window is observed. It is planned to stir the liquid in the bomb to assure that no large thermal gradients exist between the window and the bulk of the solution. A magnetic stirrer is being considered as the means for stirring. No experimental work has yet been done on this problem.

**METALLURGY**

E. C. Miller, Group Leader

W. J. Leonard, Metallurgy Division	A. R. Olsen, REED
W. J. Fretague, Metallurgy Division	F. J. Lambert, Y-12
T. W. Fulton, Metallurgy Division	J. C. Wilson, SSD
R. G. Berggren, SSD	

**SERVICE AND MISCELLANEOUS WORK**

E. C. Miller      T. W. Fulton

The service work performed by the Metallurgy group for other groups in HRP has increased substantially during the past quarter. Most of this work is reported in the sections prepared by the groups receiving the service, and only a few of the items will be listed here.

Metallographic service has been furnished in connection with examination of corrosion attack in the case of a type 304 stainless steel sample holder that apparently suffered a combination of intergranular attack and crevice corrosion and a type 347 stainless steel tube liner that split along a weld. The type 304 stainless steel sample holder exposed to uranyl sulfate solution containing 100 g of uranium per liter at 100°C for 1123 hr underwent severe deterioration beneath a tightly fitting type 347 stainless steel band, but it was apparently unaffected on the freely exposed surface. Metallographic examination revealed severe intergranular corrosion attack, which is assumed to be partly due to oxygen depletion of the stagnant solution beneath the band. Specimens cut from the unattacked material were subjected to the boiling nitric acid (Huey) test in the as-machined, sensitized, and fully annealed conditions. Characteristic results were obtained for the sensitized and fully annealed specimens, but the as-machined material was severely attacked, which indicated that the original stock had not been given a full anneal prior to machining of the sample holder.

Specimens from this sample holder are being prepared by various sensitizing and annealing treatments for controlled exposure under loop conditions. The severity of the attack indicates the necessity of using in the homogeneous reactor system only those materials and components that have been completely stabilized against intergranular attack.

Experimental assistance has been given to both the Design and Instrument groups in the development of suitable materials for service in valve parts. This assistance has included efforts to hard-surface titanium poppets, experimental fabrication of titanium parts, procurement and heat treatment of special stainless steels for nongalling applications, and the microscopic examination of such parts after removal from service. Considerable effort has been given to the metallurgical preparation of materials for both the Static and Dynamic Corrosion Test groups, and still further attention will be given to evaluating the results of corrosion testing of these variously prepared materials.

In connection with the longer range requirements of the Design group, attention has been given to the procurement, availability, fabrication, properties, and specifications of various potential construction materials for service in the dynamic, pressurized, moderate-temperature ISHR system.

**WELDING OF TYPE 347 STAINLESS STEEL**

W. J. Leonard

Plates of type 347 stainless steel 1 in. thick were welded by using

## HRP QUARTERLY PROGRESS REPORT

type 347 stainless steel bare rod and a type 347 stainless steel lime-coated electrode. A 60-deg included angle and a 1/8-in. root face with a single V groove were the pertinent variables in the welding design. The first three weld passes in the root were made by the inert gas or heliarc process, and 3/32-in. filler rod was used. The balance of the welding was completed by using a conventional 1/8-in. lime-coated-metal arc-welding electrode. The 1/8-in. root face was too large to permit complete and uniform penetration through the base of the root. Radiographs of the finished weld indicated that the weld was sound. The weld was sectioned transversely and macroscopic and microscopic examinations were made of the base metal, heat-affected zone, and weld metal. The constituents and conditions observed were normal for a type 347 stainless steel weld.

One-inch plates were welded by using a single U groove, a 50-deg included angle, a radius in root of 3/16 in., and a root face of 1/16 +0.015 -0.000 inch. The first four passes were made with 3/32-in. filler rod and the heliarc process. The remaining passes were made with 3/16-in. lime-coated electrodes. Penetration through the base of the root was normal. Radiographs, macrographs, and photomicrographs showed a normal, sound weld.

One-inch plates were welded by using the same U design on four more welds. The first of these was made from type 347 base plates by using four root passes with the heliarc process and 3/32-in. bare filler rod. The remaining passes were made with a 3/16-in. lime-coated type 307 stainless steel electrode. The composition of this welding rod is similar to that of type 347 stainless steel, except that it is about 1% higher in chromium, 1% less in nickel, and about 3% more in manganese; there

is no columbium or other stabilizing element present. Penetration in the root and soundness of the weld were satisfactory. Microscopic examination showed normal conditions and constituents in the weld and adjacent area.

Work was also done on welding type 347 stainless steel base plate to a boiler-grade carbon steel (type AISI 1028). The welding rods and procedures were exactly the same as those for the stainless steel to stainless steel welds. The root penetration and weld metal soundness were satisfactory, as shown by radiograph. Metallurgical conditions were normal in the weld area.

Type 347 stainless steel base plate was also welded to type AISI 1028 steel by using the same welding procedures, except that type 347 stainless steel lime-coated electrodes were used instead of type 307 stainless steel in the metal arc welding. Radiographs and metallurgical examination revealed a normal sound weld. The next weld of the same stainless steel and carbon steel base plates was performed by the coated metallic arc process by using a 1/8-in. type 307 stainless steel lime-coated electrode for the first two root passes and filling the groove with a 3/16-in.-dia electrode of identical composition. Again, nondestructive and microscopic examination showed a sound weld with the proper root penetration and a normal area surrounding the weld.

These welds were sectioned into strips containing a particular weld for which the mechanical properties are to be determined. They are being machined into standard tensile- and bend-test specimens.

Tentative specifications have been written for heavy section welding of type 347 stainless steel plate, pipe, and shapes. Procedural specifications and a welder's qualification outline are included in these specifications.

Two-inch plates of type 347 stainless steel have been obtained and machined to proper size to incorporate a definite welding design. Preliminary welding evaluation has been begun on these plates.

#### RADIATION DAMAGE STUDIES

R. G. Berggren      A. R. Olsen  
                                  N. E. Hinkle

Impact tests of a normalized carbon steel (described previously<sup>(1)</sup> as SAE 1040 steel, but found by analysis to be of the following composition: 0.167% C, 0.68% Mn, 0.208% S, 0.12% P, 0.04% Al) were made and the data plotted<sup>(2)</sup> for unirradiated control specimens and for specimens irradiated for periods of four and ten weeks (integrated flux above 0.1 Mev equal to  $8.3 \times 10^{17}$  nvt and  $3.0 \times 10^{18}$  nvt), respectively, in hole 1867 (donut hole) of the ORNL graphite reactor. The curves show that the transition temperature increases and the fracture energy decreases with increasing irradiation. This is in accord with the results of tests on ASTM type A-70 steel reported previously.<sup>(3)</sup> One fracture was made on a specimen that was heated for 1 hr to 305°C after irradiation in an attempt to anneal out the damage. The impact strength agrees with that of similar specimens that were only irradiated.

Samples of type 304 ELC stainless steel and the steel described above, irradiated in C-59 (vertical beryllium exposure piece) of the LITR, will be fractured when the impact tester has been installed in the hot cell. A new coolant system and hydraulic sample

positioner are being fabricated for the impact tester.

An experimental assembly was irradiated in hole HB-4 (horizontal beam hole) of the LITR. This assembly contained impact specimens of type 347 stainless steel, type 304 stainless steel, Ti-75A commercial-purity titanium, and arc-melted iodide titanium at 250°C in a helium atmosphere.

#### PROPERTIES OF TITANIUM

W. J. Fretague

**Impact Tests on Commercial Titanium (Ti-75A).** Impact tests have been performed on eight Ti-75A specimens that had been exposed to uranyl sulfate solution at 250°C in a type 347 stainless steel loop (loop A) by the Dynamic Corrosion group. Prior to exposure in the uranyl sulfate solution, these specimens were machined from 0.238-in.-dia Ti-75A rod. To produce this rod, 1-in.-dia commercial titanium bar (Ti-75A, Item 24, Heat L782) was swaged to 0.238-in.-dia rod, sand blasted to remove surface oxide, pickled in 2% HF, 8% HNO<sub>3</sub>, and 90% H<sub>2</sub>O for 15 min, rinsed in water and then in alcohol, and dried in a warm air blast. The material was then vacuum annealed at 500°C for 1 hr and furnace cooled prior to machining into corrosion-impact specimens. Table 10 lists the corrosion test history prior to impact testing.

Samples of broken impact specimens have been submitted for H<sub>2</sub>, O<sub>2</sub>, and N<sub>2</sub> analysis by the vacuum-fusion method. In most cases, three identical samples were submitted from each specimen in the following groups of specimens:

1. Ti-75A Specimens 18, 24, 26, and 28. These specimens were vacuum annealed at 500°C for 1 hr, furnace cooled, machined, and impact tested.<sup>(4)</sup>

(1) R. G. Berggren and R. H. Kernohan, *Solid State Quar. Prog. Rep. Jan. 31, 1952*, ORNL-1261, p. 20.

(2) R. G. Berggren and N. E. Hinkle, *Solid State Quar. Prog. Rep. Nov. 10, 1952*, ORNL-1429 (in press).

(3) R. G. Berggren, *Solid State Quar. Prog. Rep. Aug. 10, 1952*, ORNL-1359, p. 9.

(4) Fig. 54, p. 124, *HRP Quar. Prog. Rep. Oct. 1, 1952*, ORNL-1424.

# HRP QUARTERLY PROGRESS REPORT

**TABLE 10. TEST HISTORY OF EXPOSURE OF TITANIUM IN DYNAMIC CORROSION LOOPS**

SOLUTION	GAS PRESSURIZING	TEMPERATURE (°C)	TIME OF EXPOSURE (hr)	
			In H <sub>2</sub> O	In UO <sub>2</sub> SO <sub>4</sub>
Specimens 3, 5, 6, and 7				
3% Na <sub>3</sub> PO <sub>4</sub>	200 psi He	150	4.2	
5% HNO <sub>3</sub>	200 psi He	100	2	
H <sub>2</sub> O	200 psi He	100	2.2	
H <sub>2</sub> O	200 psi O <sub>2</sub>	250	76.0	
UO <sub>2</sub> SO <sub>4</sub> (300 g of U per liter)	140 psi H <sub>2</sub> , 70 psi O <sub>2</sub>	250		3.4
H <sub>2</sub> O	200 psi O <sub>2</sub>	250	84.0	
UO <sub>2</sub> SO <sub>4</sub> (291 g of U per liter)	140 psi H <sub>2</sub> , 70 psi O <sub>2</sub>	250		9.4
UO <sub>2</sub> SO <sub>4</sub> (296 g of U per liter)	200 psi O <sub>2</sub>	250		19.8
UO <sub>2</sub> SO <sub>4</sub> (296 g of U per liter)	140 psi H <sub>2</sub> , 70 psi O <sub>2</sub>	250		67.1
		Total	168.4	99.7
Specimens 1, 2, 4, and 8				
UO <sub>2</sub> SO <sub>4</sub> (300 g of U per liter)	200 psi H <sub>2</sub> , 100 psi O <sub>2</sub>	250		671

2. *Ti-75A Specimens 9, 10, 11, and 12.* These specimens received the same treatment as the first group plus 10 days of exposure in uranyl sulfate solution containing 40 g of uranium per liter at 250°C prior to impact testing.<sup>(4)</sup>

3. *Ti-75A Specimens 13, 14, 15, and 16.* These specimens received the same treatment as the first group plus cathodic treatment in 1 M H<sub>2</sub>SO<sub>4</sub> at 70°F for 8 hr prior to impact testing.<sup>(4)</sup>

4. *Ti-75A Specimen 19.* This specimen received the same treatment as the third group, except that the duration of the cathodic treatment was 168 hr instead of 8 hr. (See Fig. 29 for impact test results.)

5. *Ti-75A Specimens 3, 5, 6, and 7.* These specimens received the same treatment as the first group plus

99.7 hr of exposure in loop A to uranyl sulfate solution containing 300 g of uranium per liter at 250°C. (See Table 11 for corrosion test history and Fig. 29 for impact test results.)

6. *Ti-75A Specimens 1, 2, 4, and 8.* These specimens received the same treatment as the first group plus 671 hr of exposure in loop A to uranyl sulfate solution containing 300 g of uranium per liter at 250°C. (See Table 11 for corrosion test history and Fig. 29 for impact test results.)

Table 11 gives the vacuum-fusion analyses completed to date.

An examination of the experimental data presented in Fig. 29 and a comparison with the results obtained for annealed and untreated Ti-75A show that both short-time exposure

TABLE 11. TREATMENT OF IMPACT SPECIMENS

SPECIMEN NO.	MATERIAL	TREATMENT PRIOR TO IMPACT TESTING	H <sub>2</sub> (wt %)
18-6	Ti-75A	Vacuum annealed at 500°C for 1 hr and furnace cooled	0.011
26-1	Ti-75A	Vacuum annealed at 500°C for 1 hr and furnace cooled	0.008
9-3	Ti-75A	Exposed in UO <sub>2</sub> SO <sub>4</sub> solution (40 g of U per liter) at 250°C for 10 days; H <sub>2</sub> and O <sub>2</sub> in a 2:1 ratio at 750 psi at room temperature was maintained in the type 347 stainless steel bomb	0.010*
10-9	Ti-75A	Exposed in UO <sub>2</sub> SO <sub>4</sub> solution (40 g of U per liter) at 250°C for 10 days; H <sub>2</sub> and O <sub>2</sub> in a 2:1 ratio at 750 psi at room temperature was maintained in the type 347 stainless steel bomb	0.012**
11-6	Ti-75A	Exposed in UO <sub>2</sub> SO <sub>4</sub> solution (40 g of U per liter) at 250°C for 10 days; H <sub>2</sub> and O <sub>2</sub> in a 2:1 ratio at 750 psi at room temperature was maintained in the type 347 stainless steel bomb	0.012**, 0.011*
12-3	Ti-75A	Exposed in UO <sub>2</sub> SO <sub>4</sub> solution (40 g of U per liter) at 250°C for 10 days; H <sub>2</sub> and O <sub>2</sub> in a 2:1 ratio at 750 psi at room temperature was maintained in the type 347 stainless steel bomb	0.014*
16-9	Ti-75A	Cathodically treated in approximately 1 M H <sub>2</sub> SO <sub>4</sub> at 0.1 amp for 8 hr; temperature, 70°F	0.020
15-9	Ti-75A	Cathodically treated in approximately 1 M H <sub>2</sub> SO <sub>4</sub> at 0.1 amp for 8 hr; temperature, 70°F	0.018
14-8	Ti-75A	Cathodically treated in approximately 1 M H <sub>2</sub> SO <sub>4</sub> at 0.1 amp for 8 hr; temperature, 70°F	0.020
I-6A	Iodide titanium	Vacuum annealed at 500°C for 1 hr and furnace cooled	0.008
I-7A	Iodide titanium	Vacuum annealed at 500°C for 1 hr and furnace cooled	0.017

\*Brown corrosion product abraded.

\*\*Sample covered with brown corrosion product.

PERIOD ENDING JANUARY 1, 1953

# HRP QUARTERLY PROGRESS REPORT

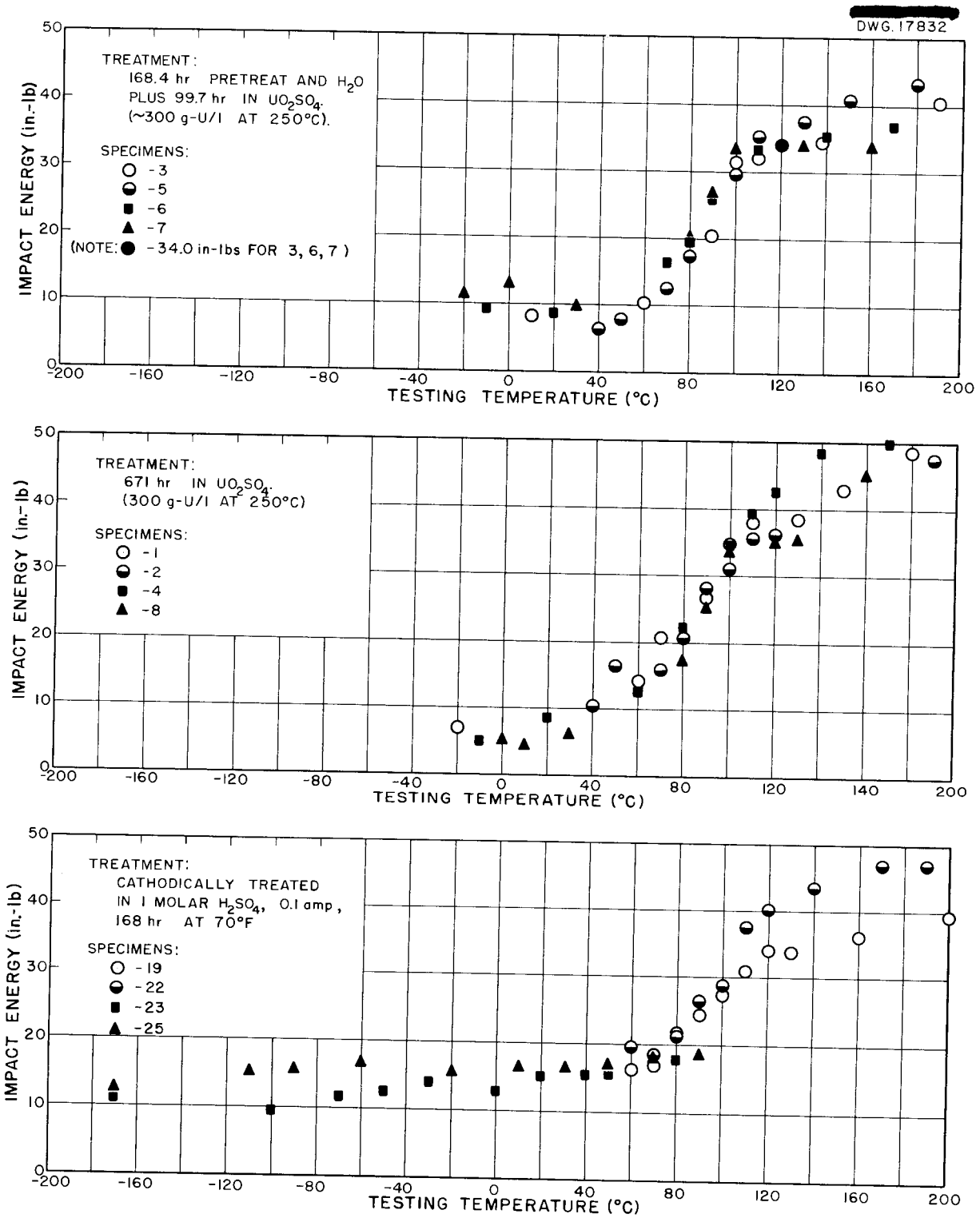


Fig. 29. Compilation of Impact Test Results on Commercial Purity Titanium (Ti-75A) Specimens.

(100 hr) and longer time exposure (671 hr) to uranyl sulfate solution containing 300 g of uranium per liter in a dynamic system (loop A) have not appreciably affected the ductility of the Ti-75A material. Similarly, the ductility of Ti-75A cathodically treated in  $H_2SO_4$  for 8- and 168-hr periods and of Ti-75A exposed to uranyl sulfate solution containing 40 g of uranium per liter at 250°C in a static system (bomb) for 10 days has not been affected.

It appears from the analytical results obtained to date that none of the environments to which Ti-75A specimens have been exposed have caused an appreciable increase in the amount of hydrogen present in the metal.

**Work in Progress.** Seventeen pounds of U. S. Bureau of Mines sponge titanium was received during the past quarter. This material is intermediate in purity between commercial titanium and iodide titanium. The chief difference between the Bureau of Mines sponge titanium and Ti-75A is in the oxygen and nitrogen content of the two materials. By employing the intermediate purity material, it is hoped that valuable information will be obtained on the effects of oxygen and nitrogen on the transition temperature observed in commercial titanium. One 96-g arc melt of this Bureau of Mines titanium sponge (Lot 1056, R 83A) has been prepared and swaged into rods for impact specimens. These rods will be vacuum annealed at 600°C for 1 hr and furnace cooled prior to machining; the finished, machined specimens will be employed to establish the transition temperature of Bureau of Mines titanium. Present plans call for several more melts of sponge titanium to be fabricated into specimens for corrosion testing prior to impact testing.

Melting stock for zirconium-titanium alloys (iodide zirconium and iodide titanium) has been weighed out and

submitted to the melting, casting, and fabrication laboratory of the Metallurgy Division for preparation of five small (approximately 185 g) arc melts of the following nominal composition: 95% Zr, 5% Ti; 90% Zr, 10% Ti; 80% Zr, 20% Ti; 70% Zr, 30% Ti; and 100% Ti. The first four zirconium-titanium alloy melts will be used for corrosion and impact specimens; part of the pure titanium melt will be used to prepare an experimental pump part, and the remaining part will be rolled into sheet and vacuum annealed for use as titanium washers.

A Ti-75A impact specimen will be used by W. J. Sturm of the Solid State Division to study the effect of cyclotron bombardment on the impact properties of vacuum-annealed Ti-75A. In these experiments, protons will be used to bombard the specimen, and each proton will cold work the specimen for the next proton; essentially, then, the hydrogen (ionized) will be entering cold-worked titanium. In the first series of tests there will be only five individual impact breaks, but more specimens can be furnished for cyclotron bombardment if the preliminary results look promising.

In order to prepare some Ti-75A specimens for fatigue testing, it was necessary to secure sheet material of approximately 0.030-in. thickness. Since this thickness of material was not readily available, it was decided to hot roll 1/4-in. titanium (Ti-75A) plate. The titanium was sealed in an evacuated, airtight container to prevent oxidation during the repeated heating cycles required for hot rolling. Eight conventional picture frames and 16 covers of cold-rolled steel plates were prepared in the Metallurgy machine shop. The pieces of 1/4-in.-thick Ti-75A plate were inserted in the picture frames and the assemblies were welded. These assemblies are now being leak checked in the rolling mill and will be evacuated and sealed for rolling as

## HRP QUARTERLY PROGRESS REPORT

soon as the necessary equipment becomes available for use. After the material has been rolled to the proper thickness, specimen blanks will be cut from the sheet and vacuum annealed. Present plans call for fatigue tests on annealed specimens, on specimens exposed to uranyl sulfate solution at 250°C in such a way that the solution contacts all parts of the specimen blank, and on specimens exposed to uranyl sulfate solution at 250°C in such a way that the solution contacts only one face of the specimen (this can be accomplished by welding two specimen blanks together).

Metallographic examination of a broken impact specimen of Ti-75A that had been treated in uranyl sulfate solution containing 40 g of uranium per liter for 10 days did not reveal any visible surface concentration of hydrogen. However, it was found that the vacuum annealing treatment of 1 hr at 500°C, followed by furnace cooling, did not cause recrystallization. To determine the recrystallization temperature of Ti-75A that has been supposedly annealed previously at 500°C, eight broken impact specimens (one from each 10 3/4-in.-long specimen) were vacuum annealed at 600°C for 1 hour. Metallographic examination of these reannealed samples revealed that the material was completely recrystallized after the latter treatment.

To investigate the effect of cold work on the transition temperature previously determined for Ti-75A, four 10 3/4-in. machined impact specimens are being vacuum annealed at 600°C for 1 hour. To investigate the effect of cold work on the rate of hydrogen absorption of Ti-75A in uranyl sulfate solution under dynamic conditions, eight 10 3/4-in.-long machined Ti-75A are being vacuum

annealed at 600°C for 1 hour and furnace cooled. Four of these specimens will be corrosion tested as described above in the annealed condition, and four will be cold worked slightly by abrading the surface with fine emery paper prior to corrosion testing. Samples of the as-annealed material prior to testing, and of the annealed and of the cold worked material after corrosion testing, will be submitted for hydrogen determination by vacuum-fusion analysis to determine the effect of cold working on the rate of hydrogen absorption by Ti-75A from uranyl sulfate solution at 250°C.

**Impact Tests of Iodide Titanium.** Impact tests were performed on specimens fabricated from six iodide titanium melts. The data obtained plus those obtained earlier on specimens I-7-1 and I-8-1 are plotted on Fig. 30. These data represent 34 individual impact tests in the temperature range between -196 and +200°C. All specimens except I-1-A were vacuum annealed at 500°C for 1 hr and furnace cooled. Specimen I-1-A was vacuum annealed at 950°C for 1 hr and furnace cooled.

Four vacuum-annealed iodide-titanium impact specimens were delivered to the Corrosion group at Y-12 for dynamic corrosion testing in uranyl sulfate solution prior to impact testing. Two iodide-titanium impact specimens were delivered to the Solid State Division for radiation damage study. It is planned to expose these two specimens in the LITR.

A trial run is planned in the Sievert's apparatus. If this is successful, a series of iodide titanium, Bureau of Mines arc-melted sponge titanium, and commercial titanium (Ti-75A) impact specimens will be loaded with hydrogen to study the effect of large amounts of hydrogen on the impact properties of titanium.

DWG. 17833

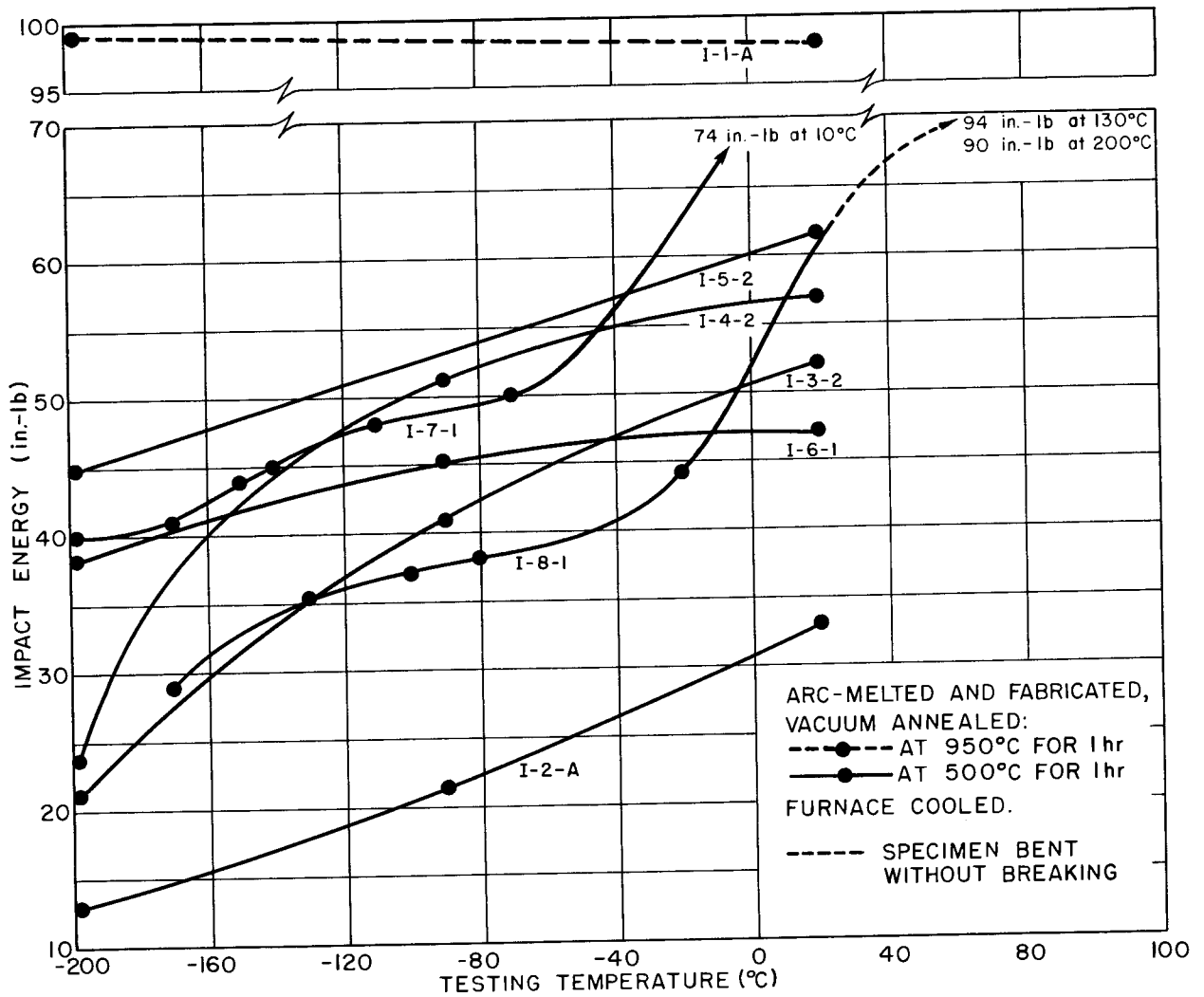


Fig. 30. Compilation of Impact Test Results on Iodide Titanium Specimens.



## AQUEOUS SOLUTION AND RADIATION CHEMISTRY

C. H. Secoy, Group Leader

### RADIATION STUDIES OF URANYL FLUORIDE AND URANYL SULFATE SOLUTIONS

F. H. Sweeton      W. C. Yee

In a recently completed experiment, uranyl fluoride solution was exposed in a stainless steel bomb in the ORNL graphite reactor. The primary differences in this experiment (H5) and the previously reported experiment H2 were the substitution of  $\text{UO}_2\text{F}_2$  for  $\text{UO}_2\text{SO}_4$  and the use of  $0.03\text{ M}$   $\text{CuF}_2$  instead of  $0.01\text{ M}$   $\text{CuSO}_4$ . In both cases, 2.5 ml of solution (room temperature) was added to 5.0-cm<sup>3</sup> bombs constructed of type 347 stainless steel. Sufficient  $\text{O}_2$  in the form of  $\text{H}_2\text{O}_2$  was added to give a partial pressure of about 900 psi at 250°C. In the fluoride test the bomb was etched with HF solution before the test but was not pretreated with chromic acid as was the sulfate bomb. Both solutions contained 40 g of uranium (93% enriched) per liter. The tests were made in a flux of approximately  $3.5 \times 10^{12}$  neutrons/cm<sup>2</sup>·sec, which gave a power density of 6 kw per liter. Both irradiations were carried out at 250°C; however, during the fourth and fifth weeks of the fluoride test the temperature was raised to 260°C in order to control the total pressure. The fluoride test was run for nine weeks, and the total uranium burnup is calculated to be about 1.0%. The oxygen partial pressure during the fluoride irradiation was about 1100 psi at the start and 500 psi at the end. The oxygen partial pressure at the end of the test was produced by the remaining excess oxygen plus the oxygen produced by the decomposition of the water.

The amount of excess oxygen remaining each week was determined in the same manner as described in the previous report. The quantity remaining

has been converted to average corrosion over the surface of the bomb wetted by the solution. The results of both the fluoride and sulfate tests are shown in Fig. 31. The sulfate solution data are those given in the previous report except for a correction in error in calculation that amounts to about 20% for each of the points. The average corrosion rate over the nine-week period is 3.5 mpy. An out-of-reactor control test indicated a corrosion rate of approximately 0.9 mpy over a six-day period. Thus neutron irradiation appears to make  $\text{UO}_2\text{F}_2$  solutions, as well as  $\text{UO}_2\text{SO}_4$  solutions, more corrosive to type 347 stainless steel. The fluoride solution appears to have essentially the same initial rate of corrosion as the sulfate solution, but a more increased rate later.

The  $\text{UO}_2\text{F}_2$  solution, like the  $\text{UO}_2\text{SO}_4$  solution, appeared to gradually lose uranium as a precipitate. Pressure data recorded immediately after a periodic lowering of the temperature to 210°C were analyzed and used to

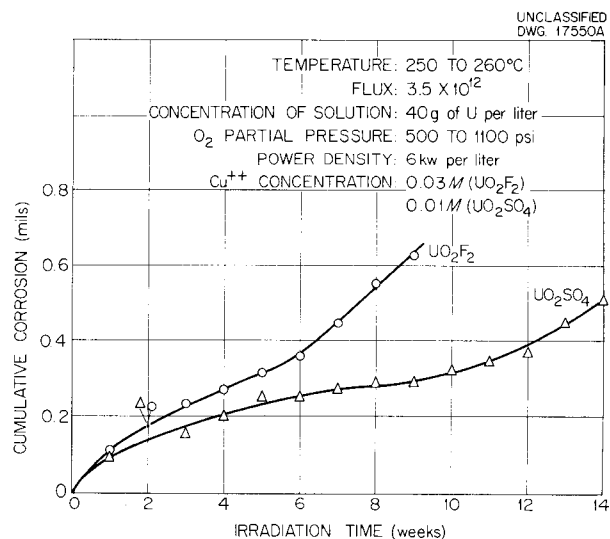


Fig. 31. Corrosion of Type 347 Stainless Steel by  $\text{UO}_2\text{F}_2$  and  $\text{UO}_2\text{SO}_4$  Under Neutron Irradiation.

## HRP QUARTERLY PROGRESS REPORT

calculate the uranium in solution by making use of the known G value. The results are shown in Fig. 32, where the calculated fraction of uranium still in solution is plotted against the loss in partial pressure of excess oxygen. Since the data appear to fall on a straight line, there is indication that the loss of uranium is directly related to the corrosion process. The slope of the line drawn through these points corresponds to the precipitation of 1 mole of uranium for each mole of nickel oxidized and gives circumstantial support to the belief that the oxidized nickel converts an equivalent amount of  $UO_2F_2$  to  $UO_3$ , which precipitates.

The analysis of the solution after the irradiation showed that about 20% of the uranium was still in solution, which is a reasonable check with that indicated by Fig. 32. Only about 30% of the copper originally added was found in solution after completion of the irradiation. The oxygen absorption data indicated that 23 mg of nickel should have been oxidized, but only about 15% of this was found in the solution.

### EFFECT OF LOW OXYGEN PRESSURE ON CORROSION OF TYPE 347 STAINLESS STEEL IN RADIATION

In a recent experiment (H7), a uranium sulfate solution containing 40 g of uranium per liter and 0.01 M  $CuSO_4$  was irradiated in a stainless steel bomb at 250°C. The excess oxygen present in the bomb was much less than that in experiment H2; consequently, the oxygen partial pressure during irradiation was only about one-third of that in the earlier experiment. The resulting corrosion was significantly less during the first week but then increased to significantly more for the remaining week and a half of the test. This experiment will be reported in detail after the solution has been analyzed.

UNCLASSIFIED  
DWG. 17549A

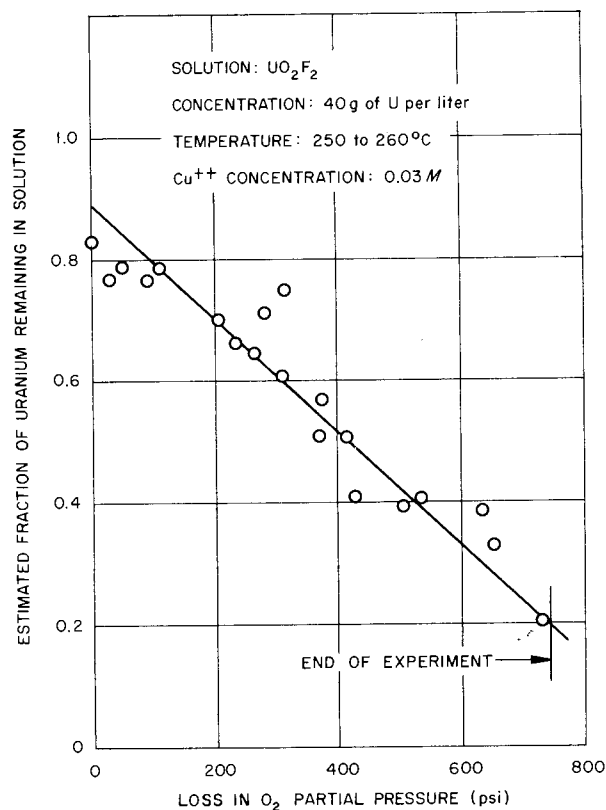


Fig. 32. Uranium Precipitation as Calculated from Apparent G Value.

### RADIATION CHEMISTRY OF AQUEOUS REACTOR SOLUTIONS

J. W. Boyle

**Effect of pH on Gas Production.** It has been shown<sup>(1)</sup> that acidity has an effect on  $G_{H_2}$  for a uranyl sulfate solution containing 105 g of uranium per liter and for a uranyl fluoride solution containing 377 g of uranium per liter. The amount of gas produced per unit energy input was decreased by an increase in acidity.

In the work reported here, the acidity has been varied from pH 0.60 to 3.48 by adding either  $H_2SO_4$  or NaOH to a  $UO_2SO_4$  solution containing approximately 40 g of uranium (93.2%

(1) J. W. Boyle et al., *Radiation Chemistry of Aqueous Reactor Solutions*, ORNL CF-52-8-103.

enriched) per liter. Eight ampoules were irradiated at 120°C for 3 min each at a power density of about 1 kw per liter. All the gas produced (99.7% or better) was identified as hydrogen, oxygen, and condensable CO<sub>2</sub>. G<sub>H<sub>2</sub></sub> for the unaltered (pH) UO<sub>2</sub>SO<sub>4</sub> solution agreed exactly with previously found values.<sup>(1)</sup> The results are presented in Fig. 33.

No acid effect was found in the pH range of 1.4 to 3.5, but a lowering in G<sub>H<sub>2</sub></sub> of about 3% was observed in going from pH 1.41 to 0.60. The studies of the effect of pH will be extended to solutions of greater uranium concentrations in which acidity appears to have a more pronounced effect.

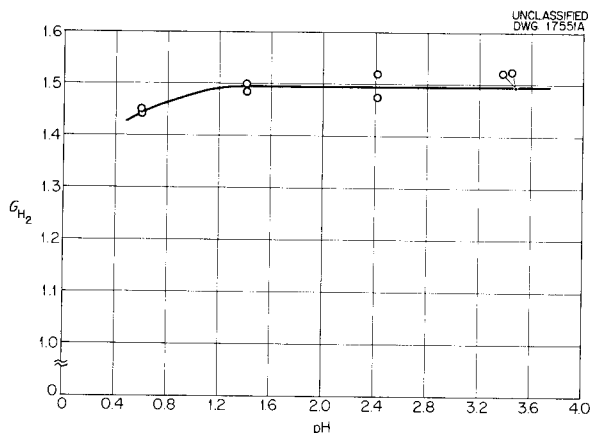


Fig. 33. Effect of pH on G<sub>H<sub>2</sub></sub> for UO<sub>2</sub>SO<sub>4</sub> Solution Containing 40 ± 1 g of Uranium per Liter (93.2% U<sup>235</sup>).

**MECHANISM OF THE HYDROGEN-OXYGEN  
RECOMBINATION REACTION IN SOLUTIONS**

H. F. McDuffie                      L. F. Woo

During the past quarter attention has been focused upon the mechanism of the homogeneous recombination reaction catalyzed by dissolved copper salts. Previous work<sup>(2)</sup> with copper sulfate dissolved in uranyl sulfate

<sup>(2)</sup>H. F. McDuffie et al., *HRP Quar. Prog. Rep.* Mar. 15, 1952, ORNL-1280, p. 161-172.

solutions has indicated the following information about the reaction:

1. It is first order in dissolved copper from 0.005M to at least 0.05 M.
2. It is first order in hydrogen and independent of oxygen pressure at least from a 2:1 ratio of hydrogen to oxygen to a 1:1 ratio.
3. It is effective in recombining hydrogen and oxygen formed *in situ* from fissioning solutions.
4. It is responsive to geometry and diffusion in such a way as to permit inference of the rate of the reaction in the solution phase from measurement of the pressure changes in the associated gas phase.
5. It presumably involves a slow rate-controlling reaction of dissolved hydrogen with cupric copper (in a 1:1 ratio), followed by a very rapid oxidative regeneration of the cupric copper with simultaneous formation of water.

6. A rate constant for the reaction was expressed as  $k_{Cu} = [Cu]^1 \times 5.9 \times 10^{13} \exp(-24,000/RT) \text{ hr}^{-1}$ .

The particular items concerning the mechanism of the reaction to be discussed in this quarterly report include the significance of the frequency factor and the effects of added sulfate-containing solutes.

**Frequency Factor.** For bimolecular reactions between neutral molecules (or presumably between a neutral molecule and an ion if there are no substantial changes in hydration), there are two values that may be considered as normal for the frequency factor: 10<sup>11</sup> and 10<sup>7</sup>. The first value corresponds to a reaction every time the molecules come within a distance of the order of a molecular diameter of each other; the second value requires that in the activated complex the two molecules are essentially bonded to each other.<sup>(3)</sup> When the frequency factor in the expression for the rate constant for copper

<sup>(3)</sup>G. K. Rollefson, *J. Phys. Chem.* 56, 976 (1952).

## HRP QUARTERLY PROGRESS REPORT

(presented above) is divided by 60 to express the constant in appropriate units ( $\text{min}^{-1}$  instead of  $\text{hr}^{-1}$ ), it becomes approximately  $10 \times 10^{11}$ . This is considered as very good agreement for the case in which there is a reaction every time the copper ion and hydrogen molecule approach each other in the solution (if they have the required energy); that is, there is no evidence here that a highly specific orientation of the reacting species is necessary.

**Effect of Added Solutes.** By using the technique for determining  $k_{\text{Cu}}$  described earlier,<sup>(2)</sup> values have been determined at  $250^\circ\text{C}$  for solutions  $0.0008\text{ M}$  in  $\text{CuSO}_4$  and containing

various amounts of added sodium sulfate, sulfuric acid, sodium bisulfate, and potassium sulfate. These values are presented in Table 12 and are shown also in Fig. 34.

It seems probable that both sulfate ions and hydrogen ions may be involved in the reaction, possibly in opposite ways. It is planned to attempt to separate and elucidate these effects by using the perchloric acid-lithium perchlorate system, if this system is stable under the experimental conditions. The competitive effects of copper vs. stronger sulfate complexing agents, for example, zirconium, will be considered as a possible indication of the relative complexing power of

**TABLE 12. EFFECT OF ADDED SOLUTES ON HYDROGEN-OXYGEN RECOMBINATION RATE OVER  $0.0008\text{ M}$   $\text{CuSO}_4$ \* AT  $250^\circ\text{C}$**

EXPERIMENT NO.	SOLUTE ADDED	MOLARITY AT ROOM TEMPERATURE	pH AT ROOM TEMPERATURE	$k_{250^\circ\text{C}}$
B-18	None		5.13	6,708
24	$\text{Na}_2\text{SO}_4$	0.0005	5.38	3,629
25	$\text{Na}_2\text{SO}_4$	0.0010	5.42	1,644
26	$\text{Na}_2\text{SO}_4$	0.0015	5.38	800
23	$\text{Na}_2\text{SO}_4$	0.002	5.44	761
22	$\text{Na}_2\text{SO}_4$	0.004	5.45	638
21	$\text{Na}_2\text{SO}_4$	0.006	5.44	624
19	$\text{Na}_2\text{SO}_4$	0.010	5.44	519
20	$\text{Na}_2\text{SO}_4$	0.100	5.68	396
47	$\text{H}_2\text{SO}_4$	0.0004	3.1	11,208
33	$\text{H}_2\text{SO}_4$	0.001	2.7	20,638
34	$\text{H}_2\text{SO}_4$	0.002	2.43	19,728
35	$\text{H}_2\text{SO}_4$	0.003	2.25	19,273
40	$\text{NaHSO}_4$	0.001		12,648
41	$\text{NaHSO}_4$	0.002		13,891
36	$\text{K}_2\text{SO}_4$	0.001		2,525
37	$\text{K}_2\text{SO}_4$	0.002		1,720
38	$\text{K}_2\text{SO}_4$	0.003		1,443

\* $0.001\text{ M}$  at room temperature.

various cations at high temperatures. The effect of changes in the total ionic strength will be determined to gain information as to the charge type of the reaction. Since one of the reactants (hydrogen) is neutral, it is rather expected that changes in ionic strength will not materially affect the recombination rate constants.

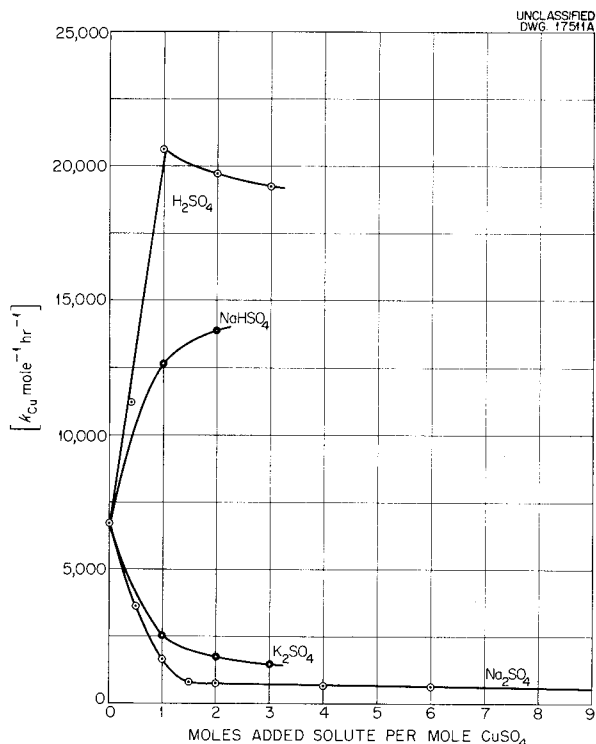


Fig. 34. Effect of Added Solute on Rate of H<sub>2</sub>-O<sub>2</sub> Recombination at 250°C for Solutions with 0.008 M CuSO<sub>4</sub> (0.001 M at Room Temperature).

CATALYTIC DECOMPOSITION OF HYDROGEN PEROXIDE IN URANYL SULFATE SOLUTIONS

M. D. Silverman

Several series of experiments have been conducted in the study of the catalytic decomposition of hydrogen peroxide in uranyl sulfate solutions since the last report. More detailed studies of the decomposition of hydrogen peroxide at 100°C in uranyl

sulfate solutions have revealed that iron added as Fe(III) is a better catalyst than Fe(II) by a factor of approximately 1.5. However, promoter action by cupric ion is slightly more effective with Fe(II) than with Fe(III). Furthermore, it has been found that Cu(II) in a concentration of 6 to 10 ppm is sufficient for promoter action. In all previous work a copper concentration of 793 ppm had been used.

Another potential corrosion catalyst, Mn(II), was investigated, and its catalytic properties were found to be negligible in these systems.

A safe power level for operation of the HRE at 100°C, indicated as approximately 400 kw in the previous quarterly report, is based on a steady-state concentration in the reactor of 15 ppm of both iron and ruthenium. It is doubtful whether the ruthenium will ever reach such a concentration in solution because hydrolysis is extremely rapid at this temperature and at the pH of the reactor solution. However, it is probable that the iron concentration will exceed 15 ppm. Promoter action by added Cu(II) would increase the permissible power level to approximately 600 kw.

SOLUBILITY OF URANIUM TRIOXIDE IN AQUEOUS URANYL SULFATE AND URANYL FLUORIDE

E. V. Jones J. S. Gill  
W. L. Marshall

In previous reports on the solubility of UO<sub>3</sub> in aqueous UO<sub>2</sub>SO<sub>4</sub> and UO<sub>2</sub>F<sub>2</sub> at 175°C<sup>(4)</sup> and at 250°C,<sup>(4,5)</sup> it was pointed out that the behavior of the sulfate system in the low concentration region was uncertain.<sup>(4)</sup> The question as to whether the equilibrium ratio, U to SO<sub>4</sub>, drops below

(4) E. V. Jones, J. S. Gill, and W. L. Marshall, HRP Quar. Prog. Rep. Oct. 1, 1952, ORNL-1424, p. 105.

(5) J. S. Gill, E. V. Jones, and W. L. Marshall, HRP Quar. Prog. Rep. July 1, 1952, ORNL-1318, p. 144.

## HRP QUARTERLY PROGRESS REPORT

1.00 in this region is still unanswered, partly because of analytical difficulties for very low concentrations of sulfate. Efforts are being made to resolve these difficulties.

In the previous reports it was stated that, "In most of the experiments on the fluoride system at 250°C, corrosion of the titanium filter bombs and some reduction of uranium was noted, but this attack was not evident at 175°C." This statement must now be revised as follows: the corrosion of the titanium filter bombs and some reduction of uranium have been found in the sulfate system also and in the fluoride system at 175°C, as well as at 250°C. However, at 175°C this reduction of uranium, which occurred in two or three days in the filter bombs with titanium plated iron stirrers operated by solenoid, had not occurred even in ten or twelve days in titanium filter bombs that were "rocked" in heated aluminum cylinders without stirrers. A black deposit on one side of a stirrer from a filter bomb that had been placed in a slightly inclined position suggested that the corrosion and reduction of uranium might be due to the rubbing of the stirrer against the side of the bomb. Snugly fitted teflon caps were put over the ends of the stirrers, and eleven runs at 250°C and three at 175°C in  $\text{UO}_2\text{SO}_4$  solutions have shown no reduction of uranium.

Studies are being made of the solubilities of  $\text{UO}_3$  in aqueous  $\text{UO}_2\text{F}_2$  at

25°C and at 100°C; the data will be presented in a later report.

Studies are also being made on the equilibration time for  $\text{UO}_3$  in 1.25 M  $\text{UO}_2\text{SO}_4$  and in 1.25 M  $\text{UO}_2\text{F}_2$  at 25°C. Preparations are being made for similar studies at 100°C.

### OXIDATION STATES OF FISSION PRODUCTS IN REACTORS

D. W. Sherwood

A study of the chemical states of iodine in environments related to those likely to prevail in homogeneous reactors has been started. Apparatus has been built, and a search of the applicable literature is being made. The immediate objective is the determination of the rates of oxidation and reduction of the several oxidation states of iodine.

**Other Work.** Phase study of the two-liquid phase region in the three-component system,  $\text{UO}_3\text{-SO}_3\text{-H}_2\text{O}$ , is in progress. Most of the past quarter has been devoted to the construction of apparatus by which a thermostatic method involving volume measurements can be employed. This technique, if successful, will yield information about the vapor phase, as well as about each of the liquid phases.

Corrosion of type 347 stainless steel by  $\text{UO}_2\text{F}_2\text{-NaF}$  solutions is being investigated. Results will be reported later.

## SLURRY CHEMISTRY

F. R. Bruce, Section Chief

UO<sub>3</sub> CHEMISTRY

**Preparation of Pure UO<sub>3</sub>·H<sub>2</sub>O Platelets** (J. O. Blomeke, L. E. Morse). A more thorough investigation of the methods of preparing high-purity platelets has become necessary because the preparation of UO<sub>3</sub>·H<sub>2</sub>O slurries in the platelet form with small particle size is tedious and lengthy, and trace quantities of soluble uranium salts have been shown to markedly promote crystal growth and caking. The obvious criteria for a suitable preparation would be: (1) the starting material should be commercially available or easily prepared from such a material; (2) the method should be as short and as simple as possible; and (3) the resulting product should be both of a suitable particle size for use in a slurry and of sufficient purity that its slurry properties do not become impaired during its use as a slurry fuel. Past experience has dictated that a satisfactory product should contain uniform platelets that average 3 μ or less on a dimension and yield less than 10 ppm of soluble uranium on being heated in water at 250°C at a concentration of 250 g of uranium per liter.

*Preparation with Mallinckrodt or Harshaw UO<sub>3</sub> Starting Material.* The most logical starting material for large-scale slurry preparation would be either the Mallinckrodt oxide or the Harshaw oxide, which are commercially available. Both are prepared by the thermal decomposition of uranyl nitrate. In addition, the Harshaw product is subjected to a size reduction step. Both materials contain 1.4 to 1.5 wt % of soluble uranium as uranyl nitrate. Either would be suitable for use as a starting material if the soluble uranium could be efficiently removed.

Exhaustive washing of the Mallinckrodt material was found to reduce the soluble uranium to 0.3 to 0.5%. Hydration of the washed oxide at 100°C and calcination at 400°C resulted in a product composed of very hard lumps that were difficult to break up and slow to hydrate. Upon autoclaving at 250°C, platelets were obtained that were about 25 to 30 μ on an edge. After five cycles of calcination at 400°C and hydration at 250°C, the average particle size was about 7 μ, which was too large for use as a slurry and indicated that there was a substantial uranium content in the supernatant.

After the Harshaw oxide was washed at 850°C and treated further by 3 cycles of alternate calcination (350°C) and hydration (250°C), it yielded a product containing large and very irregular platelets. The supernatant contained 38 ppm of soluble uranium calculated on the basis of 250 g of uranium per liter (Table 13). Additional treatment would, of course, be necessary to produce a satisfactory slurry.

Autoclaving the Harshaw oxide at 250°C without previous washing resulted in considerable caking. Heating at 400°C and at 520°C for 16 hr reduced the amount of uranium extracted by washing at 85°C. Subsequent hydration at 250°C resulted in the formation of very bad cakes and the release of a large amount of soluble uranium.

An attempt was made to remove the nitrate impurity from the Harshaw oxide by passing superheated steam through a bed of the material maintained at 230°C. Tests of the effluent steam indicated an acid component. When the apparatus was disassembled, a partial decomposition to U<sub>3</sub>O<sub>8</sub> was noted, which was evidence, presumably, of overheating. Channeling had also occurred within the oxide bed. The product oxide yielded 0.2% soluble uranium on

# HRP QUARTERLY PROGRESS REPORT

TABLE 13. PREPARATION OF SLURRY-GRADE  $UO_3 \cdot H_2O$  FROM  $UO_3$  (HARSHAW)

OPERATION	TEMPERATURE (°C)	TIME (hr)	SOLUBLE URANIUM IN SUPERNATANT
Water wash	85	0.5	1.4% of total weight
Hydration	250	16	540 ppm*
Calcination and hydration (I)	350	16	154 ppm*
	250	16	
Calcination and hydration (II)	350	16	95 ppm*
	250	16	
Calcination and hydration (III)	350	16	38 ppm*
	250	16	

\* Solubility calculated on the basis of a slurry containing 250 g of uranium per liter as  $UO_3 \cdot H_2O$ .

extraction with hot water. Experimental difficulties with the high-temperature autoclave prevented a study of the behavior of this material on hydration at 250°C. Further investigation of this nitrate removal procedure is planned.

It would appear from the above that neither of the commercially available oxides is a suitable starting material for the production of  $UO_3 \cdot H_2O$  platelets by the calcination-hydration procedure without some pretreatment.

*Preparations with  $UO_4 \cdot H_2O$  and  $UO_3 \cdot H_2O$  Rods as Starting Material.* Both  $UO_4 \cdot 2H_2O$  and  $UO_3 \cdot H_2O$  rods may be easily prepared from an acid solution of the oxide by simple precipitation of the peroxide and hydration of this material at 250°C to the rods. Either type of rod, presumably, could be a starting material for the production of monohydrate platelets.

Calcination of  $UO_4 \cdot 2H_2O$  at 350°C yielded an oxide easily processed further by the calcination-hydration procedure previously described. (1)  $UO_3 \cdot H_2O$  platelets that were about 10  $\mu$  on the large dimension and several microns thick were formed after the

first autoclaving. After five cycles, the platelets had been reduced to an average particle size of about 5 microns. The concentration of uranium in the supernatant from the fifth autoclaving was 23 ppm.

$UO_3 \cdot H_2O$  rods were the most difficult crystals to break down. Long, thin platelets were formed after two cycles of calcination at 375°C and subsequent hydration at 250°C. A total of five cycles resulted in platelets that were about 4  $\mu$  on a dimension. The uranium concentration following the fifth autoclaving was 4 ppm, which indicated a high-purity product.

These results indicate that either the peroxide or the rods would be suitable for the preparation of platelets by a calcination-hydration procedure, with the rods being slightly more attractive.

*Preparations with  $(NH_4)_4UO_2(CO_3)_3$  as Starting Material.* It has been noted that many metallic oxides when prepared by the thermal decomposition of the carbonate or an organic salt of the metal are obtained as powders of low bulk density and high surface area, which should enhance the removal of volatile materials by a calcination

(1) J. O. Blomeke, *HRP Quar. Prog. Rep. Oct. 1, 1952*, ORNL-1424, p. 28.

PERIOD ENDING JANUARY 1, 1953

procedure. Accordingly, an investigation is being made of the possibility of utilizing ammonium uranyl carbonate (AUC) in the preparation of  $UO_3$  for use in the calcination-hydration procedure for the production of platelets. Preliminary results indicate that pure  $UO_3 \cdot H_2O$  platelets may be obtained more easily from this material than from the other materials investigated (cf., Table 14).

Two methods were used to prepare the AUC. In one method, ammonium diuranate was precipitated from a uranyl nitrate solution and then metathesized to AUC in a concentrated solution of ammonium carbonate. In the second method, uranyl ion was adsorbed from a nitrate solution onto Dowex-50 cation resin. The resin was then washed free of nitrate and the uranium eluted with ammonium carbonate. Details of the latter method are being investigated with the cooperation of I. R. Higgins and T. J. Roberts of the Ion Exchange group in this division.

The AUC products so obtained were subsequently decomposed at  $350^\circ C$ . The oxide products were washed for 1 hr at  $90$  to  $100^\circ C$ , recalcined at  $350^\circ C$ , and hydrated to platelets at  $250^\circ C$ . After

a second calcination-hydration cycle, the supernatants in all cases (cf., Table 14) were found to contain not more than 10 ppm of uranium, which indicated the oxide to be of the desired purity. Further investigation of this method of preparing the platelets is planned.

**Particle Size Determinations and Sedimentation Rates (L. E. Morse).** The work on the relation between particle size measurements and sedimentation rates in slurries containing 250 g of uranium per liter as  $UO_3 \cdot H_2O$  in water has been continued. In the previous quarterly report,<sup>(2)</sup> an expression relating particle size and sedimentation rates was shown to be applicable to slurries containing 100 g of uranium per liter but not to slurries with higher concentrations of uranium.

Hatch and Isakoff,<sup>(3)</sup> by proceeding from the consideration that sedimentation in concentrated suspensions of solid particles is one aspect of the flow of fluids through porous

(2) L. E. Morse, *HRP Quar. Prog. Rep. Oct. 1, 1952*, ORNL-1424, p. 29.

(3) L. P. Hatch and S. Isakoff, *Fluid Dynamics of Porous Systems*, BNL-1106.

TABLE 14. CONVERSION OF  $2(NH_4)_2CO_3 \cdot UO_2CO_3$  TO SLURRY-GRADE  $UO_3 \cdot H_2O$

OPERATION	TEMPERATURE (°C)	TIME (hr)	SOLUBLE URANIUM IN SUPERNATANT* (ppm)		
			ADU-I**	AUC-I***	AUC-II***
Conversion of $2(NH_4)_2CO_3 \cdot UO_2CO_3$ to $UO_3$	350	16			
Water wash	90 to 100	1	100	130	100
Calcination and hydration	350	16			
	250		10	88	10
Calcination and hydration	350	16			
	250	16	9	10	

\* Calculated on the basis of a slurry containing 250 g of uranium per liter as  $UO_3 \cdot H_2O$ .

\*\* AUC prepared by metathesizing ammonium diuranate with concentrated  $(NH_4)_2CO_3$  solution.

\*\*\* AUC prepared by ion-exchange methods.

## HRP QUARTERLY PROGRESS REPORT

media, presented an equation relating particle size and sedimentation rates. The equation is

$$\frac{dH}{dt} = \frac{g}{k} \frac{(d_s - d_l)}{M} D_{sv}^2 \frac{e^3}{(1 - e)},$$

where

$\frac{dH}{dt}$  = rate of subsidence of solid phase boundary,

$g = 980 \text{ cm/sec}^2$ ,

$d_s$  = density of solid,

$d_l$  = density of liquid,

$D_{sv}$  = particle size diameter, defined as surface area per volume of particles,

$e$  = porosity =  $\frac{\text{volume of liquid}}{\text{total volume}}$ ,

$k = 5$  or  $12.7$  (the choice of values will be discussed),

$M$  = viscosity of liquid.

Hence, if  $dH/dt$  is determined for slurries of several different concentrations and plotted against  $e^3/(1 - e)$  for each slurry, the resultant curve should be a straight line passing through the origin with slope equal to

$$\frac{g(d_s - d_l)}{kM} D_{sv}^2;$$

the value of  $e^3/(1 - e)$  is obtained, of course, from the average of the

initial and final values of  $e$  in each sedimentation experiment. If the equation holds, it should be possible to calculate  $D_{sv}$  from the slope, since all other terms in the expression are known.

The equation has been tested with slurries containing 200 to 500 g of uranium per liter and has been found to give particle size measurements in good agreement with those obtained from surface area measurements by nitrogen adsorption.

Slurries were prepared from both rods and platelets of measured surface area (nitrogen adsorption) and the sedimentation data obtained. Two particle sizes ( $D_{sv}$ ) were calculated from each set of data by using the two values for  $k$  (see below). Table 15 illustrates the agreement between these sizes and those that were calculated from the surface areas by the following equations:

$$S_w = \frac{6}{\rho D_{sv}}, \quad \text{for platelets,}$$

$$S_w = \frac{4}{\rho D_{sv}}, \quad \text{for rods,}$$

where

$S_w$  = surface area in  $\text{cm}^2/\text{g}$ ,

$\rho$  = density of  $\text{UO}_3 \cdot \text{H}_2\text{O} = 5.7$ .

TABLE 15. PARTICLE SIZE MEASUREMENTS IN  $\text{UO}_3 \cdot \text{H}_2\text{O}$  SLURRIES BY SEDIMENTATION METHODS

URANIUM CONCENTRATION (g/l)	DIAMETER OF SEDIMENTATION TUBE (cm)	PARTICLE SIZE, $D_{sv}$ (microns)		
		Sedimentation		Nitrogen Adsorption
		$k = 5$	$k = 12.7$	
200 to 500 ( $\text{UO}_3 \cdot \text{H}_2\text{O}$ platelets)	2.10	1.5	2.4	1.8
250 ( $\text{UO}_3 \cdot \text{H}_2\text{O}$ platelets)	0.95	1.7	2.7	1.8
250 ( $\text{UO}_3 \cdot \text{H}_2\text{O}$ rods)	0.96	2.5	4.0	2.7
250 ( $\text{UO}_3 \cdot \text{H}_2\text{O}$ platelets)	0.12 (0.2-ml serological pipette)	1.6	2.6	1.8

Although the two platelet preparations investigated were both prepared from uranyl peroxide by alternate calcinations and hydrations, one differed from the other in that it was also micronized between each calcination and hydration. No significant difference in particle size resulted.

It is seen from Table 15 that the particle size measurement by sedimentation is independent of the sedimentation tube diameter. This emphasizes the utility of the method in that a measurement can be made on a sample as small as 0.2 ml.

In Table 15, particle size values obtained from sedimentation data are given for two different values of  $k$ . In evaluating flow through porous media, it has been demonstrated that the value of  $k$  is very close to 5. However, there is some evidence to indicate that when the ratio of the volume of solids to total system volume is low, as in the case of a slurry containing 250 g of uranium per liter, the value of  $k$  increases. In this case, the value of  $k$  appears to be about 12.7. A large value of  $k$  will, of course, be reflected in an increased value of  $D_{sv}$ .

Further justification for the higher value of  $k$  may be seen by comparing the results obtained by using the two different values of  $k$  with the nitrogen adsorption results. In the nitrogen adsorption determination, the assumption that the surface of the solid is covered by a monolayer of nitrogen gas makes it possible to calculate a surface area. Analogously, it is generally considered that a film is formed about a particle on its immersion into a liquid. This film, which moves with the particle through the fluid, should result in an increase in the effective particle size of the solid. Since the  $D_{sv}$  values calculated by using  $k = 5$  are nearly the same as those obtained from the nitrogen adsorption data, and the

$D_{sv}$  values calculated by using  $k = 12.7$  are larger, the higher figure for  $k$  appears to be more reasonable.

#### UO<sub>2</sub>CO<sub>3</sub> CHEMISTRY

Project literature references to the preparation of pure UO<sub>2</sub>CO<sub>3</sub> by the reaction of CO<sub>2</sub> at high pressure on freshly prepared UO<sub>3</sub><sup>(4,5)</sup> prompted an investigation of this reaction with both natural and irradiated material. The results were very promising in that the resulting product was produced in a very finely divided form and showed excellent slurry properties in both high and low concentration. The addition of Na<sub>2</sub>CO<sub>3</sub> to the system resulted in considerable peptization and a reduction in average particle size. Further interest in the reaction is warranted, not only because of the understanding it may give of the technique of producing fine particles, but also because the UO<sub>2</sub>CO<sub>3</sub> itself may be useful (1) as a slurry fuel, (2) as an intermediate in the production of UO<sub>3</sub> slurries, and (3) in the chemical processing of slurry systems.

**Preparation of UO<sub>2</sub>CO<sub>3</sub> Slurries** (J. P. McBride, W. L. Pattison). Scouting experiments have indicated that reaction between CO<sub>2</sub> and UO<sub>3</sub> is possible over a wide range of pressure and temperature, from 500 to 1000 psi and 100 to 250°C. Such variables as the state of subdivision of the oxide, its previous history, and, especially, its state of suspension appear to be important in determining the completeness of reaction.

Relatively pure UO<sub>2</sub>CO<sub>3</sub> (CO<sub>3</sub>/U = 0.96) was obtained in a rocking autoclave at 600 to 1000 psi CO<sub>2</sub>, 250°C, and 15-hr reaction time by using high-purity UO<sub>3</sub>·H<sub>2</sub>O platelets as a starting material. The platelets were prepared

(4) P. D. Miller, H. A. Pray, and H. P. Munger, *The Preparation of Uranyl Carbonate and Measurement of Its Solubility*, BMI-JDS-206 (AECD-2740), p. 15 ff.

(5) K. B. Brown and C. F. Coleman, *Uranium Chemistry of Raw Materials*, Y-622, p. 11 (June 22, 1950).

## HRP QUARTERLY PROGRESS REPORT

from solid precipitated initially as  $\text{UO}_4$  and carried through three cycles of calcination at  $400^\circ\text{C}$  and subsequent rehydration at  $250^\circ\text{C}$ . The  $\text{UO}_2\text{CO}_3$  prepared in this way gave a pale yellow suspension that at a concentration of 160 g of uranium per liter settled slowly but uniformly in about 1/2 hr to a bulk density of one-third the original volume of slurry. The solid was mainly composed of five-particle agglomerates that were 10 to 20  $\mu$  in size.

The addition of 0.005 M  $\text{Na}_2\text{CO}_3$  to the oxide before reaction with  $\text{CO}_2$  brought about a radical change in the resulting slurry. The product in this case was milk white in appearance, very fluid, and virtually stable in comparison with the previous  $\text{UO}_2\text{CO}_3$  slurry or the usual oxide slurries. A suspension containing 224 g of uranium per liter prepared in this way showed complete settling of only 25% of its solids in 17 hr of standing, and the residual material was still dispersed. The pH of the slurry was 7.4. The suspending fluid was water white, which indicated a very low uranium solubility and, correspondingly, indicated the complete adsorption of the added electrolyte.

An attempt to prepare the  $\text{UO}_2\text{CO}_3$  under the above conditions by using as a starting material a  $\text{UO}_4$  precipitate that had been calcined at  $325^\circ\text{C}$  resulted in only partial reaction. The references cited point out the fact that the commercially available  $\text{UO}_3$  prepared by  $\text{UO}_2(\text{NO}_3)_2$  calcination is unreactive. The pretreatment of the uranium necessary to give the most reactive oxide or the best conditions for reaction has not as yet been determined.

**The Properties of  $\text{UO}_2\text{CO}_3$  and  $\text{UO}_2\text{CO}_3$  Slurries** (J. P. McBride, W. L. Pattison, R. G. Mansfield).  $\text{UO}_2\text{CO}_3$  has been described as a pale-yellow, crystalline solid, only slightly soluble in water (3 to 28 ppm), and of density 5.7.<sup>(4,5)</sup>

Electron micrographs of a slurry prepared in the presence of  $\text{Na}_2\text{CO}_3$  showed the  $\text{UO}_2\text{CO}_3$  to be in the form of elongated platelets rounded or cut by crystalline faces at the ends and of about 0.6- $\mu$  average size. X-ray diffraction studies confirmed the crystalline nature of the substance.

$\text{UO}_2\text{CO}_3$  prepared in the absence of  $\text{Na}_2\text{CO}_3$  was found to decompose readily at  $250^\circ\text{C}$  to produce uniform rods that could be readily slurried. Prolonged boiling of a  $\text{Na}_2\text{CO}_3$  stabilized  $\text{UO}_2\text{CO}_3$  slurry through which  $\text{CO}_2$  was bubbled resulted in partial decomposition (7%) and the production of a viscous but quite stable slurry. The presence of 0.005 M  $\text{Na}_2\text{CO}_3$  alone or in the presence of a 200 psi partial pressure of  $\text{CO}_2$  prevented the decomposition to oxide in a closed system for at least 60 hr at  $250^\circ\text{C}$ . The resulting slurries were gray rather than white in color, presumably because of corrosive attack on the stainless steel container, and they exhibited a "silkeness" on stirring. Analysis of the slurries for Fe, Ni, and Cr indicated the corrosive attack to be less than 0.5 mpy but gave evidence that the "dissolution" of Cr was more pronounced than in the case of the oxide slurries. Table 16 gives the corrosion data obtained. Examination of the steel surfaces in contact with the slurry showed them to have acquired a violet cast, which indicated interaction. That the presence of  $\text{CO}_2$  tends to minimize the attack is indicated by the data of Table 16 and the milk-white appearance of the slurries prepared at high  $\text{CO}_2$  pressures. Whether the surface may be protected by an oxide coat or would eventually stabilize itself against attack has not been determined.

The addition of  $(\text{NH}_4)_2\text{CO}_3$  in a stoichiometric ratio of 3:1 readily converts the  $\text{UO}_2\text{CO}_3$  to a partially soluble crystalline substance, presumably  $(\text{NH}_4)_4\text{UO}_2(\text{CO}_3)_3$ . Complete dissolution of this material to give

TABLE 16. CORROSION PRODUCTS IN  $UO_2CO_3$  SLURRIES

Conditions: 200 g of uranium per liter; 0.005 M  $Na_2CO_3$ ; 250°C

	COMPOSITION ( $\mu$ g per g of uranium)		
	Fe	Cr	Ni
Original oxide	150	7	<0.2
$UO_2CO_3$ slurry with 200 psi $CO_2$	256	89	<0.01
$UO_2CO_3$ slurry with no $CO_2$	382	139	<0.01

a stable red-colored solution was obtained by the addition of  $H_2O_2$  and gentle treating at less than 100°C. Prolonged boiling of the solution with  $CO_2$  bubbling through it gave a yellow solid containing  $NH_4$ ,  $CO_3$ , and U in a ratio of 1:1:1. Heating a slurry of this material at 250°C in a closed system resulted in the reduction of the uranium to a black oxide.

**URANIUM OXIDE SLURRY IRRADIATION STUDIES**

J. P. McBride

The results of an irradiation experiment in which a natural uranium oxide slurry was exposed in a stainless steel bomb in the ORNL graphite reactor have indicated that at a relatively low fission density (0.2 watts/g of uranium oxide) the slurry properties of platelets are essentially unimpaired. The irradiated slurry was readily recovered from the radiation bomb, and there was no evidence of the caking that had been observed in previous experiments. The high purity of the oxide used (0.01%  $NO_3$ ) and complete control of the in-reactor temperature were probably the important factors in this successful experiment.

The experiment was carried out in hole 11 of the graphite reactor at full flux, and the material exposed was a slurry of  $UO_3 \cdot H_2O$  platelets containing 250 g of uranium per liter. The platelets were prepared from a  $UO_4$  precipitate by four successive calcinations to anhydrous oxide and subse-

quent rehydrations at 250°C. The slurry was irradiated 21 days at 250°C. Gas production was insignificant (150 psi). Table 17 gives the data obtained.

The growth of the average particle dimension from 3 to 6.7  $\mu$  is particularly interesting. Apparently, little degradation of particle size occurs because of fission in the natural uranium. In addition, the high purity of the platelet preparation is confirmed by the comparatively slight growth that occurred over the three-week period at 250°C.

The usual color change from yellow to nearly jet black was observed as in the previous irradiations. Heating the solid at 400°C overnight failed to produce a color change. Subsequent heating at 250°C in a water slurry to which sufficient  $H_2O_2$  was added to give a 300 psi partial pressure of  $O_2$  restored the yellow color to the slurry, which indicates that the color change induced by radiation is due to the partial reduction of the uranium.

**EFFECT OF FISSION PRODUCTS ON CORROSION**

J. O. Blomeke J. L. Fulmer

As a conclusion of the slurry corrosion work described in the last quarterly report, studies were made of the corrosion of type 347 stainless steel by  $UO_3 \cdot H_2O$  slurries containing fission-product ions in the same concentrations as would be expected after 30 hr of irradiation. Test

## HRP QUARTERLY PROGRESS REPORT

specimens of type 347 stainless steel were exposed to slurries in rocking-bomb autoclaves for 20 hr at 250°C. After each test, the corrosion film was electrolytically stripped from the specimen, and a penetration rate was calculated from the observed weight loss.

The results of this work are given in Table 18, together with the previously reported corrosion rate of pure  $\text{UO}_3 \cdot \text{H}_2\text{O}$  platelets. It was concluded that the presence of traces of fission products in a  $\text{UO}_3 \cdot \text{H}_2\text{O}$  slurry would not be expected to appreciably change the corrosion rate.

TABLE 17. SUMMARY OF SLURRY IRRADIATION EXPERIMENT

OBSERVATION	IRRADIATED SLURRY
Uranium recovered (%)	97
Reduced uranium (%)	2.6
Average corrosion (mpy)	<0.2
Corrosion products ( $\mu\text{g}$ per g of U)	
Fe	400
Cr	26.6
Ni	293
Plutonium distribution (%)	
Solid	95
Supernatant	4.5
Sludge*	0.5
Fission-product distribution (%)	
Solid	88
Supernatant	1
Sludge*	11
Particle growth	From 3 to 6.7 $\mu$

\* Insoluble in 4 M  $\text{HNO}_3$ .

TABLE 18. CORROSION RATES OF TYPE 347 STAINLESS STEEL EXPOSED TO  $\text{UO}_3 \cdot \text{H}_2\text{O}$  SLURRIES AT 250°C

Duration of tests: 20 hr  
Uranium concentration: 250 g/l

SLURRY AND ADDITIVES	CORROSION RATE (mpy)
$\text{UO}_3 \cdot \text{H}_2\text{O}$ rods plus air and 0.012 g of KI per liter	1.1
$\text{UO}_3 \cdot \text{H}_2\text{O}$ platelets plus air and 0.026 g of $\text{BaSO}_4$ per liter	0.2
$\text{UO}_3 \cdot \text{H}_2\text{O}$ platelets plus air and 0.052 g of $\text{BaSO}_4$ and 0.024 g of KI per liter	0.9
$\text{UO}_3 \cdot \text{H}_2\text{O}$ platelets plus air and 0.052 g of $\text{BaSO}_4$ , 0.024 g of KI, and 0.062 g of $\text{Zr}(\text{OH})_4$ per liter	0.3
$\text{UO}_3 \cdot \text{H}_2\text{O}$ platelets (evacuated)	0.6

## PHYSICAL STUDIES OF SLURRIES

A. S. Kitzes            P. R. Crowley  
 R. B. Gallaher        W. Q. Hullings  
                           C. A. Gifford

## THORIUM OXIDE STUDIES

A portion of the effort on slurry studies was devoted to investigating slurries of thorium oxide as possible blanket material for breeder or converter reactors such as the ISHR. Thorium oxide was chosen because it is expected to be more stable than the carbonate in the presence of radiation and because many of the other insoluble thorium compounds, such as the fluoride and oxyfluoride, form gelatinous mixtures in water. Thorium oxide particles remain discrete, but they settle rather rapidly even in slurries of more than 1000 g per liter. At 2000 g per liter, further compacting takes place slowly. In the concentration range between 1000 and 2000 g per liter, the slurry is thixotropic. That is, it becomes more fluid with agitation and retains its fluidity for a short time after the agitation is stopped. This is of importance in considering the power required to circulate the slurry in the system. The evidence to date indicates that these slurries are pseudoplastic in nature, that is, that they will flow to some extent under any applied force, but the possibility still exists that on standing for a long period the slurry will become compacted enough to require a finite force to cause flow. In a circulating system, this property could cause considerable inconvenience.

In tests so far, there is no indication of caking that would prevent agitation from reforming a smooth, homogeneous slurry after standing.

In a preliminary loop test, it was found, as reported last quarter,<sup>(1)</sup>

(1) R. N. Lyon *et al.*, *HRP Quar. Prog. Rep.* Oct. 1, 1952, ORNL-1424, p. 35.

that the thorium oxide particles are extremely abrasive. Further studies with the abrasion tester previously described<sup>(2)</sup> have confirmed the abrasive character of the oxide both with type 347 stainless steel and titanium. In these tests, the slurry flowed between a rotating wheel and a polished test plate parallel to the axle of the wheel. A gap of 0.008 in. was maintained between the rim of the wheel and the plate. The tests are being continued to obtain more quantitative results.

## THORIUM OXIDE CIRCULATING LOOPS

Two loops for circulating thorium oxide slurries are planned - one will operate at 150°C and the other at 250°C. In both these systems, pressure drop and heat transfer determinations will be made.

The loop for operation at 150°C was described in a previous report<sup>(3)</sup> in connection with its use for studying uranium slurries. It has now been modified by substituting a Richardson-Frithsen "bearingless" canned-rotor pump for the original conventional pump, since the stuffing box in the original pump was found to be unusable with the abrasive thorium oxide particles. The loop with the new pump has been tested with water and is now ready for operation with slurry.

Preliminary design of the thorium oxide slurry loop for operation at 250°C and 1000 psi has been completed. A sketch of the proposed loop is shown in Fig. 35. It will be observed that only part of the stream will pass through the pressurizer. Thus, although some flow is required through

(2) A. S. Kitzes *et al.*, *HRP Quar. Prog. Rep.* Aug. 15, 1951, ORNL-1121, p. 156.

(3) *Ibid.*, p. 160.



the bearings. It is expected that if the bearings were not flushed, they would have a very short life.

#### URANIUM SLURRY PUMP LOOPS

A glass loop has been built and operated at atmospheric pressure to aid in interpreting some of the difficulties with the uranium oxide circulating loop that operates at 250°C and 1000 psi. It was learned quickly that a vortex is established in the pressurizer unless baffles are provided to prevent formation of the vortex. The vortex extends all the way around the loop to the pump and apparently accounts for the fluctuations in pump power that were observed previously in the slurry loop and sometimes in the solution loops. Vertical baffles in the pressurizer completely eliminate the vortex if the flowing stream passes through the pressurizer as in the slurry loop. They do not eliminate the vortex if the stream is connected to the pressurizer by a straight vertical pipe as in the solution loops, presumably because the vortex originates in the connecting pipe.

Baffles of this type were installed in the uranium slurry loop (250°C, 1000 psi), and the pump power was found to become unusually steady. After a total of over 2000 hr of intermittent operation with  $\text{UO}_3 \cdot \text{H}_2\text{O}$  slurries, no erosion or corrosion has been detected in the loop. The most serious problem is still that of maintaining the slurry concentration.

Installation of the baffles in the pressurizer has essentially stopped caking of the solids on the pipe wall, perhaps because the vortex which formed without the baffles threw solids out to the walls. Solids still tend to accumulate in the pressurizer, however, and there is a corresponding reduction in concentration of the circulating stream.

#### CRITICAL EXPERIMENTS

In cooperation with the ORNL Criticality group, a system has been built and tested for critical experiments with uranium slurries. An aluminum tank with an agitator and with a water reflector is fed from a continuously circulating loop containing the enriched slurry. The circulating loop is equipped with a Richardson-Frithsen pump. When enough slurry has been added to the tank to make the system almost critical, the feed is stopped and the agitator is slowed. The changes in reactivity are then followed as the solids begin to settle while the reflector is held at the same height as the original slurry level. As yet, no data are available.

Concentrations ranging from 50 to 400 g of uranium per liter will be tested in tanks 10 and 12 in. in diameter. The results will be compared with predictions based on recent calculations for the system by P. R. Kasten.

#### SEDIMENTATION STUDIES

Sedimentation experiments have been performed to provide data for interpretation of the criticality experiments. The settling rate of  $\text{UO}_3 \cdot \text{H}_2\text{O}$  rod slurries at room temperature was determined as a function of concentration. The tests were conducted in a 100-ml graduated cylinder, and the rate was determined by timing the fall of the water-slurry interface. The slurry was mixed by shaking, inverting, and rotating the cylinder for several minutes. The settling rates are shown in Table 19. These values are only approximate, since at the higher concentration, channeling took place and caused the settling rate to vary from test to test. The values reported are an estimate of the settling rate without channeling.

B. F. Ruth of Ames Laboratory has developed equations to correlate

# HRP QUARTERLY PROGRESS REPORT

**TABLE 19. SETTLING RATE DATA FOR UO<sub>3</sub>·H<sub>2</sub>O SLURRY**

CONCENTRATION (g of UO <sub>3</sub> ·H <sub>2</sub> O per liter)	OBSERVED SETTLING RATE, <i>u</i> (in./sec)	CALCULATED VOLUME FRACTION OF LIQUID, <i>ε</i>
25	0.094	0.996
50	0.040	0.992
75	0.023	0.988
100	0.007	0.983
150	0.004	0.975

sedimentation data in the hindered settling range.<sup>(4)</sup> One of his equations is

$$u = \frac{u_s}{1 + \frac{2K(1 - \epsilon)}{\epsilon^3}} \quad (1)$$

where

- u* = settling rate of the interface,
- u<sub>s</sub>* = settling rate of a single particle,
- ε* = porosity (volume fraction of liquid),
- K* = Kozeny constant, 4.5.

By plotting

$$\log \frac{1}{1 + \frac{2K(1 - \epsilon)}{\epsilon^3}} \text{ vs. } \log \frac{u}{u_s},$$

a straight line should be obtained with a slope of 1.0. This plot is shown in Fig. 36, and although the line is straight, the slope is not 1.0. According to Ruth, this indicates that the particles have a lysphere, that is, a layer of water around the particle. Equation 2 is an equation developed by Ruth to predict the nature of the lysphere.

$$\sqrt[3]{\frac{(1 + \nu)^2}{\frac{u_s}{u} - 1}} = (\nu - \nu_0) \sqrt[3]{\frac{\psi^{3/2}}{2K(1 + \nu_0)}}, \quad (2)$$

where

*ν* = *ε*/(1 - *ε*), the ratio of liquid to solid (by volume),

*ν<sub>0</sub>* = ratio of lysphere volume to solid volume,

*ψ* = sphericity, the ratio of surface area of sphere to surface area of particle with same volume.

The value of *u<sub>s</sub>* may be obtained, by extrapolation, from Fig. 36 at

$$\frac{1}{1 + \frac{2K(1 - \epsilon)}{\epsilon^3}} = 1.0;$$

UNCLASSIFIED  
DWG. 17835

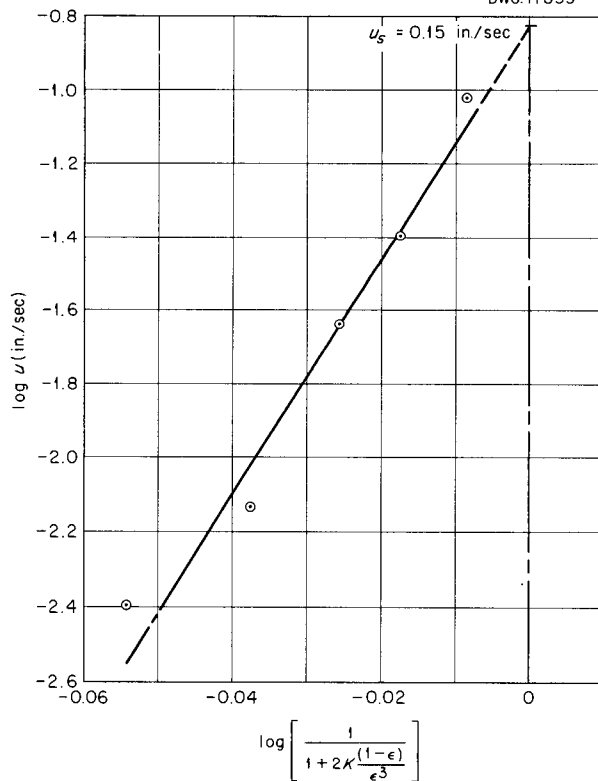


**Fig. 36. Plot of log *u* vs. log 1/{1 + [2*K*(1 - *ε*)]/*ε*<sup>3</sup>}.**

(4) B. F. Ruth; Lectures on Dynamics of Fluid-Solid Systems, Iowa State College, Ames, Iowa, summer term, 1951.

$u_s$  is found to be 0.15 in./sec. Then by plotting

$$\nu \text{ vs. } \sqrt[3]{\frac{(1 + \nu)^2}{\frac{u_s}{u} - 1}},$$

the value of  $\nu_0$  is obtained, by extrapolation, as the value of  $\nu$  when

$$\sqrt[3]{\frac{(1 + \nu)^2}{\frac{u_s}{u} - 1}} = 0,$$

as shown in Fig. 37. Also the value of  $\psi$ , the sphericity of the particle, may be found from Fig. 36 since

$$\sqrt[3]{\frac{\psi^{3/2}}{2K(1 + \nu_2)}}$$

is the slope of the line. The lysphere was found to be approximately  $19 \text{ cm}^3$  of liquid per cubic centimeter of solid, and the sphericity to be 0.98; that is, the particle is very nearly spherical. After the ratio of solid to liquid in the particle was determined, the pseudo density was

calculated to be 1.25. Then by using the values for density and the velocity (determined by using Stokes' law), the diameter of the particle was found to be 0.167 mm. A particle of this size would contain about 300  $\text{UO}_3 \cdot \text{H}_2\text{O}$  rod particles; that is, it would be an agglomerate.

#### THERMAL CONDUCTIVITY OF SLURRIES

Preliminary values of the thermal conductivities of uranium oxide and thorium oxide slurries at  $25^\circ\text{C}$  have been determined. A transient method of measuring thermal conductivity, developed by W. D. Powers, was used and the experimental work was done in cooperation with Powers. The oxides were suspended in Kelcosol gelatin solution of high viscosity in order to keep the particles dispersed during the measurement. The results of these studies are shown in Table 20. They are, in general, within 5% of actual value on the basis of determination on pure water. Measurement of the thermal conductivity of these slurries at temperatures up to  $250^\circ\text{C}$  is planned for the future. The equipment for such work has been constructed and is being tested.

#### CRYSTAL STRUCTURE OF $\text{UO}_3 \cdot \text{H}_2\text{O}$

In an effort to study the transformations of the various crystal habits of  $\text{UO}_3 \cdot \text{H}_2\text{O}$  (rod, platelet, and bipyramid) and possibly discover the mechanism of these transformations, a means of identification more positive than microscopic examination was sought. Samples of rods, platelets, and bipyramids were submitted to R. Ellison for x-ray analysis and G. White for index of refraction studies.

The results of the x-ray analysis are: rods are pure alpha structure, bipyramids are pure beta structure, and platelets (as produced by the Chemical Technology Division) are beta structure, with traces of the alpha structure present. The indices

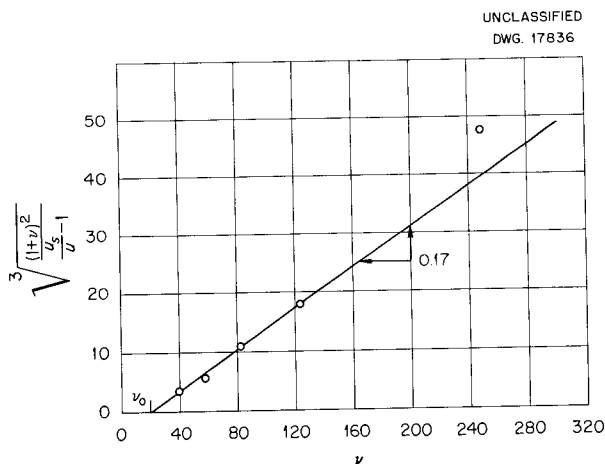


Fig. 37. Plot of  $\nu$  vs.

$$\sqrt[3]{(1 + \nu)^2 / [(u_s/u) - 1]}.$$

# HRP QUARTERLY PROGRESS REPORT

**TABLE 20. THERMAL CONDUCTIVITY OF URANIUM OXIDE AND THORIUM OXIDE SLURRIES (ROOM TEMPERATURE)**

URANIUM OXIDE SLURRY		THORIUM OXIDE SLURRY	
CONCENTRATION (g of $UO_3 \cdot H_2O$ per liter)	CONDUCTIVITY (kcal/sec·cm·°C)	CONCENTRATION (g of Th per liter)	CONDUCTIVITY (kcal/sec·cm·°C)
0	0.00142	0	0.00146
250	0.00146	500	0.00168
350	0.00150	1000	0.00194
1140	0.00149	1500	0.00205

of refraction of these crystal habits are: rods, 1.847; bipyramids, 1.730 and 1.773; and platelets, 1.730 and 1.773. (The alpha and beta structures are those reported by Zachariassen,<sup>(5)</sup> with the difference being in the size of a unit cell.) From these results it is possible by either x-ray analysis or index of refraction determination to identify the crystal structure of  $UO_3 \cdot H_2O$ , but not necessarily the crystal habit.

It was observed that when  $UO_3 \cdot H_2O$  in the form of rods was circulated in the loop operated at 250°C, the rods changed to small spherical or oval particles, probably because of the breaking and rounding action caused by circulation. Samples taken periodically from the loop during operation showed a transformation from the alpha structure of the initial rods to the beta structure associated with plates and bipyramids of the resulting spherical or oval particles. Table 21 gives the percentages of alpha and beta structures at various times during the runs. The percentages are only approximate because no standard mixtures of alpha and beta structures are available for comparison at the present time.

(5) W. H. Zachariassen, *Physics Division Report for Month Ending February 15, 1945 - Part I*, CK-2737, p. 12.

**TABLE 21. CONVERSION OF ALPHA STRUCTURE TO BETA STRUCTURE IN  $UO_3 \cdot H_2O$  RODS (AS A FUNCTION OF TIME) WHEN CIRCULATED IN A LOOP OPERATED AT 250°C**

TIME (hr)	ALPHA STRUCTURE (%)	BETA STRUCTURE (%)
0	100	0
2	100	0
44	60	40
73	40	60
151	20	80
164	5	95

The results of this study show that  $UO_3 \cdot H_2O$  rods not only change form during circulation but also change structure. Therefore the possibility exists that it may be desirable to use the beta structure as a starting material in reactor fuel slurries.

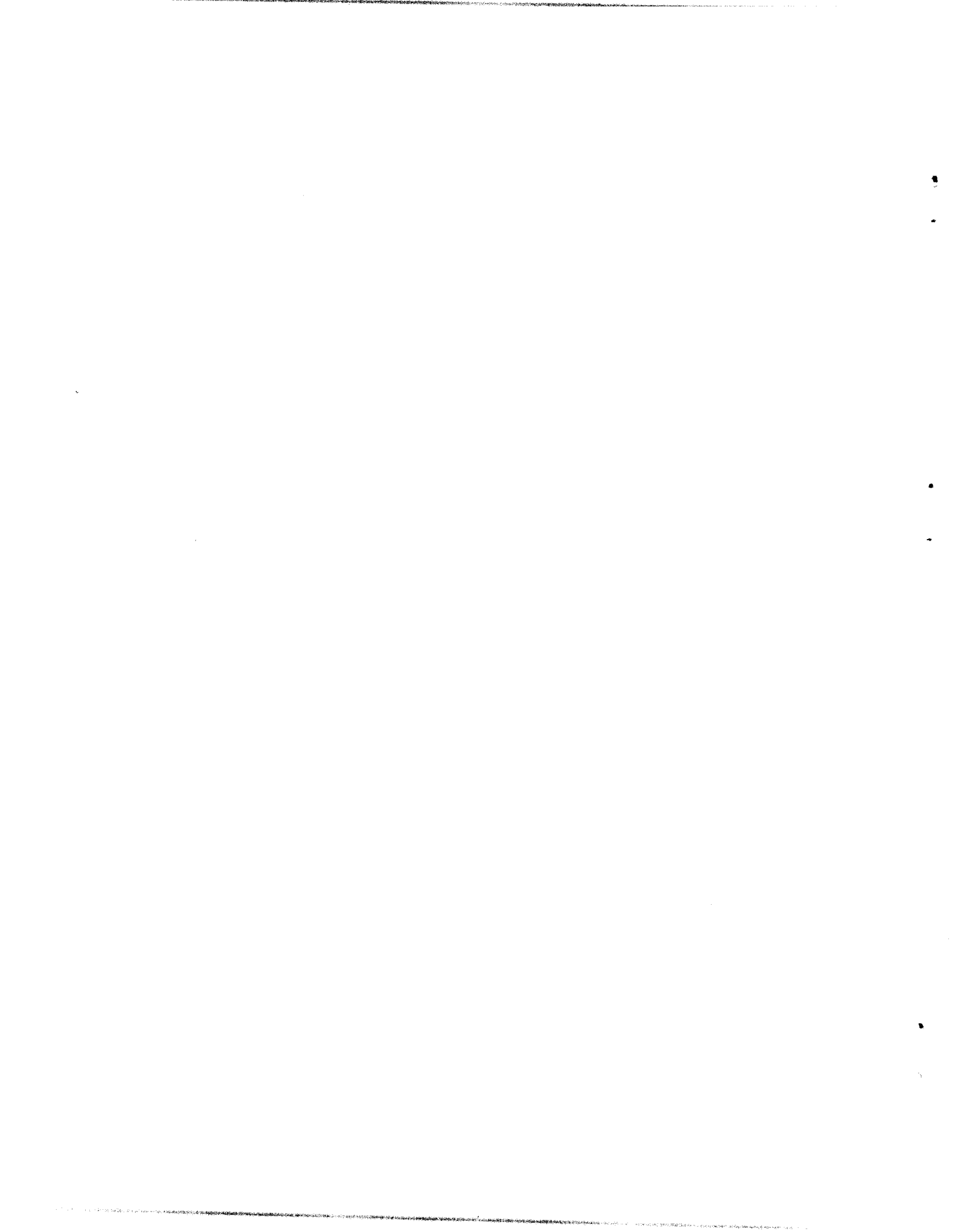
The present method of producing platelets (beta structure) employs rods as the starting material and involves several cycles of calcination, hydration, washing, and autoclaving. Because a certain amount of time and effort is spent in producing rods, and much more is involved in transforming the rods to platelets, it seemed necessary to find a better method of producing platelets. By using  $UO_4 \cdot 2H_2O$

## PERIOD ENDING JANUARY 1, 1953

as the starting material, bipyramids and large platelets were produced after one calcination at 400°C and hydration and autoclaving at 250°C. This material was found to be beta-structure  $\text{UO}_3 \cdot \text{H}_2\text{O}$ , with a very small amount of alpha structure, but it contained a relatively large amount of soluble uranium and nitrate ion (from 25 to 150 ppm of soluble uranium and less than 10 to 40 ppm of nitrate). After a second cycle, the material contained a number of small platelets and a large amount of irregular material that appeared to be highly

agglomerated platelets. This material was beta structure with trace amounts of alpha structure, and it contained very little soluble uranium and nitrate ion. Although this is not a method for producing platelets, it is a relatively short method for producing beta-structure  $\text{UO}_3 \cdot \text{H}_2\text{O}$  of high purity.

It is possible that iron, chromium, and nickel, or other impurities may influence the stable crystal form of the uranium oxide. Studies have been started to investigate this possibility, but results are not yet available.



## CHEMICAL PROCESSING

F. R. Bruce, Section Chief

D. E. Ferguson                      W. B. Howerton  
G. I. Cathers                        O. K. Tallent  
W. E. Tomlin

### PLUTONIUM CHEMISTRY IN URANYL SULFATE SOLUTIONS

**Effect of Mixtures of Hydrogen and Oxygen on the Behavior of Plutonium in 1 M Uranyl Sulfate Solution.** The composition of the gas mixture in contact with the fuel solution in a homogeneous, plutonium-producing reactor will vary throughout the reactor. In the reactor core, the gas phase will contain approximately the stoichiometric ratio of hydrogen and oxygen. In the gas separator and external system, there will be a large excess of oxygen. The conditions used in the following series of experiments were designed to investigate the effect on plutonium valence state of this range of gas mixtures at both 250 and 100°C.

The results at 250°C indicate that Pu(VI) will be rapidly reduced to the

insoluble tetravalent state and will precipitate (Table 22). There was some indication that the highest oxygen pressure, 400 psi, stabilized about 0.015 mg/ml of Pu(VI); however, the concentration of oxygen in solution attained in this experiment will probably not be reached in the reactor.

At 100°C the reaction rates are much slower. When a 1 M UO<sub>2</sub>SO<sub>4</sub> solution containing both Pu(VI) and Pu(IV) was exposed to mixtures of hydrogen and oxygen at 100°C, some reduction of Pu(VI) to Pu(IV) was observed, but no precipitation of plutonium occurred even after 72 hr (Table 23).

Based on these results, the equilibrium amount of plutonium in solution would not exceed 0.01 mg/ml in a reactor operating at 250°C, and in a reactor operating at 100°C, the equilibrium concentration would exceed

**TABLE 22. EFFECT OF MIXTURES OF HYDROGEN AND OXYGEN ON THE BEHAVIOR OF PLUTONIUM IN 1 M URANYL SULFATE SOLUTION AT 250°C**

Starting Solution: 1 M UO<sub>2</sub>SO<sub>4</sub> containing 0.14 mg of Pu(VI) per ml and 0.14 mg of Pu(IV) per ml

Conditions: 24 hr at 250°C, 120 psi of H<sub>2</sub>, and O<sub>2</sub> pressure as indicated

OXYGEN PRESSURE (psi at 250°C)	FINAL Pu(VI) CONCENTRATION IN SOLUTION (mg/ml)	FINAL TOTAL Pu CONCENTRATION IN SOLUTION (mg/ml)
60	0.0000	0.0016
120	0.0000	0.0017
240	0.0001	0.0017
400	0.0006	0.0019
400	0.012	0.016
400	0.017	0.021

## HRP QUARTERLY PROGRESS REPORT

TABLE 23. EFFECT OF MIXTURES OF HYDROGEN AND OXYGEN ON THE BEHAVIOR OF PLUTONIUM IN 1 M URANYL SULFATE SOLUTION AT 100°C

Starting solution: 1 M UO<sub>2</sub>SO<sub>4</sub>  
 Temperature: 100°C  
 Hydrogen pressure: 75 psi  
 Oxygen pressure: as indicated

OXYGEN PRESSURE (psi at 100°C)	HEATING TIME (hr)	Pu(VI) CONCENTRATION BEFORE HEATING (mg/ml)	Pu(VI) CONCENTRATION AFTER HEATING*
38	24	0.196	0.185
75	24	0.195	0.171
150	48	0.181	0.153
250	72	0.165	0.146

\*No precipitation occurred; therefore all the Pu(IV) remained in solution.

0.1 mg/ml. These concentrations in the reactor correspond to a Pu<sup>240</sup> content of 0.2 and 2%, respectively, in the product.

**Reduction of Plutonium in the Fuel Solution by Hydrogen.** When a 1 M UO<sub>2</sub>SO<sub>4</sub> solution containing a mixture of Pu(IV) and Pu(VI) was exposed to a partial pressure of 39 psi of hydrogen at 250°C for 6 hr, all the Pu(VI) was reduced. The concentration of plutonium remaining in solution after 6 hr, as Pu(IV), was 0.005 mg/ml; and after 12 hr, only 0.002 mg/ml of plutonium remained in solution. Thus, it is possible to remove plutonium from a uranyl sulfate solution fuel in 6 hr by reducing with a small amount of hydrogen gas at 250°C.

**Removal of PuO<sub>2</sub> Precipitated from Reactor Fuel Solution.** It was found that the average particle size of PuO<sub>2</sub> precipitated at 250°C from a 1 M UO<sub>2</sub>SO<sub>4</sub> solution was less than 1 micron. There was no significant increase in particle size of PuO<sub>2</sub> precipitated during agitation in a rocking autoclave, even when the solution was seeded with preformed PuO<sub>2</sub>.

The settling rate of this finely divided material is about 0.2 cm/min.

A settling rate of at least five times this value, or 1 cm/min, would be required to remove plutonium from the fuel solution adequately by a simple settling technique.

### RADIATION DAMAGE

It was anticipated that economic chemical processing of homogeneous reactor fuel solutions might require operation at a radiation level that would damage a solvent extraction process employing tributyl phosphate. Some experimental work has been carried out to determine what effect radiation has on tributyl phosphate, and how this damage changes the effectiveness of the Purex process. This was done by exposure of solvent to high intensity gamma emission from a Co<sup>60</sup> source to simulate the beta absorption that would occur in the processing of short-cooled material.

Preliminary tests on exposed solvent showed that radiation-induced hydrolysis of tributyl phosphate to monobutyl and dibutyl phosphate was the major result of radiation damage. However, the magnitude of this effect made it probable that radiation damage

PERIOD ENDING JANUARY 1, 1953

would only be noticeable in a Purex process operating at ten to one hundred times the radiation level expected in the processing of 15-day cooled material from a homogeneous reactor.

The two series of Purex batch countercurrent tests that have now been completed confirm this conclusion. Series A (Table 24) consists of runs made with 30% tributyl phosphate-Amsco solvent that had received various energy dosages, specified in watt-hours per liter. Processing 15-day cooled material in the first cycle of Purex would be equivalent to dosages of about 0.25 watt-hr per liter.

Series B (Table 24) consists of analogous runs with the solvent irradiated in the presence of the nitric acid and uranyl nitrate complexes that would be present in actual processing. Table 24 lists only those variables that were affected by radiation, that is, the fission-product decontamination factors, the plutonium loss from the strip column, the nonstrippable uranium, and the residual activity in the used solvent.

The effect of radiation damage was noticeable, particularly in the losses, at ten times the radiation exposure expected in the processing of 15-day cooled material. The effect of radiation is even more pronounced in the second series, in which the radiation was made in the presence of nitric acid and uranium. Very large changes in decontamination factors and residual solvent activity occurred, however, only at 30 watt-hr per liter.

The above summarizes the general results of radiation-induced hydrolysis in tributyl phosphate extraction processes. Another type of damage, which has not been so well evaluated, is that due to evolution of relatively large amounts of hydrogen and methane from the tributyl phosphate, as well as from the hydrocarbon diluent. This apparently leads to an increase in solvent acidity and unsaturation. The formation of emulsions and crud in the process may be due to the surface-active agents and polymers produced by radiation.

TABLE 24. PUREX COUNTERCURRENT RUNS WITH RADIATION-DAMAGED 30% TBP-AMSCO SOLVENT

RADIATION EXPOSURE (watt-hr per liter)	Pu DECONTAMINATION FACTOR	U DECONTAMINATION FACTOR	Pu LOSS IN PU STRIP COLUMN (%)	U LOSS IN U STRIP COLUMN (%)	BETA ACTIVITY OF USED SOLVENT (c/min/ml)
Series A					
0	7000	5000	0.08	0.0004	550
2.4	140	1300	0.05	0.007	225
27	30	220	0.22	0.2	$4 \times 10^3$
280		21	0.62	2.1	$1.4 \times 10^5$
Series B					
0	6400	1700	0.08	0.002	90
4.3	690	2200	0.31	0.02	110
30	37	600	38.0	0.6	$1.3 \times 10^5$



## RELATED BASIC CHEMISTRY RESEARCH

S. C. Lind, Director

### CAPTURE CROSS SECTION OF PROTACTINIUM-233

J. Halperin      R. W. Stoughton

Work on the determination of the capture cross section of protactinium-233 has been completed and will be reported in ORNL-1462.<sup>(1)</sup> The thermal-neutron capture cross section of Pa<sup>233</sup> has been measured as  $125 \pm 15$  barns.

### CHEMISTRY OF CORROSION

G. H. Cartledge

It has been discovered that potassium pertechnetate,  $\text{KTcO}_4$ , has the properties of a corrosion inhibitor under a variety of conditions. The results to date will be presented in the forthcoming Chemistry Division quarterly progress report.

### NUCLEATION OF BUBBLES IN SUPERHEATED SOLUTIONS BY FISSION RECOILS

J. A. Ghormley

A knowledge of the conditions under which fission recoil tracks can serve as nuclei for bubbles in superheated solutions is essential in predicting the behavior of homogeneous boiling reactors. From studies made in the temperature range from 114 to 250°C, it was shown that single fissions provide bubble nuclei that cause ebullition in uranyl sulfate solutions superheated above a definite minimum temperature at any given pressure.

<sup>(1)</sup> J. Halperin, Capture Cross Section of Pa<sup>233</sup>, ORNL-1462 (to be issued).

At 250°C, the maximum possible superheating in the presence of fissions is about 2°C. Expressed in terms of vapor pressure, the superheat necessary for fission tracks to nucleate bubbles at any pressure, in  $\text{UO}_2\text{SO}_4$  solution containing 44 g of uranium per liter, is that temperature which gives a vapor pressure of about 110 cm Hg above the existing pressure in the system. Results are described in more detail in the Chemistry Division quarterly progress reports for periods ending September 30 and December 31, 1952.

### URANYL-SENSITIZED REACTION OF HYDROGEN AND OXYGEN

T. J. Sworski

The yield of hydrogen in the decomposition of water by fission recoils is proportional to the square root of the uranium concentration for solutions in which more than 99.5% of the absorbed energy is fission energy.

SOLUTE	FORMULA FOR $G_{\text{H}_2}$
$\text{UO}_2\text{F}_2$	$1.83 - 0.0428 \sqrt{\text{g of U per liter}}$
$\text{UO}_2\text{SO}_4$	$1.83 - 0.0488 \sqrt{\text{g of U per liter}}$
$\text{U}(\text{SO}_4)_2$	$1.83 - 0.0585 \sqrt{\text{g of U per liter}}$

It is suggested that uranyl ion lowers the hydrogen yield through a radiation-induced chemical reaction. The reaction of hydrogen and oxygen is photosensitized by uranyl sulfate. This work is described more fully in the Chemistry Division quarterly progress report for December 31, 1952.

**OXIDATION OF URANIUM(IV) BY GAMMA RAYS**

C. Hochanadel

The gamma-ray induced oxidation of uranium(IV) is being studied. Uranium(IV) is oxidized completely to uranium(VI) with yields ranging from

1.6 ions oxidized per 100 ev in degassed solutions to 7.8 ions per 100 ev with oxygen present. The effects of several variables are being studied. Results are presented in more detail in the Chemistry Division quarterly progress report for period ending September 30, 1952.